AN IN-FLIGHT INVESTIGATION TO DEVELOP CONTROL SYSTEM DESIGN CRITERIA FOR FIGHTER AIRPLANES

Volume I

T. PETER NEAL
ROGERS E. SMITH

FOREWORD

This report was prepared for the United States Air Force by the Cornell Aeronautical Laboratory, Inc. (CAL), Buffalo, New York in partial fulfillment of Contract No. F33615-69-C-1664, and describes the results of the first flight program under that contract.

The investigation reported here was performed by the Flight Research Department of CAL under sponsorship of the Air Force Flight Dynamics Laboratory, Wright-Patterson Air Force Base, Ohio, as part of Project 8219, Task 821905. The Air Force Project Engineer was Mr. David K. Bowser (FGC).

This report represents the combined efforts of many members of the Flight Research Department. Fred D. Newell is the program manager for the overall variable stability T-33 program. Ronald W. Huber is responsible for modifications, calibration, and maintenance of the T-33 variable stability system. The CAL project engineer for this investigation was T. Peter Neal, and the assistant project engineer was Rogers E. Smith. The evaluation pilots were G. Warren Hall (Pilot W), and T. Michael Harris (Pilot M). Rogers E. Smith, Robert P. Harper, Jr., and Nello L. Infanti acted as safety pilots on the evaluation flights. The engineering assistance of Alan B. Adler, James R. Lyons, and C. Macey Poppenberg is also gratefully acknowledged.

This report was submitted by the authors in June 1970.

This report has been reviewed and is approved.

C. B. Westbrook
Chief, Control Criteria Branch
Air Force Flight Dynamics Laboratory

Unclassified

Security Classification

DOCUMENT CONTROL DATA - R & D

(Security classification of title, body of abstract and indexing annotation must be entered when the overall report is classified)

1. ORIGINATING ACTIVITY *(Corporate author)*
Cornell Aeronautical Laboratory, Inc.
Buffalo, New York 14221

2a. REPORT SECURITY CLASSIFICATION
Unclassified

2b. GROUP

3. REPORT TITLE
AN IN-FLIGHT INVESTIGATION TO DEVELOP CONTROL SYSTEM DESIGN CRITERIA FOR FIGHTER AIRPLANES, Volume I

4. DESCRIPTIVE NOTES *(Type of report and inclusive dates)*
Final report

5. AUTHOR(S) *(First name, middle initial, last name)*
Neal, T. Peter and Smith, Rogers E.

6. REPORT DATE	7a. TOTAL NO. OF PAGES	7b. NO. OF REFS
December 1970	132	21

8a. CONTRACT OR GRANT NO.	9a. ORIGINATOR'S REPORT NUMBER(S)
F33615-69-C-1664	CAL Report No. BM-2821-F-4
b. PROJECT NO. 8219	
c. Task No. 821905	9b. OTHER REPORT NO(S) *(Any other numbers that may be assigned this report)*
d.	AFFDL-TR-70-74, Volume I

10. DISTRIBUTION STATEMENT
Approved for public release; distribution unlimited.

11. SUPPLEMENTARY NOTES	12. SPONSORING MILITARY ACTIVITY
	Air Force Flight Dynamics Laboratory Wright-Patterson Air Force Base Ohio 45433

13. ABSTRACT

The effects of control system dynamics on the longitudinal flying qualities of fighter airplanes were investigated in flight, using the USAF/CAL variable stability T-33 airplane. Two pilots evaluated a total of 57 different combinations of control system and short-period dynamics at two flight conditions, while performing tasks representative of the "combat" phase of a fighter's mission. The pilot rating and comment data from this investigation indicate that the dynamic modes of the flight control system can cause serious flying qualities problems, even if the short-period mode is well behaved. The data do not correlate with the control system requirements of MIL-F-8785B. In addition, the data demonstrate that the C* criterion does not adequately account for the effects of control system dynamics. Pilot-in-the-loop analysis of the data is shown to describe effectively the pilot's difficulties in control of pitch attitude, providing insight into how the pilot flies the airplane. A design criterion, based on this analysis, is shown to be applicable to a wide range of short-period and control system dynamics. A simplified version is also presented to provide the designer with preliminary estimates of flying qualities. Volume I contains the body of the report, while Volume II consists of the Appendices.

DD FORM 1 NOV 68 1473

Unclassified
Security Classification

14. KEY WORDS	LINK A		LINK B		LINK C	
	ROLE	WT	ROLE	WT	ROLE	WT
Longitudinal Flying Qualities Control System Dynamics Short-Period Dynamics Fighter Airplane Evaluations In-Flight Simulation Variable-Stability Airplane						

TABLE OF CONTENTS

TABLE OF CONTENTS (cont.)

LIST OF ILLUSTRATIONS

LIST OF ILLUSTRATIONS (cont.)

LIST OF ILLUSTRATIONS (cont.)

LIST OF TABLES

LIST OF SYMBOLS

a_E	Equivalent time delay (sec)
BW	Bandwidth; the frequency at which the phase angle of the θ/θ_c transfer function = -90 deg (rad/sec)
$(BW)_{min}$	The value of the closed-loop bandwidth which the pilot is trying to achieve in precision tracking tasks (rad/sec)
c	Wing mean aerodynamic chord (ft)
C_L	$= \frac{L}{\bar{q}S}$, Airplane lift coefficient
C_{L_α}	$= \frac{\partial C_L}{\partial \alpha}$ (1/rad)
$C_{L_{\delta_e}}$	$= \frac{\partial C_L}{\partial \delta_e}$ (1/rad)
C_m	$= \frac{M}{\bar{q}Sc}$, Airplane pitching moment coefficient
C_{m_α}	$= \frac{\partial C_m}{\partial \alpha}$ (1/rad)
$C_{m_{\dot{\alpha}}}$	$= \frac{\partial C_m}{\partial \left(\frac{\dot{\alpha} c}{2V_T}\right)}$ (1/rad)
C_{m_q}	$= \frac{\partial C_m}{\partial \left(\frac{q c}{2V_T}\right)}$ (1/rad)
$C_{m_{\delta_e}}$	$= \frac{\partial C_m}{\partial \delta_e}$ (1/rad)
C^*	Particular blend of the airplane's n , $\dot{\theta}$ and $\ddot{\theta}$ responses (g's) (Reference 15)
dB	Decibel units for Bode amplitude, where amplitude in dB = $20 \log_{10}$ [amplitude]
$\left(\frac{dA}{d\chi}\right)_{ad}$	Rate of change of Bode amplitude with phase for the airplane plus pilot time delay at $\omega = (BW)_{min}$ (dB/deg)
F_{AS}	Aileron stick force, positive to the right (lb)
F_{RP}	Rudder pedal force, positive for right rudder (lb)
F_S	Elevator stick force, positive for a pull (lb)
$\frac{F_S}{n}$	Steady-state stick force per unit normal acceleration change, at constant speed (lb/g)
$\frac{F_S}{\theta_e}$	Transfer function of the pilot model

g Acceleration of gravity (ft/sec^2)

h_d Density altitude (ft)

h_p Pressure altitude (ft)

I_y Moment of inertia about airplane y axis ($slug\text{-}ft^2$)

$K_{\theta W}$ Pilot gain at $\omega = (BW)_{min}$ (lb/deg)

K_L Total closed-loop gain, $K_L = K_p K_\theta$ (1/sec)

K_p Steady-state pilot gain (lb/deg)

K_θ Gain of airplane's θ/F_s transfer function $\left(\frac{deg/sec}{lb}\right)$

K'_θ Gain of airplane's θ/δ_s transfer function $\left(\frac{deg/sec}{in.}\right)$

ℓ_p Distance of the pilot's station ahead of the center of gravity (ft)

L Airplane lift, positive for positive angles of attack (lb)

$L_\alpha = \frac{\bar{q} S C_{L_\alpha}}{m V_T}$ (1/sec)

$L_{\delta_e} = \frac{\bar{q} S C_{L_{\delta_e}}}{m V_T}$ (1/sec)

m Mass of airplane (slugs)

M Airplane pitching moment, positive nose up (ft-lb)

$M_\alpha = \frac{\bar{q} S c C_{m_\alpha}}{I_y}$ ($1/sec^2$)

$M_{\dot{\alpha}} = \frac{\bar{q} S \left(\frac{c^2}{2V_T}\right) C_{m_{\dot{\alpha}}}}{I_y}$ (1/sec)

$M_q = \frac{\bar{q} S \left(\frac{c^2}{2V_T}\right) C_{m_q}}{I_y}$ (1/sec)

$M_{\delta_e} = \frac{\bar{q} S c C_{m_{\delta_e}}}{I_y}$ ($1/sec^2$)

n Normal acceleration at c.g., positive for a pull up (g's) ($n = 1$ for level flight)

$\frac{n}{\alpha}$ Steady-state normal acceleration change per unit angle-of-attack change, when the airplane is maneuvered at constant speed (g's/radian) $n/\alpha \approx \frac{V_T}{g} \frac{1}{t_{\theta_2}}$

$P_E = \frac{2\pi}{\omega_E}$, Period of equivalent short-period mode (sec)

$\bar{q} = \frac{1}{2}\rho V_T^2$, Dynamic pressure (lb/ft^2)

q Airplane pitch rate about y body axis. For wings-level flight $q = \dot{\theta}$

s Laplace operator (1/sec)

S Wing area (ft^2)

t Time (sec)

T_p Phugoid period (sec)

V_{ind} Trimmed indicated airspeed, (knots)

V_T Trimmed true airspeed (ft/sec)

α Airplane angle of attack, positive for relative wind from below (rad)

β Airplane angle of sideslip, positive for relative wind from right (rad)

δ_{AS} Aileron stick deflection at grip, positive to the right (inches)

δ_e Airplane elevator deflection, positive trailing edge down (rad)

δ_{RP} Rudder pedal deflection, right rudder is positive (inches)

δ_S Elevator stick deflection at grip, positive aft (inches)

$\left(\frac{\delta_e}{F_S}\right)_{SS}$ Steady-state gearing between elevator deflection and elevator stick force (rad/lb)

$\left(\frac{\delta_e}{\delta_S}\right)_{SS}$ Steady-state gearing between elevator deflection and elevator stick displacement (rad/in.)

ζ_d Dutch-roll damping ratio

ζ_E Equivalent short-period damping ratio

ζ_p Phugoid damping ratio

ζ_{SP} Short-period damping ratio

ζ_3 Damping ratio of second-order control system lag

ζ_ϕ	Damping ratio of second-order numerator term in bank-angle-to-aileron transfer function
θ	Airplane's pitch attitude with respect to horizon, positive nose up (deg or rad)
θ_c	Commanded change in airplane pitch attitude (deg or rad)
θ_e =	(θ_c - θ), Error between the commanded pitch attitude and the airplane pitch attitude (deg or rad)
$\frac{\theta}{F_s}$	Constant-speed transfer function of θ to F_s for airplane plus control system
$\frac{\theta}{\theta_e}$	Open-loop transfer function of airplane plus control system plus pilot
$\left(\frac{\theta}{\theta_e}\right)^*$	$\frac{\theta}{\theta_e}$ transfer function with uncompensated pilot ($F_s/\theta_e = K_p e^{-0.3s}$)
$\frac{\theta}{\theta_c}$	Closed-loop transfer function of airplane plus control system plus pilot
$\left\lvert\frac{\theta}{\theta_c}\right\rvert_{max}$	Magnitude of resonant peak in the θ/θ_c Bode amplitude plot (dB)
$\left\lvert\frac{\ddot{\theta}}{F_s}\right\rvert_{max}$	Maximum Bode amplitude of $\ddot{\theta}/F_s$ $\left(\frac{rad/sec^2}{lb}\right)$
ρ	Air density (slug/ft^3)
σ	Real part of $s = \sigma + j\omega$
τ_1	Time constant of control system lead element (sec)
τ_2	Time constant of control system lag element (sec)
τ_E	Equivalent lead time constant of airplane (sec)
τ_{p_1}	Time constant of pilot's lead element (sec)
τ_{p_2}	Time constant of pilot's lag element (sec)
τ_R	Roll mode time constant (sec)
τ_s	Spiral mode time constant (sec)
τ_{θ_2}	Airframe lead time constant in θ/F_s transfer function (sec)
$\lvert\phi/\beta\rvert_d$	Absolute value of control-fixed roll-to-sideslip ratio evaluated at $\omega = \omega_d$

ω	Bode frequency (rad/sec)
ω_c	Gain crossover frequency, where the open-loop Bode amplitude curve crosses 0 dB line (rad/sec)
ω_d	Dutch roll undamped natural frequency (rad/sec)
ω_E	Undamped natural frequency of equivalent short-period mode (rad/sec)
ω_{fs}	Undamped natural frequency of longitudinal feel system (rad/sec)
ω_{sp}	Short-period undamped natural frequency (rad/sec)
ω_3	Undamped natural frequency of second-order control system lag (rad/sec)
ω_ϕ	Undamped natural frequency of second-order numerator term in bank-angle-to-aileron transfer function (rad/sec)
$\lvert\ \rvert$	Signifies Bode amplitude of a transfer function
$\angle$	Signifies Bode phase angle of a transfer function
$\angle_{ad}$	Phase angle of the airplane plus pilot time delay at $\omega = (BW)_{min}$ (deg)
$\angle_{pc}$	Phase angle of the pilot compensation at $\omega = (BW)_{min}$ (deg)
$\dot{(\ )} = \frac{d}{dt}(\ )$	First derivative with respect to time
$\ddot{(\ )} = \frac{d^2}{dt^2}(\ )$	Second derivative with respect to time

ABBREVIATIONS

FCS	Flight control system
CAL	Cornell Aeronautical Laboratory, Inc.
c.g.	Center of gravity
HOS	Higher-order-system program (Reference 6)
IFR	Instrument flight rules
log	Logarithm to base 10
norm.	Normalized
PIO	Pilot-induced oscillation
PIOR	Pilot-induced-oscillation rating
PR	Pilot rating (Cooper-Harper scale)
USAF	United States Air Force
VFR	Visual flight rules

SECTION I

INTRODUCTION

The study reported herein is the continuation of a series of experimental investigations into the longitudinal flying qualities problems of fighter airplanes, using the USAF/CAL variable stability T-33 airplane (References 1 through 8). The experiment is directed at the "combat" phase of the fighter's mission. The major area of concern is the influence of control system dynamics on maneuvering response characteristics, though the effects of turbulence are also considered.

For fighters having "fast" control system dynamics, the maneuvering response usually can be described adequately in terms of the following dominant parameters:

(1) The short-period frequency (ω_{sp}) and damping ratio (ζ_{sp})

(2) The pitch attitude numerator term $\left(1/T_{\theta_2} \right)$ and the response ratio (n/α)

(3) The maneuvering stick force gradient (F_s/n)

In recent years, however, complex flight control systems (FCS), employing various combinations of feedback and feedforward loops, have become increasingly common. Many such systems being designed and tested today introduce additional dynamic modes which have natural frequencies of the same order of magnitude as the short-period frequency. When this is the case, the airplane's flying qualities can be completely unacceptable even if the short-period mode itself is well behaved (as shown in Reference 6).

Because of the significance of control system dynamics, it is important that new criteria for the design of FCS be developed, to ensure satisfactory maneuvering characteristics. The criteria should have the following characteristics:

(1) They should describe, as directly as possible, those characteristics of the control system plus airframe which can cause the pilot difficulties in performance of the mission.

(2) They should be applicable to the higher-order maneuvering dynamics of airplanes having complex FCS, as well as to airplanes whose dynamics can be adequately described by the short-period characteristics.

(3) They should enable the designer to readily explore various combinations of feedback and feedforward loops, compensation networks, and filters in his attempts to achieve good flying qualities.

The purpose of the present investigation is to provide data on the effects of FCS dynamics and to develop a preliminary set of design criteria satisfying the above three conditions.

This report presents detailed descriptions of the design and conduct of the experiment, the results, analysis of the results, and proposed design criteria resulting from the analysis.

SECTION II

BACKGROUND

In planning the experiment, it was first deemed necessary to identify what types of control system dynamics are likely to occur in practice. This was accomplished by studying a number of current FCS designs. The next step in the planning was a detailed examination of the results of the USAF/CAL higher-order-system (HOS) investigation (Reference 6). After these studies, the configurations to be evaluated in the present experiment were selected to provide a broad base of data on the effects of FCS dynamics for the development of design criteria.

2.1 Study of Current FCS Designs

The study was begun with a literature search, during which many different types of FCS mechanizations were examined. The study showed that the most popular FCS concepts being designed and tested today appear to have certain similar effects on the airplane's overall maneuvering characteristics. One example of this type of FCS is an experimental adaptive system tested in an F-102 airplane (described in References 10 and 11). A simplified block diagram of this system is shown below.

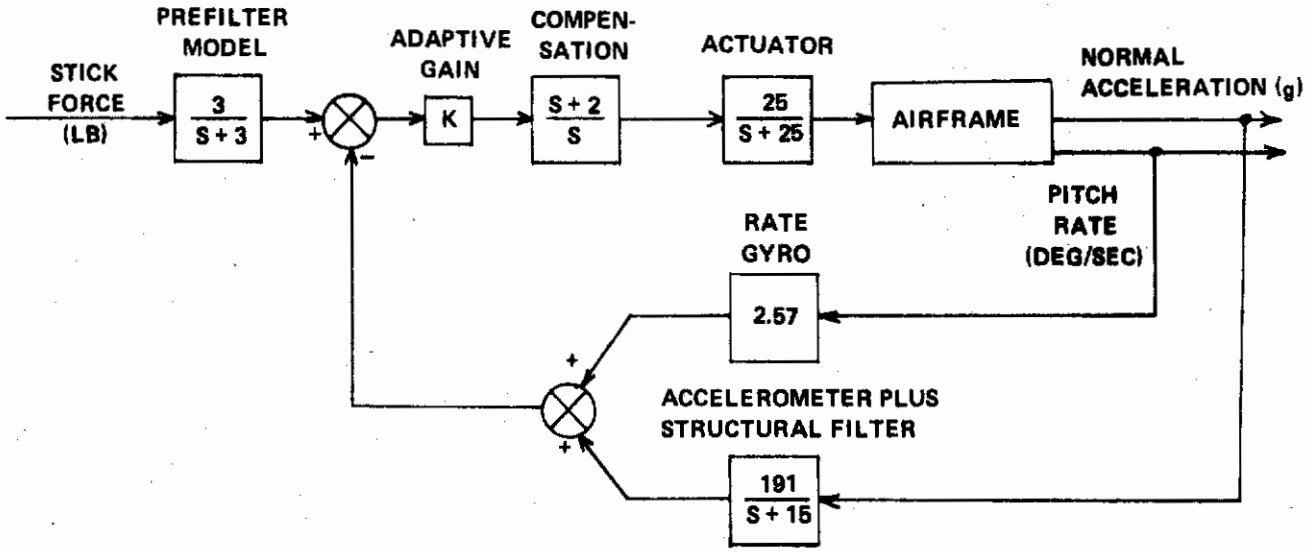

The closed-loop poles and zeros of the constant-speed pitch-rate-to-stick-force transfer function, for a high-$\bar{q}$ flight condition, are shown in the following s-plane plot.

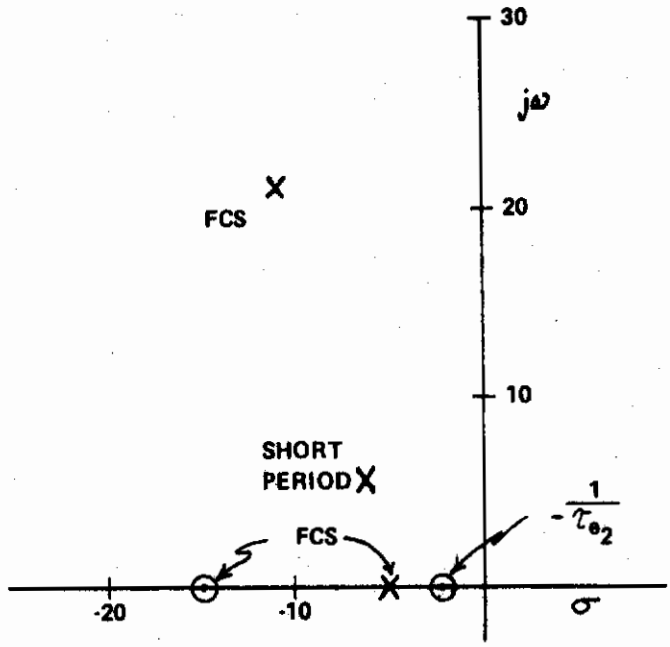

This plot is fairly typical of the FCS designs studied, in that the closed-loop dynamics are characterized by one or more complex poles having natural frequencies above that of the short period, plus a series of first-order poles and zeros having frequencies near or below that of the short period.

2.2 Discussion of the HOS Experiment

From the pilot's viewpoint, the maneuvering characteristics of the configurations evaluated in Reference 6 can be represented as follows:

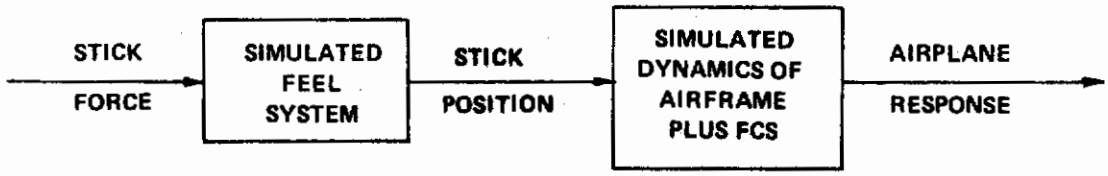

The maneuvering dynamics were varied during the HOS experiment by altering the simulated feel system, short period, and FCS.

The feel system dynamics were varied by changing the feel system natural frequency through a range of 6 to 31 rad/sec. The comments showed that the pilots noticed changes in the feel characteristics, per se. But the primary effect of feel system dynamics on the overall flying qualities appeared to be attributable to their influence on the airplane's response to

stick-force inputs.

Three sets of short-period dynamics were selected to show the effects of both short-period frequency and damping ratio. For each set of short-period dynamics, various types of FCS dynamics were investigated. Each set of FCS dynamics was arranged in a Butterworth configuration, so that each FCS pole had the same natural frequency. The dynamics were then changed by varying the natural frequency of the Butterworth configuration from 6 to 63 rad/sec, and varying its order from second to fifth.

In order to illustrate the combined effects of the feel system, short period, and FCS dynamics, a typical s- plane plot of the airplane's pitch-rate response to stick force inputs is shown in Figure 1.

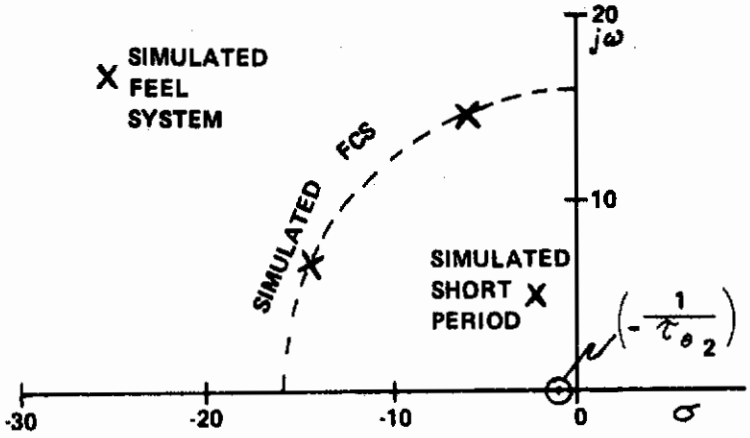

Figure 1. s-Plane Plot of a Typical FCS/Airframe Configuration from HOS Program

The time history of pitch-rate response to a step stick-force input for this example is shown in Figure 2.

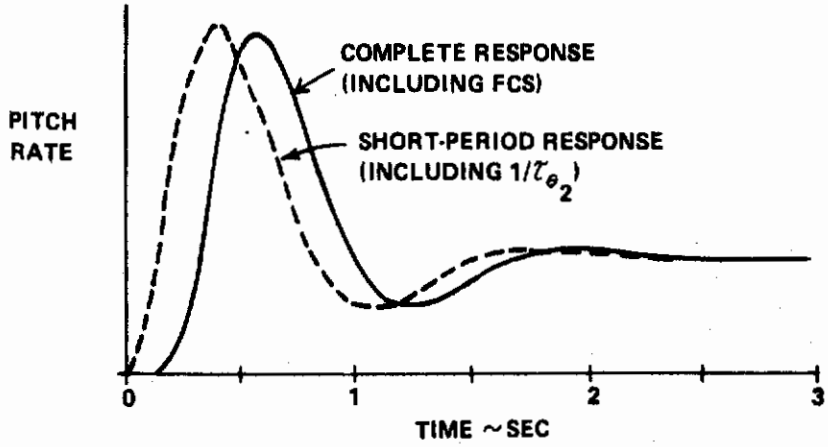

Figure 2. Pitch-Rate Response to a Step Stick-Force Input for HOS Configuration of Figure 1.

Notice that the airplane's maneuvering response to pilot inputs looks very much like the short-period response (including $1/\tau_{\theta_2}$) plus a pure time delay. This is typical of the configurations evaluated in the HOS experiment. Most of the pilot's difficulties in flying such configurations were related to the size of the time delay and the rapidity of the response following the delay. For the extreme cases, violent pilot-induced oscillations (PIO's) occurred whenever precise attitude tracking was attempted.

2.3 Purpose of the Present Experiment

From the above discussion, it is evident that the effects of FCS complex poles on flying qualities were studied in some detail during the HOS program, but that other forms of FCS dynamics often occur in practice. The primary objective of the present experiment, then, is to study the effects of first-order FCS poles and zeros. As will be shown in the following sections, the results of the two experiments combine to provide considerable insight into many of the problems which FCS dynamics are likely to cause.

SECTION III

DESIGN OF THE EXPERIMENT

On the basis of the considerations expressed in Section II, the specific configurations to be simulated were selected. The purpose of Section III is to describe the control system and airplane characteristics for each of these configurations. The reader is referred to Appendix IV for detailed discussion of airplane longitudinal transfer functions and equations of motion. In addition, Appendix V explains how the simulated configurations were mechanized in the variable stability T-33 airplane, as well as how the longitudinal characteristics discussed in this section were measured.

3.1 Basic Dynamic Configurations

To restrict the study of first-order FCS singularities to a reasonable size, the majority of the configurations were designed to evaluate the effects of a single FCS zero and a single FCS pole on eight basic short-period configurations. A second-order FCS pole was also included, but its natural frequency was fixed at 63 rad/sec for most of the experiment. Stick-force commands to the FCS were used because this is typical of the current FCS designs discussed in Section 2.1. The block diagram of Figure 3 represents how the pilot would view the pitch attitude response to stick-force inputs for these configurations.

The eight basic short-period configurations were selected to span fairly wide ranges, relative to the requirements of MIL-F-8785B (Reference 12). Five of the configurations were flown at an indicated airspeed of 250 knots (n/α = 18.5 g's/rad), and the other three at 350 knots (n/α = 50 g's/rad). Figure 4 compares the eight configurations to the specification requirements.

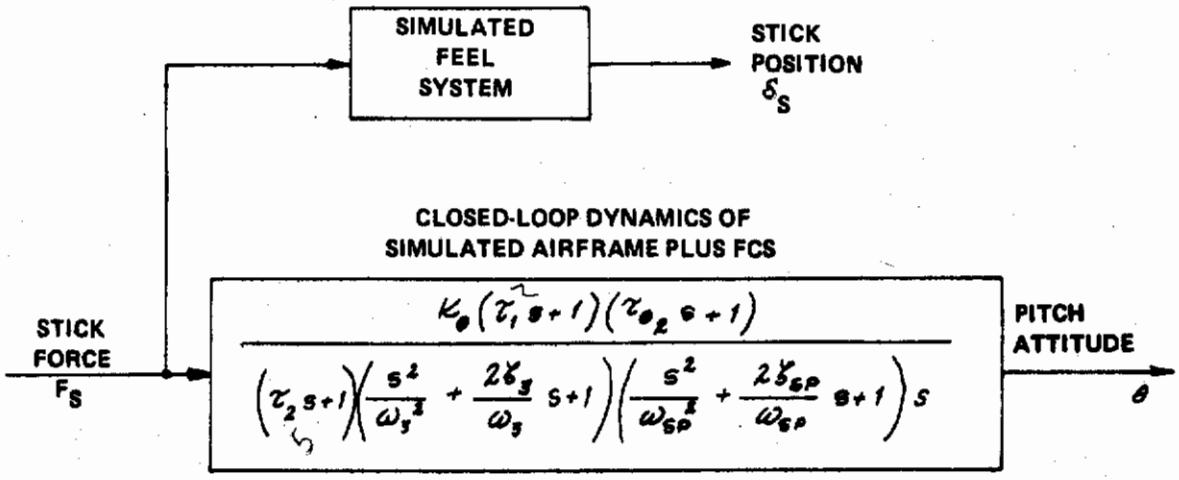

Figure 3. Block Diagram for Basic Configurations Simulated

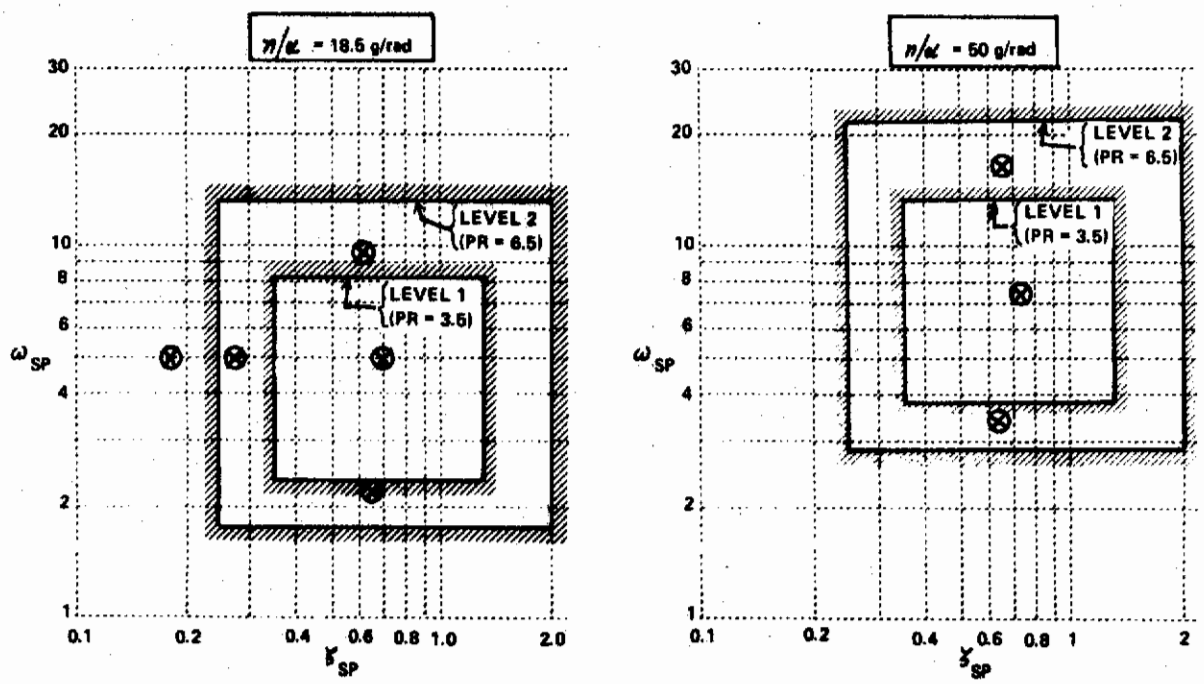

Figure 4. Comparison of Basic Short-Period Configurations with MIL-F-8785B Requirements

A complete summary of parameters related to flight conditions is as follows:

V_{ind} (knots)	n/α (g/rad)	Density Alt (ft)	V_T (ft/sec)	$\bar{q}$ (lb/ft^2)	$1/\tau_{\theta_2}$ (sec^{-1})
250	18.5	9500	480	205	1.25
350	50	9500	675	405	2.4

The original intent was to evaluate separately the effects of the first-order zero (τ_1) and the first-order lag (τ_2) on the eight short-period configurations. However, the use of τ_1 with τ_2 =0 caused noise problems in the T-33's variable stability system; therefore, τ_1 was always accompanied by a small value of τ_2 . The specific values of τ_1 and τ_2 simulated were chosen to span typical values for the FCS designs discussed in Section 2.1.

A total of 51 basic FCS/short-period configurations was evaluated, as shown in Figure 5. It should be noted that most of the 51 configurations had very high values of ω_3 (63 rad/sec), which corresponds to the frequency of the fastest FCS poles evaluated in the HOS program (Section 2.2). Four of the configurations, however, were selected to show the effects of reducing ω_3 to 16 rad/sec, which is equal to the frequency of the medium-frequency FCS poles evaluated in the HOS program (see Figure 1).

CONTROL SYSTEM CHARACTERISTICS			SHORT PERIOD CHARACTERISTICS							
			n/α = 18.5 g/RAD, V_{ind} = 250 KT, $1/\tau_{\theta_2}$ = 1.25 SEC^{-1}, V_T = 480 ft/s					n/α = 50 g/RAD, V_{ind} = 350 KT, $1/\tau_{\theta_2}$ = 2.4 SEC^{-1}, V_T = 675 ft/s		
			ω_{SP}/ζ_{SP}					ω_{SP}/ζ_{SP}		
$1/\tau_1$	$1/\tau_2$	ω_3	2.2/.69	4.9/.70	9.7/.63	5.0/.28	5.1/.18	3.4/.67	7.3/.73	16.5/.69
0.5	2	63	1A							
0.8	3.3							6A		
2	5		1B	2A						
3.3	8							6B	7A	
5	12			2C						
8	19								7B	
∞	∞	75	1D	2D	3A	4A	5A	6C	7C	8A
	19	63							7D	8B
	12			2E	3B	4B	5B			
	8							6D	7E	8C
	5		1E	2F	3C	4C	5C			
	3.3							6E	7F	8D
	2		1F	2H	3D	4D	5D		7G	
	0.8							6F	7H	8E
	0.5		1G	2J	3E	4E	5E			
2	5	16	1C	2B						
∞	5			2G						
	2			2I						

NOTE: (1) Numbers/Letters Indicate Configurations Simulated

(2) ζ_3 = .75 for ω_3 = 63, 16; ζ_3 = .67 for ω_3 = 75 ← actuator dynamics

Figure 5. Basic FCS/Short-Period Configurations Simulated in Present Experiment

Typical s-plane plots and time histories for the present program are shown in Figure 6. If these time histories are compared with the HOS time histories of Figure 2, certain fundamental differences will be seen. In the HOS program, the primary effect of the FCS dynamics was to introduce a time delay in the short-period response to pilot inputs. In the present program, however, the shape of the airplane's short-period response is completely altered by the FCS dynamics.

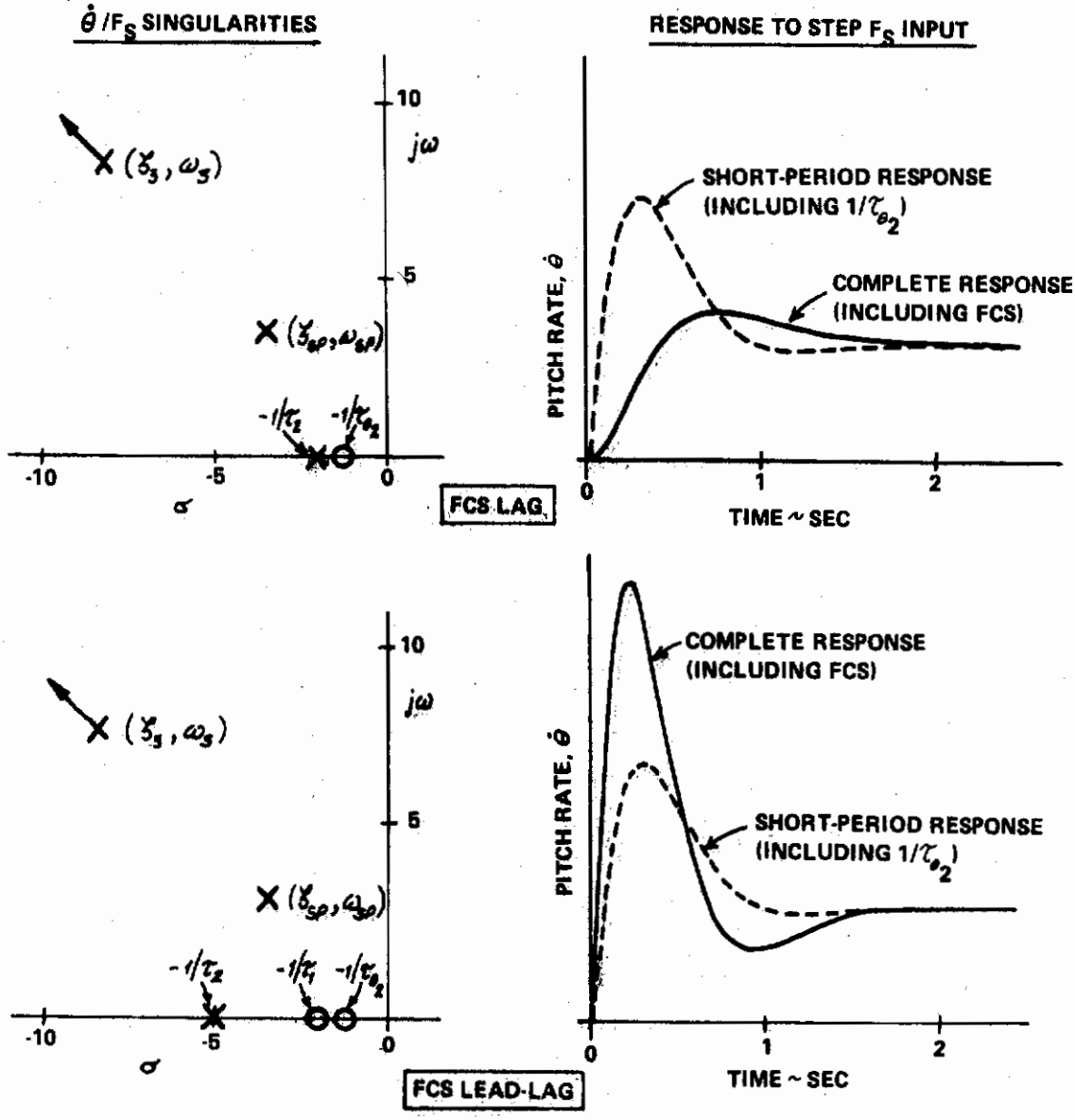

Figure 6. Typical s-Plane Plots and Time Histories for Present Experiment

3.2 Six Additional Configurations

As part of the present program, six additional short-period configurations were evaluated with a nominal set of control system dynamics. These configurations had rather extreme combinations of ζ_{sp} and ω_{sp}, and were selected to compare with the short period requirements of MIL-F-8785B in areas where the data supporting the requirements is rather sparse. The characteristics of the six configurations are compared to the specification requirements in Figure 7.

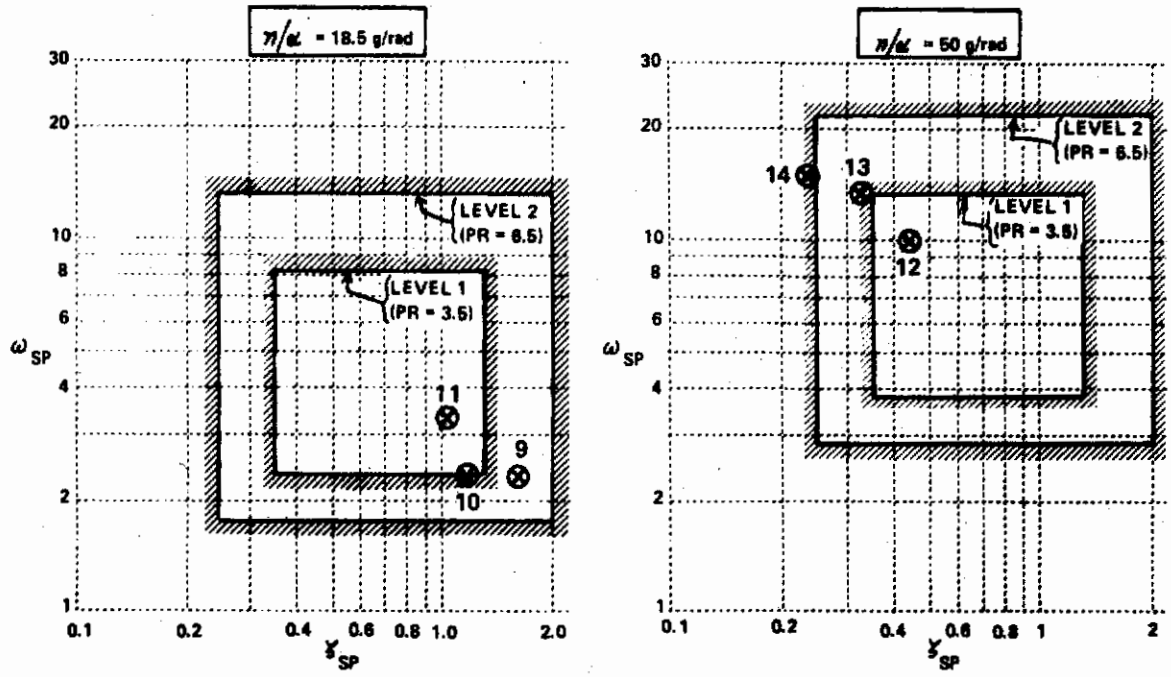

Figure 7. Comparison of Six Additional Short-Period Configurations with MIL-F-8785B Requirements

To make the control system characteristics of these configurations compatible with the control systems for which most of the specification data was obtained, stick position commands were used instead of the force commands used in the 51 basic configurations. A block diagram of the pitch-attitude dynamics for the six configurations is as follows:

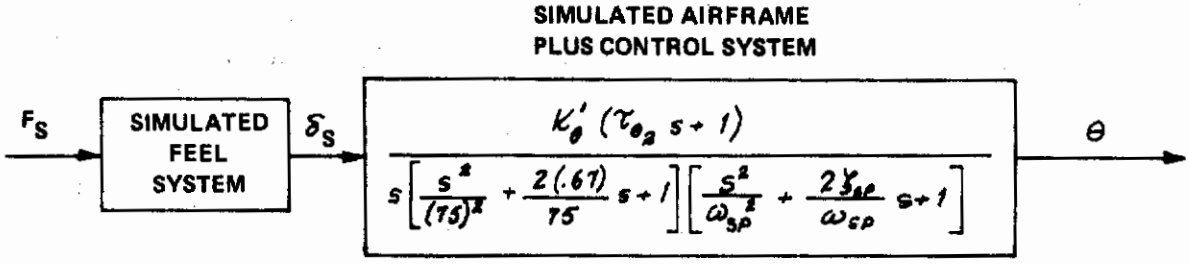

3.3 Feel System Characteristics

The feel system characteristics were held fixed for all 57 configurations evaluated in the program. The spring gradient was 22 lb/inch. The feel system dynamics can be approximated reasonably well with the following transfer function:

$$\frac{\delta_s \text{ stick position}}{F_s \text{ stick force}} = \frac{.046}{\left(\frac{s^2}{(31)^2} + \frac{2(1.0)}{31} s + 1\right)} \quad \text{(in. /lb)}$$

3.4 Elevator Gearing

The gearing ratio between the elevator and stick force was selected by the pilot at the beginning of each evaluation, as discussed in more detail in Section 4.1. The purpose of this process was to avoid having pilot opinion degrade because of the stick forces being either too high or too low. Ideally, each dynamic configuration should have been evaluated with several values of the elevator gearing ratio, but this would have required a much larger flight program.

3.5 Phugoid Characteristics

Since phugoid dynamics do not normally have a strong influence on flying qualities for the "combat" phase of a fighter's mission, no attempt was made to control the phugoid dynamics. In-flight phugoid measurements were made for each short-period configuration evaluated, however, and it was found that the phugoid characteristics did not vary significantly as the short-period characteristics changed. A summary of the measured phugoid

characteristics is shown below.

V_{ind} ~ Kt	n/α ~ g/rad	T_p ~ sec	ζ_p
250	18.5	65-80	0.07 to 0.12
350	50	90-110	0.15

Since the phugoid periods are long, and since none of the pilot comments appeared to be related to phugoid characteristics, all the analysis contained in this report will use constant-speed longitudinal transfer functions.

3.6 Lateral-Directional Characteristics

A "good" set of lateral-directional characteristics was selected for each flight condition. These characteristics were held fixed throughout the program, except for the variations due to the changes in moments of inertia as fuel was used. The characteristics were adjusted during the pre-evaluation calibration flights until the pilots judged them to be good enough that they would not detract from the longitudinal evaluation; no attempt was made to "optimize" them.

Approximate lateral-directional characteristics, obtained from in-flight measurements, are shown below.

V_{ind} = 250 kt n/α = 18.5 g/rad	V_{ind} = 350 kt n/α = 50 g/rad
$\omega_d \approx \omega_\phi \approx$ 2.2 rad/sec	$\omega_d \approx \omega_\phi \approx$ 4.5 rad/sec
$\zeta_d \approx \zeta_\phi \approx$ 0.20	$\zeta_d \approx \zeta_\phi \approx$ 0.30
$\lvert\phi/\beta\rvert_d \approx$ 0.5	$\lvert\phi/\beta\rvert_d \approx$ 0.5
$\tau_R \approx$ 0.3 sec	$\tau_R \approx$ 0.2 sec
$\tau_s \approx$ 75 sec	$\tau_s \approx$ 75 sec

The following lateral-directional feel characteristics were held constant for all the configurations evaluated:

$$\frac{\delta_{AS}}{F_{AS}} = \frac{0.25}{\left[\frac{s^2}{(25)^2} + \frac{2(0.7)}{25}s + 1\right]} \quad \text{(in. /lb)}$$

$$\frac{\delta_{RP}}{F_{RP}} = \frac{.0067}{\left[\frac{s^2}{(25)^2} + \frac{2(0.7)}{25}s + 1\right]} \quad \text{(in. /lb)}$$

SECTION IV

CONDUCT OF THE EXPERIMENT

The control system and airplane dynamics discussed in Section III were mechanized in the USAF variable stability T-33, operated by CAL (see Figure 8). Details of this mechanization are contained in Appendix V, and a complete functional description of the variable stability system can be found in Reference 14. A total of 131 flight evaluations was carried out in this experiment, requiring 49 flights of approximately 1 1/2 hours each.

In this aircraft the evaluation pilot occupied the front cockpit, which is shown in Figure 9. The system operator in the rear cockpit, who also served as a safety pilot, could vary the handling characteristics about all three axes by changing the settings of the response-feedback gain controls on his right-hand console. In addition, through the use of switches in the rear cockpit, the safety pilot could select position or force commands for the front-seat stick, and had the capability of introducing the appropriate control-system dynamics from filter cards carried in the nose of the T-33. The evaluation pilot could not feel the control surface motions due to the variable-stability-system signals and had no prior knowledge of the configuration characteristics.

The following sections describe in detail the conduct of each flight, the pilot briefings on the overall airplane mission, the evaluation tasks performed, and the evaluation procedure.

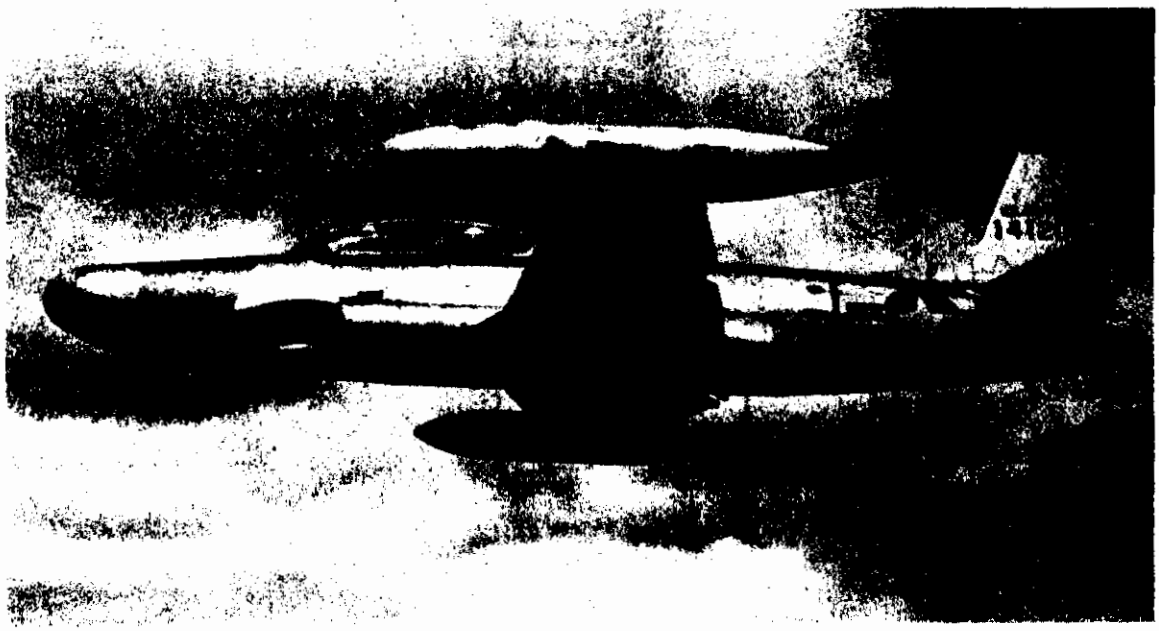

Figure 8. USAF/CAL Variable Stability T-33 Airplane

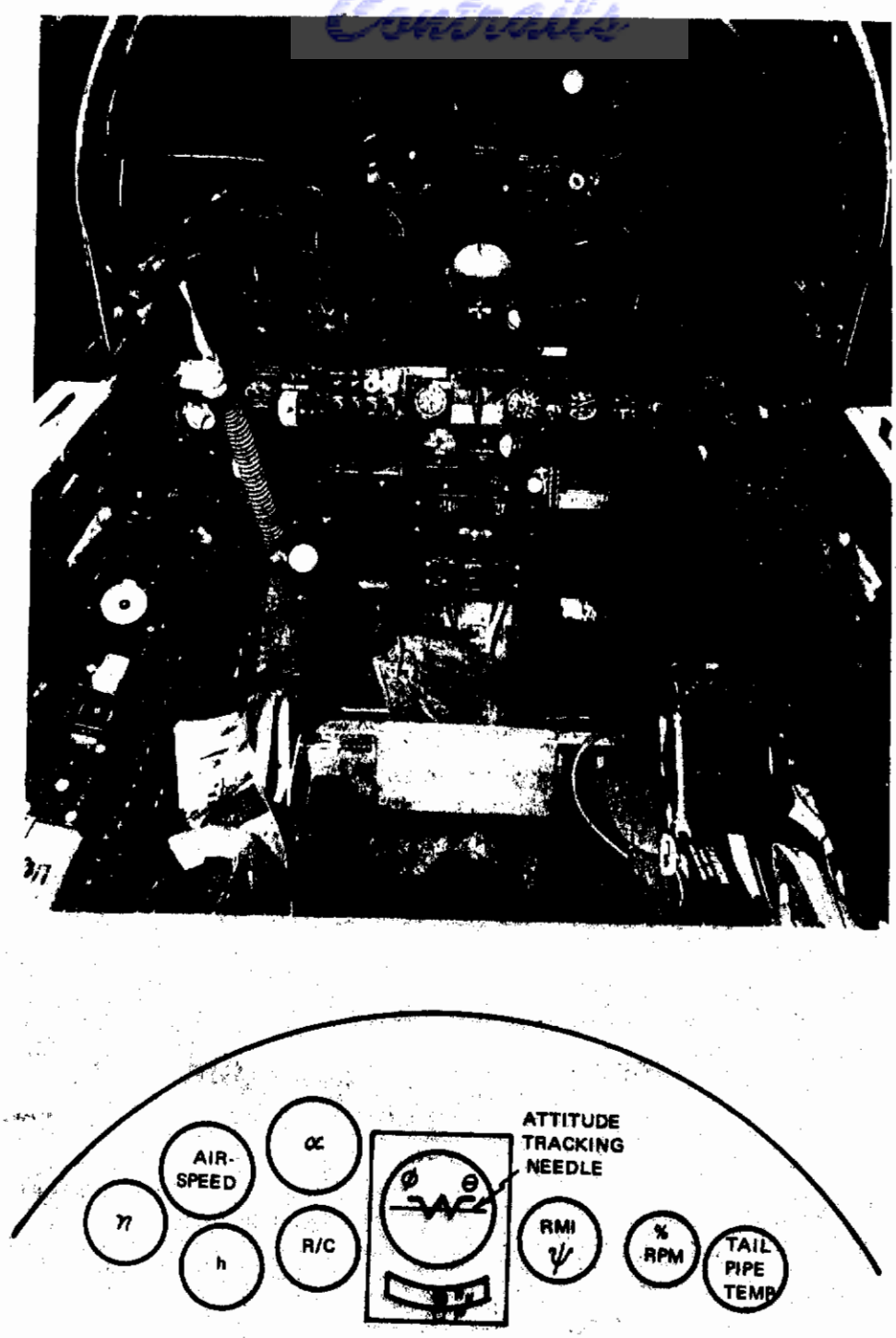

Figure 9. Evaluation Pilot's Cockpit in Variable Stability T-33

4.1 Conduct of Each Flight

As previously mentioned, the evaluations were performed at two different values of n/α (approximately 18 and 50) which were achieved by flying the T-33 variable-stability airplane at indicated airspeeds of 250 and 350 knots at 9500 feet density altitude. These are nominal values and were subject to variation because of local weather and turbulence and because of the maneuvers required in performing the tasks. For the calibration records taken during the program, the nominal indicated airspeeds were always used, but the variation in altitude was as much as ± 2000 feet. During the performance of the required fighter maneuvers the indicated airspeed variations were approximately 250 (+15, -20) knots and 350 (+20, -40) knots, while the altitude variations were ± 2000 feet.

The configurations were evaluated in a generally random order with three configurations being evaluated per flight. The 250 knot configurations were always flown first because of structural considerations related to the heavy fuel loadings. Each evaluation took approximately 25 minutes and consisted of four phases:

(1) Calibration - At the beginning of each evaluation, oscillograph records were taken to allow determination of the n/α being flown, the F_s/n selected, and the short-period characteristics (ω_{sp} and ζ_{sp}) being simulated. The n/α value was obtained by flying at the appropriate trim condition and inserting a series of separate automatic elevator steps. F_s/n was found from the automatic step records and the elevator gearing selected. The values of ω_{sp} and ζ_{sp} were determined from records of at least two manual elevator doublets made by the evaluation pilot from trimmed conditions, with no simulated control system dynamics present. During the first third of the experiment, these manual-doublet calibration records were taken after each evaluation, as well. The results indicated that the effects of changes in fuel remaining during an evaluation were not significant; and thereafter, calibration records were taken only once during each evaluation. The details of the data reduction techniques used to extract the necessary information may be found in Appendix V.

(2) Gearing Selection - During the first half of the experiment the evaluation pilot was free to select any elevator-to-stick-force gearing of his choice. The gearing selection chosen, in combination with the calibration measurements, directly determined the F_s/n for the evaluation. In order to select the optimum gearing, the evaluation pilot really had to conduct a miniature evaluation since both the steady forces, represented by F_s/n , and the initial forces, which affect the precision tracking capability, are important and sometimes conflicting factors. Although the values of F_s/n selected in the first half of the experiment were quite consistent (generally

between 4 1/2 - 7 lb/g), some excursions outside these values did occur. Values as high as 14 lb/g were selected in two instances and as low as 3 lb/g in several others. Since it is a difficult task for the evaluation pilot to be totally consistent in selecting the gearing when allowed only a "short look", limits corresponding to a range of F_s/n from roughly 4 1/2 to 7 lb/g were placed on the elevator gearing available to the pilot during the second half of the experiment. During the selection process, the pilot was allowed to explore the complete range of gearings available, but if either limit was violated in the process, the final gearing used was the limiting value. In this way the evaluation pilot could comment fairly on any problems associated with the gearing selection used.

(3) Evaluation - Performance of the required tasks.

(4) Pilot Comments and Ratings.

These last two phases of the evaluation are discussed in detail in Section 4.2.

4.2 Evaluation Procedure

Two evaluation pilots participated in this flying qualities investigation. Their backgrounds are summarized below:

Pilot M - CAL Research Pilot, experienced as an evaluation pilot in flying qualities investigations. His flight experience of 2300 hours includes 1000 hours in fighter-type airplanes, of which 500 hours were acquired in an operational air-superiority role.

Pilot W - CAL Research Pilot with extensive experience as an evaluation pilot in flying qualities investigations. His flight experience of 2700 hours includes over 1000 hours in high-performance fighter airplanes.

In the course of this experiment, Pilot M evaluated 54 configurations (each a different combination of control-system and short-period dynamics) for a total of 80 evaluations (including repeats). Pilot W evaluated 39 of the configurations for a total of 51 evaluations (including repeats).

Before any meaningful flying qualities evaluation can be performed, a clear understanding of the airplane mission requirements is essential. The basic mission of the airplane to be evaluated was that of an air-superiority fighter having a limit load factor of 7. The evaluation maneuvers were designed to be representative of those up-and-away tasks associated with air-to-air combat, including weapons delivery. In addition, some consideration was to be given to those air-to-ground tasks where high-load-factor maneuvers are required. The airplane was expected to have

instrument flying capability, although this portion of its mission was considered to be of secondary importance. The mission as described above was discussed at length with the evaluation pilots, individually and collectively, to insure that each pilot was evaluating the configurations for the same mission requirements.

Although the mission involves many tasks, an evaluation of the vehicle flying qualities can be accomplished by having the evaluation pilots perform a series of maneuvers representative of those tasks anticipated in the mission. A copy of the pilot flight card outlining the piloting tasks used to evaluate all the configurations is presented below.

PILOT EVALUATION TASKS

VFR (Bulk of Evaluation)

1. Trimmability - ability to stabilize and trim.
2. Pitch attitude tracking - ability to rapidly acquire and track distant air or ground targets.
3. Symmetric pullups and pushovers - ability to rapidly acquire and maintain a given load factor (n ranging from 0.5 g to 4 g).
4. Turning maneuvers
   a) roll into 60 deg bank and maintain altitude - reverse
   b) rapid turn reversals (90 degree bank, n = 4 g).
5. Ground attack (pullup, wingover, track, pullup).
6. Disturbance inputs - briefly check above in presence of disturbances.

IFR (Brief look)

1. Trimmability.
2. Discrete-error tracking task (record 1 minute).
3. Random-error tracking task (record 1 minute).
4. Symmetric pullups and pushovers - ability to rapidly acquire and maintain a given load factor (n ranging from 0.5 g to 2.0 g).
5. Level turns - roll into 60 deg bank and maintain altitude-reverse.
6. Briefly check above in presence of disturbance inputs.

The evaluation pilot performed these tasks in order, making comments as he desired on a wire recorder. The details of the discrete-error and random-error tracking tasks are discussed in Section 4.3, while Section 4.4 contains a discussion of the random disturbance inputs.

At the end of each evaluation, the pilot was asked to make recorded comments on the specific items listed on the Pilot Comment Card, which is reproduced below.

PILOT COMMENT CARD

Specific comments

1. Ability to trim.
2. Stick forces O.K.?
   a) any second thoughts on gearing selection?
3. Stick motions O.K.?
4. Predictability of airplane response to pilot inputs (initial vs final response).
5. Pitch attitude control and tracking capability.
6. Normal acceleration control.
7. Longitudinal control in steep turns.
8. Effects of random disturbance inputs.
9. Any IFR problems which didn't show up VFR?
10. Lateral-directional control satisfactory? Did it detract from longitudinal evaluation?

Summary comments

1. Good features.
2. Objectionable features.
3. Special piloting techniques.
4. Pilot rating and PIO rating.
   - record decision-making process on wire
   - identify deficiency(ies) which most influenced each rating.

As shown, the pilot was then asked to make summary comments and to assign an overall pilot rating and a PIO (pilot-induced-oscillation) rating for the configuration.

The overall pilot rating was assigned by the pilot to the configuration in accordance with the ten-point Pilot Rating Scale established in Reference 9 and shown in Figure 10. The pilot rating represents a numerical summary

of the airplane's suitability for performing the particular mission tasks under consideration.

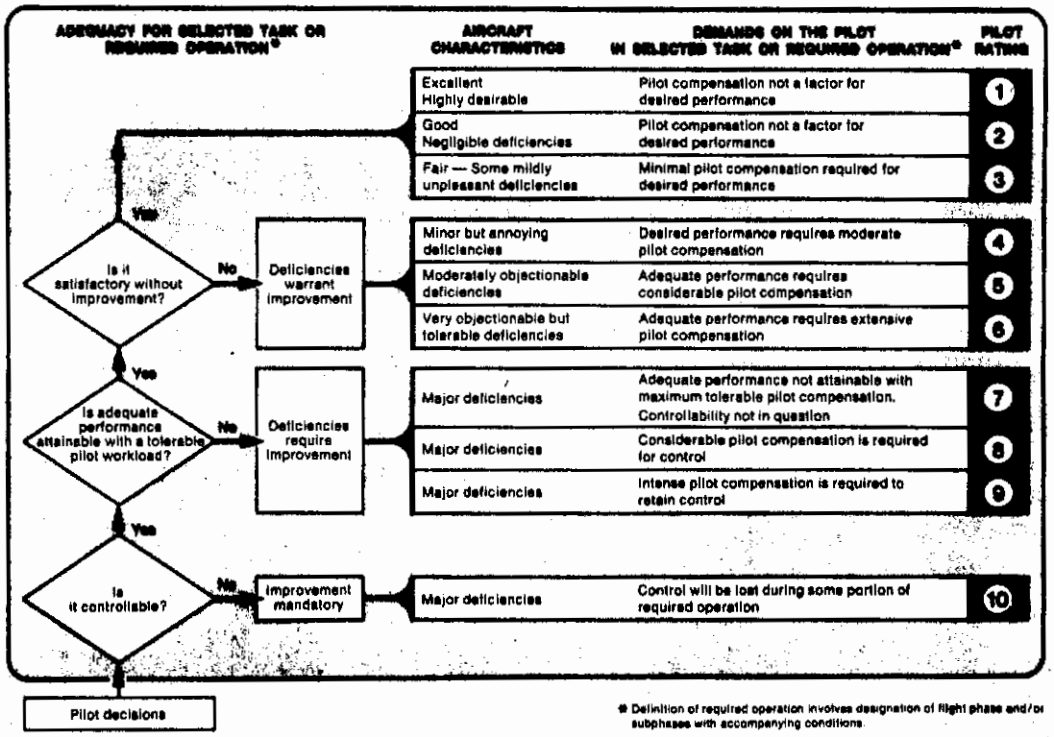

Figure 10. Pilot Rating Scale

The PIO tendency rating assigned by the pilot was based on the six-point rating scale established in Reference 6 and shown in Figure 11. The PIO rating acts as a convenient shorthand to discuss the tendency of the airplane to oscillate during performance of the task maneuvers. The scale spans the complete range from minor "undesirable motions" to "divergent oscillations". Because of this, the PIO rating data from this experiment show strong correlation with the pilot rating data. Therefore, little use was made of the PIO ratings in the analysis.

DESCRIPTION	NUMERICAL RATING
NO TENDENCY FOR PILOT TO INDUCE UNDESIRABLE MOTIONS	1
UNDESIRABLE MOTIONS TEND TO OCCUR WHEN PILOT INITIATES ABRUPT MANEUVERS OR ATTEMPTS TIGHT CONTROL. THESE MOTIONS CAN BE PREVENTED OR ELIMINATED BY PILOT TECHNIQUE.	2
UNDESIRABLE MOTIONS EASILY INDUCED WHEN PILOT INITIATES ABRUPT MANEUVERS OR ATTEMPTS TIGHT CONTROL. THESE MOTIONS CAN BE PREVENTED OR ELIMINATED BUT ONLY AT SACRIFICE TO TASK PERFORMANCE OR THROUGH CONSIDERABLE PILOT ATTENTION AND EFFORT.	3
OSCILLATIONS TEND TO DEVELOP WHEN PILOT INITIATES ABRUPT MANEUVERS OR ATTEMPTS TIGHT CONTROL. PILOT MUST REDUCE GAIN OR ABANDON TASK TO RECOVER.	4
DIVERGENT OSCILLATIONS TEND TO DEVELOP WHEN PILOT INITIATES ABRUPT MANEUVERS OR ATTEMPTS TIGHT CONTROL PILOT MUST OPEN LOOP BY RELEASING OR FREEZING THE STICK.	5
DISTURBANCE OR NORMAL PILOT CONTROL MAY CAUSE DIVERGENT OSCILLATION. PILOT MUST OPEN CONTROL LOOP BY RELEASING OR FREEZING THE STICK.	6

Figure 11. PIO Tendency Rating Scale

4.3 Details of IFR Tracking Tasks

Two pitch attitude tracking tasks were included in the IFR tasks to aid the pilot in his evaluation. Although these tasks do not have direct analogy in the real world of the fighter airplane, they did provide the pilot with useful insight into the capabilities of the configuration to perform precise, rapid tracking maneuvers.

The discrete-error pitch-attitude tracking task was mechanized by displaying the error between the actual pitch attitude and a programmed pitch attitude command signal on a horizontal needle in the Lear remote attitude indicator. A complete cycle of the pitch attitude command signal is shown in Figure 12, and the attitude indicator is shown in Figure 9. In the brief time allotted for the tracking tasks during each evaluation, the pilots never learned the pattern of the command signal.

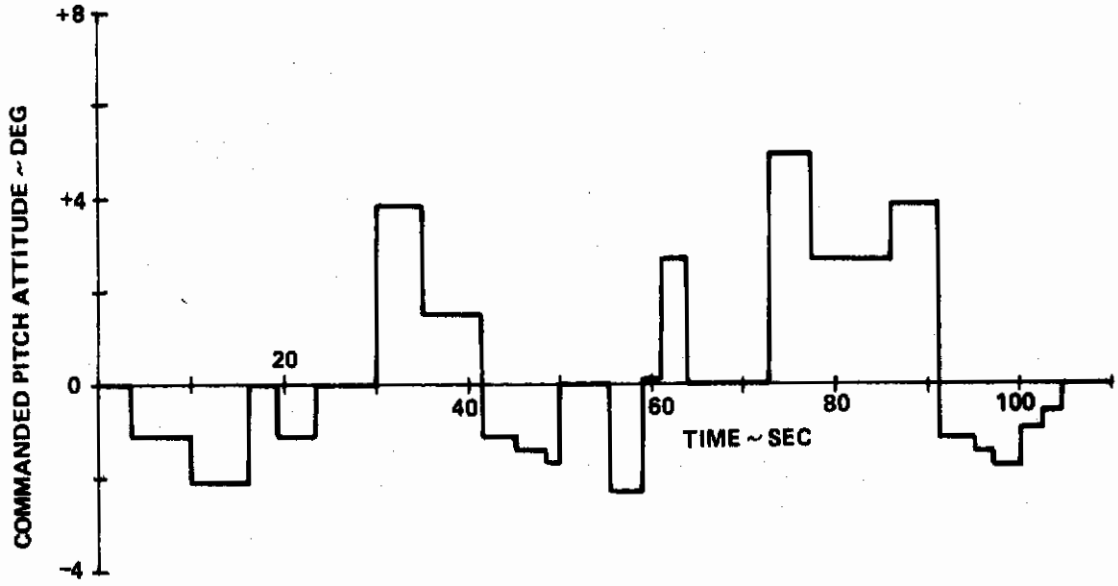

Figure 12. Discrete-Error Pitch-Attitude Command Signal

A commanded pitch attitude of ± 5 degrees represented full scale (± 1 inch) deflection of the horizontal tracking needle. The evaluation pilot's task was to keep the error to a minimum, which required rapid and precise changes in pitch attitude. In the course of the evaluation, the pilot usually experimented for a brief period to investigate the effects of different control techniques on tracking performance. After a technique consistent with the fighter mission was established, a one minute oscillograph record of the tracking task performance was taken.

The random-error pitch attitude tracking task was mechanized by displaying the error between the actual pitch attitude and that commanded by a filtered random noise signal,a sample of which is shown in Figure 13.

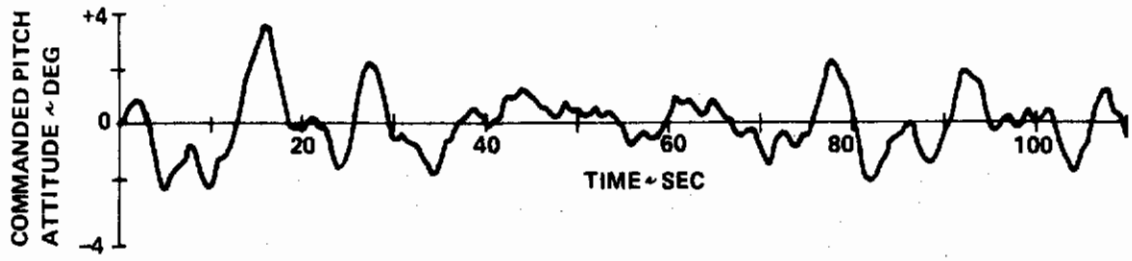

Figure 13. Random-Error Pitch-Attitude Command Signal

This task required the pilot to continuously maneuver the airplane to keep the error to a minimum. Again, after a short period of experimentation, a one-minute oscillograph record of the tracking task performance was taken.

4.4 Random Noise Disturbances

The response to atmospheric turbulence is an important factor in evaluating flying qualities of an airplane. Unfortunately, the T-33 does not possess independent control of the lift vector and therefore does not have the capability to simulate the lift response to gust-induced angle-of-attack changes. Therefore, using inputs to the elevator alone, it is not possible to provide a completely accurate turbulence simulation in both the pitching and heaving degrees of freedom. In order to provide the pilot with some insight into the airplane's flying qualities in the presence of random external disturbances, however, filtered random noise inputs were fed briefly to the elevator, ailerons and rudder of the T-33 during the required tasks. The magnitude of the random inputs to the ailerons and rudder remained constant, but at a different level for each of the two flight conditions evaluated. The level of the disturbances was selected during the calibration phase of the flight program to be consistent with the up-and-away fighter mission under consideration.

As previously mentioned, it is impossible to satisfy the conflicting requirements of the airplane θ and n responses to vertical gusts as ω_{sp} varies, using the elevator alone. To keep the θ gust responses realistic demands that the random inputs to the elevator be scaled as a function of ω^2_{sp}, which yields ridiculously large n responses for the

high ω_{sp} configurations. Alternatively, to keep the n gust responses realistic demands a constant level of random inputs that yields θ responses which are too small at high ω_{sp}. A suitable compromise was used which varied the random input signals to the elevator as a function of ω_{sp} for each flight condition. The evaluation pilots were carefully instructed that the airplane's response to these random disturbances represents only an approximation to real atmospheric turbulence.

The primary effect of the random disturbance inputs on the evaluation was to give the pilot a feeling for how well he could get the nose back on a target after an external disturbance had thrown it off.

4.5 Evaluation Limitations

The principal problem confronting the evaluation pilots during the evaluations was how to extrapolate to a 7 g fighter when the variable-stability T-33 encountered buffet onset for the 250 knot flight condition at 2 1/2 to 3 g (depending on the weight) and at 4 1/2 g for the 350 knot flight condition. The limitation at 250 knots was imposed by the buffet boundary of the T-33 itself and constituted a dual problem for the evaluation pilot. Could he realistically extrapolate to the higher g levels consistent with this mission, and could he fly the airplane as aggressively as he desired for the fighter mission? The pilots felt that they could make the necessary extrapolation, but with some reservations. There is evidence from the pilot comments during the program that, in general, the pilots did not fly the 250 knot configurations as aggressively as the 350 knot configurations. The pilots consistently commented that the 350 knot cases were more "fighter-like". The 4 1/2 g's available in the 350 knot case is representative of typical fighter maneuvers, where only occasional excursions to the limit load factor are made. The task maneuvers at 350 knots could therefore be performed without extra attention being required to keep clear of the buffet boundary.

During the evaluations, the pilots were forced to examine the airplane maneuvering characteristics and tracking capabilities using distant, stationary air and ground targets. The pilots did not have the opportunity of tracking moving targets under high g loads.

Structural oscillations, particularly at the heavy fuel weights, occasionally presented a problem during abrupt maneuvers; but the pilots did not feel that these oscillations interfered with the evaluation, except in one instance. This was the high- ω_{sp}, low-speed case with negligible control system dynamics (Configuration 3A).

As previously mentioned, the two IFR tracking tasks have no direct analogy in the fighter mission. Because of this, the VFR tracking tasks were weighted much more heavily in the evaluations than the IFR tasks.

Another evaluation limitation was the lack of a completely realistic simulation of atmospheric turbulence. The random disturbances (Section 4.4) provided some useful information to the pilot concerning the effects of turbulence, but their effects were not weighted very heavily in determining the pilot ratings.

Although there is no accurate way to estimate the effects of any of these limitations, it is worthwhile to be aware of them. In spite of the limitations, the evaluation pilots felt that good evaluations could be given of the configurations, in the context of the fighter mission considered in this program.

SECTION V

EXPERIMENTAL RESULTS

The results of the experiment described in the preceding section are in the form of pilot opinion ratings and pilot comments. A complete summary of the pilot ratings (PR), PIO ratings (PIOR), and the selected F_s/n values for each configuration evaluated is presented in Table I. The summarized pilot comments for each configuration are contained in Appendix I, which also shows Bode plots and time histories for each combination of short-period and control-system dynamics evaluated. This section will briefly discuss the pilot comments and then summarize the efforts made to correlate the pilot ratings with various open-loop criteria. As previously mentioned, and as dramatically illustrated in the time histories of Appendix I, the characteristics of the configurations evaluated vary over very wide ranges. The difficulty of finding simple open-loop parameters with which to correlate all the results of this experiment led to consideration of pilot-in-the-loop analysis, which is fully discussed in Sections VI and VII.

5.1 Pilot Comments

In any flying qualities program, the pilot comment data are at least as important as the pilot rating data. In the comments, the pilot describes the nature of his problems and, of equal interest, how he flies the airplane to achieve the desired task performance. With support from the pilot comments, a number of general observations about the conduct of the overall experiment can be made.

(1) For the fighter tasks evaluated in this program, the primary concern of the pilot was his ability to precisely control pitch attitude during tracking maneuvers. This observation is substantiated by the fact that the comments for each configuration (see Appendix I) under the headings "Predictability of Response" and "Pitch Attitude Control/Tracking Capability" typically summarize the primary reasons for a given pilot rating. It is of interest to note that the pilots often commented during the program that the VFR precision tracking tasks were more demanding than the IFR tracking tasks and were given more weight in the pilot rating.

(2) The control of normal acceleration, although of concern to the pilot, did not appear to be as important as attitude control. The specific pilot comments about normal acceleration control usually indicated the same type of problems as pitch attitude control, but the problems were usually less critical.

(3) In evaluating a given configuration, the pilots were not aware of the individual elements in the combination of control-system and short-period dynamics being simulated. The pilots evaluated the "total package". This fact may appear obvious but is worth remembering when considering the problem of correlating the pilot rating data with specific characteristics of the airframe or control system.

(4) The selection of the elevator-to-stick-force gearing, which determined the F_s/n used, was sometimes a problem to the pilot. The often conflicting demands of satisfactory initial forces for good precision tracking capability, and satisfactory steady forces for good fighter maneuverability, sometimes required a compromise in the gearing selection. Consider first those configurations with initial response characteristics described as sluggish or slow, either because of low ω_{sp} or control system lags. In these cases, the pilot used large initial inputs to "overdrive the airplane", so that the desired response would be achieved. This called for a high elevator-to-stick gearing to keep the initial forces reasonable. The final response of these configurations, however, was not predictable because the airplane tended to "dig in". This characteristic demanded low elevator gearings to provide adequate g protection during the gross fighter maneuvers; and therefore, a compromise gearing selection was required.

On the other hand, those configurations with initial response characteristics described as "abrupt, too sensitive" required the opposite gearing compromise. In these cases, the initial forces appeared too light to the pilot and called for a low elevator gearing to prevent inadvertent inputs. Such a gearing selection would produce steady forces which were too high for the gross fighter maneuvers, and would again lead to a compromise gearing selection.

The evaluation pilots in this program, when faced with a compromise in the elevator gearing selection, were willing to vary F_s/n over only a relatively small range. The pilots would not compromise their ability to pull large load factors, even if the resulting F_s/n was not compatible with the initial forces required for precision tracking. The values of F_s/n selected by the pilots in this program range approximately from 3 to 8 lb/g, although a few excursions outside this range occurred early in the program (see Table I). In the second half of the program, F_s/n limits of 4 1/2 to 7 lb/g were imposed on the gearing selection to conform with the average range of values selected in the first half (Section 4.1). In only a few cases was the pilot restricted by these limits in his gearing selection. There is no evidence, however, that the F_s/n limits influenced the pilot ratings in these cases.

The pilot comments for the base short period configurations (those with negligible control system dynamics) show the same trends as in previous longitudinal programs (e.g., References 4 and 7). The pilot

comments on the effects of adding significant control system dynamics to these configurations are extremely difficult to summarize in a few words. For this reason, the detailed discussion of the pilot comments is included in Section VII, where extensive use of the pilot comments is made in support of the pilot-in-the-loop analysis.

5.2 Correlation of Pilot Ratings With MIL-F-8785B

The pilot rating data for the 8 basic short-period configurations (those with negligible control system dynamics) are compared in Figure 14 with the requirements of MIL-F-8785B, Section 3.2.2 (Reference 12). Shown on the same plots are the pilot rating data for the 6 additional short-period configurations evaluated.

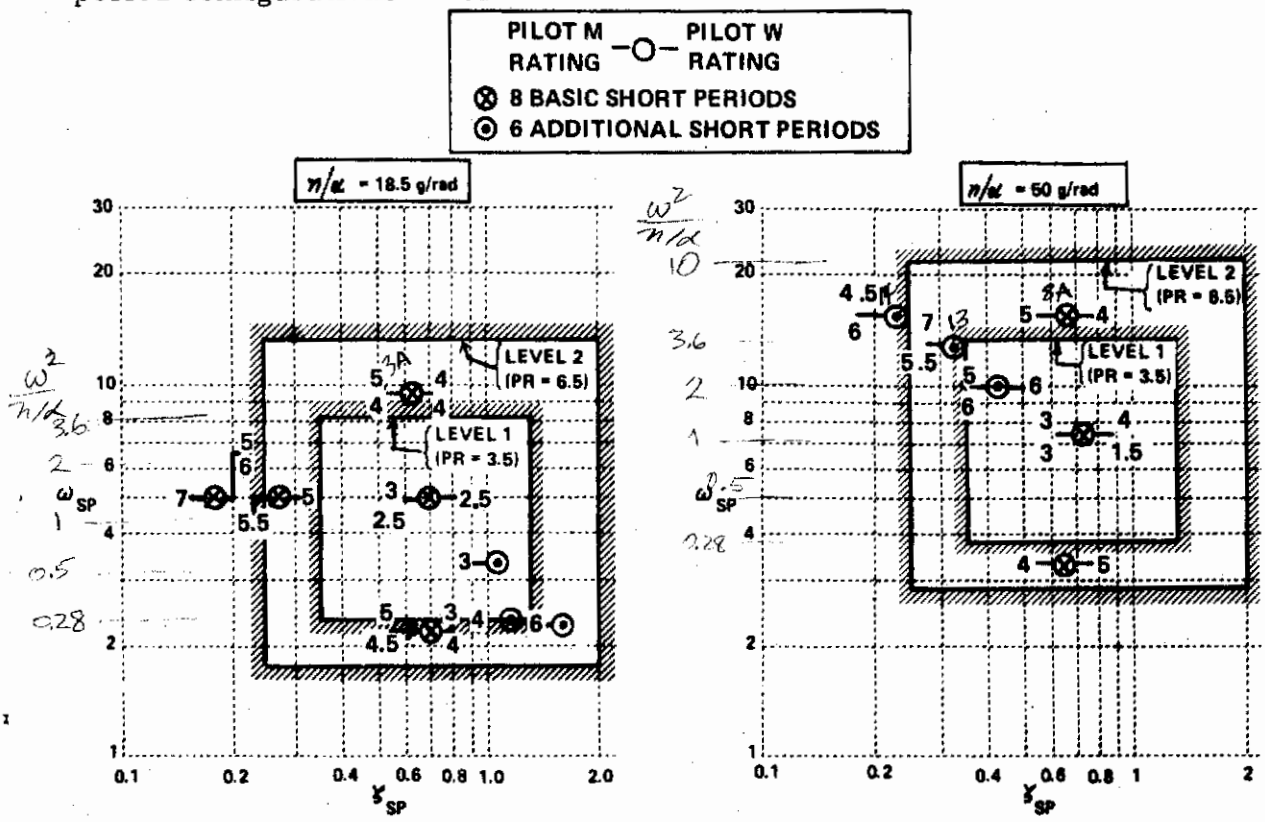

Figure 14. Correlation of Pilot Ratings with MIL-F-8785B

The correlation of the 8 basic short-period configurations with the specification boundaries is good. For the 3 additional short-period configurations at n/α =18.5, the agreement with the specification is also good; however, the 3 high-frequency, low-damping-ratio configurations at n/α = 50 show poor agreement. In fact, there seems to be very little change in PR with increasing ω_{sp} and decreasing ζ_{sp} for these last 3 cases. The lack of correlation with the boundaries is not, in itself, surprising since the specification boundaries are not well substantiated in this region. The lack of variation in PR with the changes in ω_{sp} and ζ_{sp} is, at this point, difficult to understand. More will be said in Section VII concerning these configurations.

The good correlation of the 8 basic short-period configurations with the specification boundaries provides a solid base from which to view the remainder of the pilot rating data for these same configurations evaluated with significant control-system dynamics.

Section 3.5.3 of MIL-F-8785B places limits on the control-system dynamics by restricting the phase lag, at the short-period frequency, between stick-force input and the control-surface response. The substantiating data for this requirement were drawn largely from the HOS program, Reference 6. In order to see the rating degradation due to control-system dynamics alone, the rating data of Pilot M for the configurations with good values of ω_{sp} and ζ_{sp} evaluated in this experiment are shown in Figure 15. The control system phase angles were computed from the transfer function of simulated δ_e to F_s (see Appendix V, Figure V-1). Also shown on Figure 15 is the faired line from the MIL-F-8785B background document (Reference 13) used in writing the requirement. The results of this experiment do not correlate with the specification requirement.

As observed in the previous section, the pilot evaluates the total response of the airplane to his inputs and is not concerned with, or aware of, the characteristics of the individual elements which combine to produce that response. It is evident from the time histories in Appendix I that control-system dynamics with poles or zeros close to the airplane's ω_{sp} can modify the response to the extent that characterizing the response by ω_{sp} and ζ_{sp} is difficult and loses meaning. What is needed are requirements which are not dependent on identifying certain modes of motion, such as the short-period response, but which are based on the characteristics of the total response.

A short-period flying qualities criterion for fighter aircraft called the C* criterion (Reference 15) does impose requirements on the total response to pilot inputs. The C* response is a particular blend of the airplane's n , $\dot{\theta}$ and $\ddot{\theta}$ responses. The criterion is in the form of time-history envelopes and is designed to handle the combined effects of control-system and airframe dynamics. Section 5.3 will discuss the results of

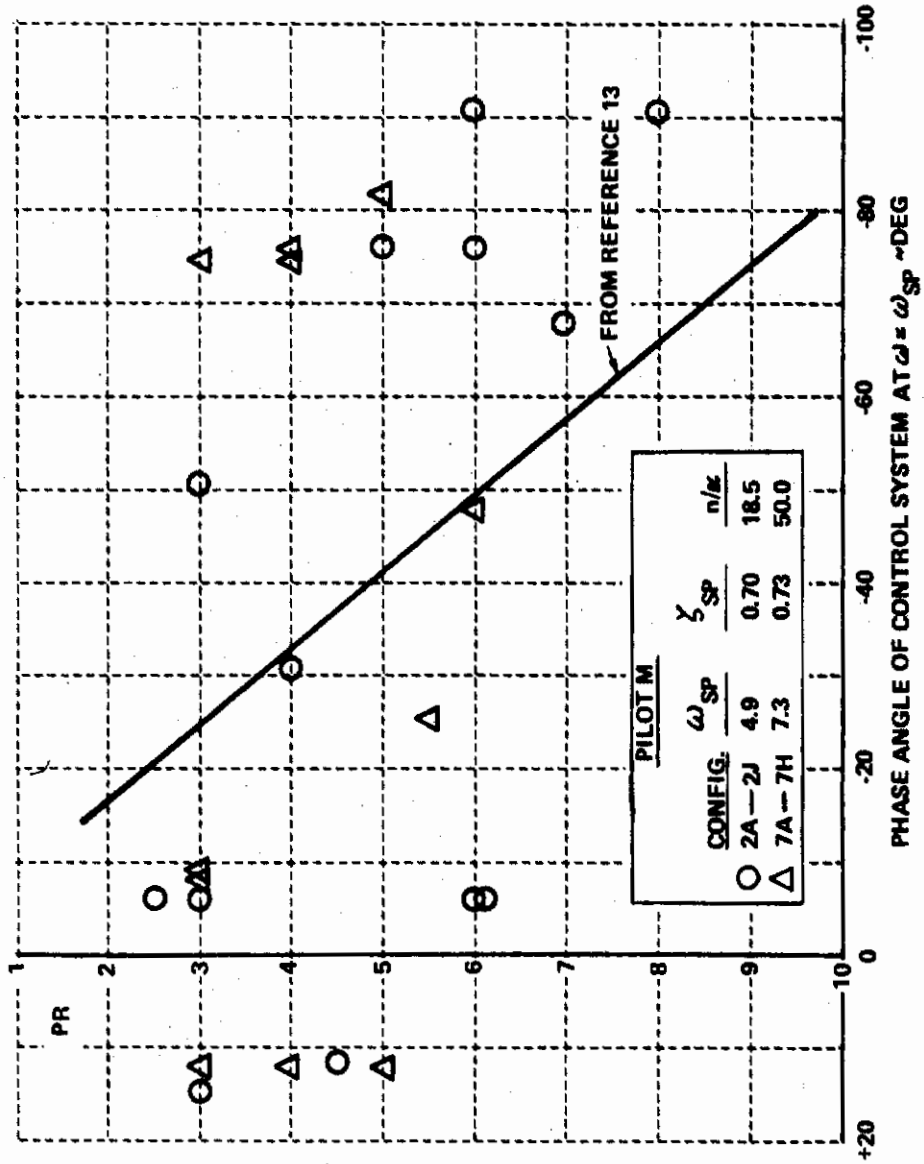

Figure 15. Variation of PR with Control System Phase Angle at $\omega = \omega_{SP}$

applying the C* criterion to the configurations evaluated in this experiment.

5.3 Correlation of Pilot Ratings with the C* Criterion

According to Reference 15, the C* response to a pilot force input is:

$$\frac{C^*}{F_s} = \frac{n}{F_s} + \frac{\ell_p}{g}\left(\frac{\ddot{\theta}}{F_s}\right) + \frac{400}{g}\left(\frac{\dot{\theta}}{F_s}\right)$$

$$= \frac{n}{F_s} + \left(\frac{\ell_p}{g}s + \frac{400}{g}\right)\left(\frac{\dot{\theta}}{F_s}\right)$$

where ℓ_p is the distance of the pilot's station ahead of the center of gravity, in feet. C^*/F_s and n/F_s have the units of g/lb, while $\dot{\theta}/F_s$ has the units of rad/sec per lb.

The normalized C* response to a step force input was calculated for each of the configurations evaluated in this experiment. These responses and their associated pilot ratings were then compared with the C* time-history boundaries of Reference 15. A time history which falls inside these boundaries should represent a satisfactory airplane (PR < 3.5). The details of these calculations and a complete summary of the C* time histories for this experiment are shown in Appendix III. Out of the 57 different configurations evaluated in this experiment, there were approximately 10 cases that disagreed with the C* criterion by either falling outside the boundaries with a PR < 3.5, or falling inside the boundaries with a PR > 3.5. There were, in addition, about the same number of cases which were considered debatable either because the PR was inconsistent or because the C* response only disagreed with the boundary briefly. This statement points up one of the difficulties in interpreting time-history boundaries such as C*. When there is a small disagreement with the boundary, how serious is the degradation in flying qualities?

It should be noted that the 8 basic short-period configurations with negligible control-system dynamics, plus the 6 additional short-period configurations, correlated with the C* criterion fairly well. This is not surprising, however, since the envelope boundaries are based on data for which the control-system dynamics were also negligible. The disagreements with the C* criterion were caused by the effects of control-system dynamics, the very effects the criterion was designed to handle. In fact, at least one control-system configuration for each of the 8 basic short-period configurations resulted in a disagreement with the boundaries.

To summarize the problems encountered in applying the C* criterion to the data of the present experiment, the following examples are given:

Example 1

ω_{SP} = 5 RAD/SEC, ζ_{SP} = 0.7

n/α = 18.5 g/RAD

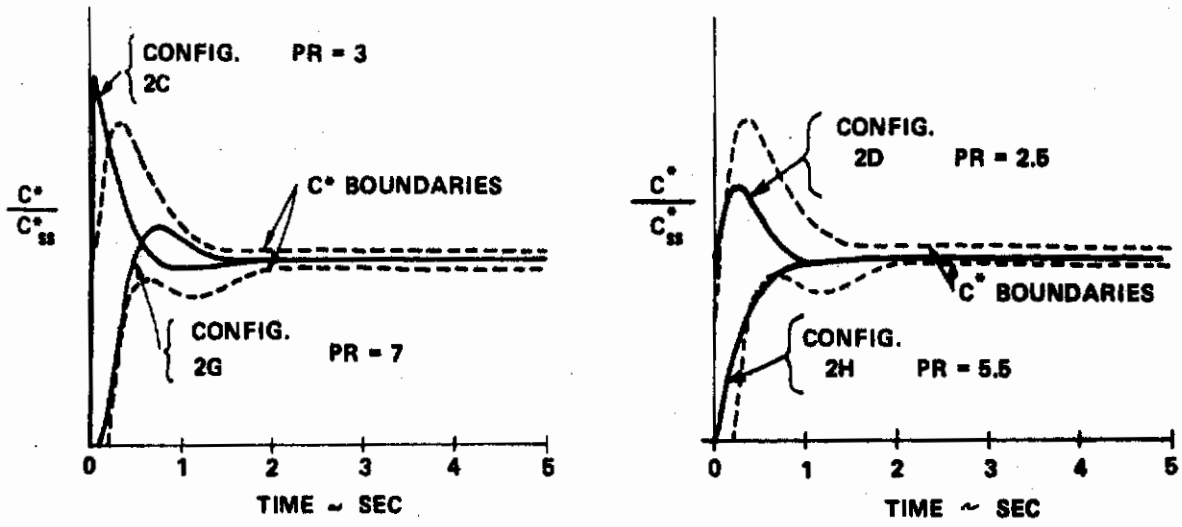

There are two clear disagreements: the configuration with a first-order lead/lag network in the control system (2C) and the configuration with a first-order lag and a low-frequency second-order lag (2G). In addition, Configuration 2H only slightly disagrees with the boundary, and yet the PR is a 5.5.

Example 2

ω_{SP} = 5 RAD/SEC, ζ_{SP} = 0.28

n/α = 18.5 g/RAD

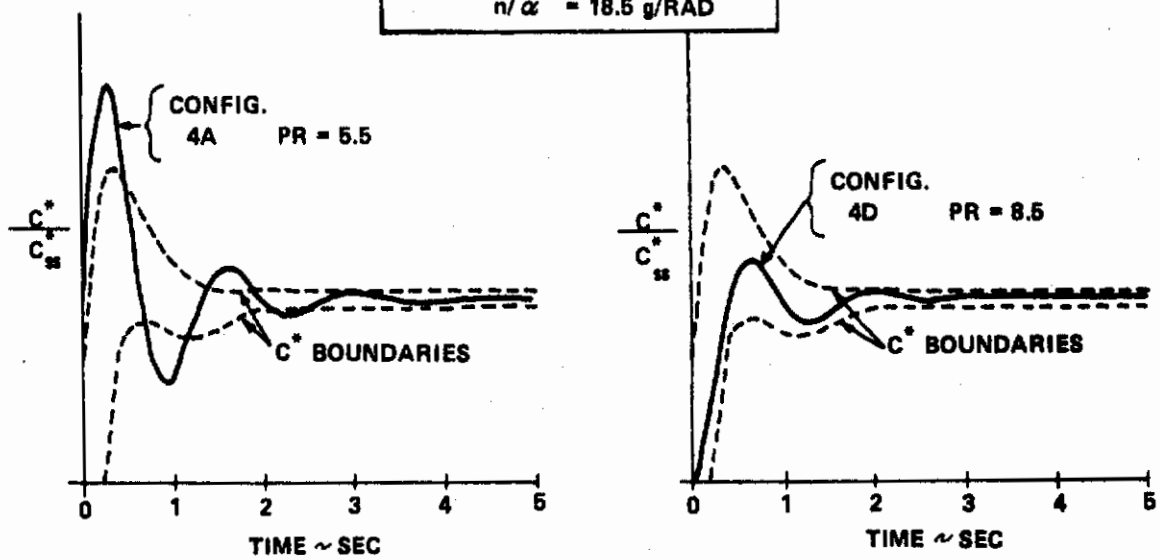

The trend of pilot opinion for both this short-period group (4A to E) and the group with lower short-period damping (5A to E) clearly indicates that any additional control-system lags cause serious degradations in the flying qualities (see Appendix I). In both groups, increasing the control-system lag will eventually reduce the oscillations in the C* response until the time history falls within the boundaries, as in the example above, but will be rated unacceptable by the pilot (Figure 40 shows an in-flight PIO record for configuration 4D).

The appeal of a criterion such as C* to the designer is obvious. As long as the C* response falls within the time history boundaries he has a satisfactory airplane without regard to the details of the control system and airframe dynamics under consideration. Based on the results of this experiment, however, the C* criterion does not appear to have this general application.

5.4 Correlation of Pilot Ratings with Equivalent Dynamics

In the HOS program (Reference 6), the response of each control-system/short-period combination was approximated by an equivalent second-order system plus a transport time lag. The frequency and damping ratio of the equivalent system were generally very close to the short-period characteristics because the frequencies of the control-system roots were high relative to ω_{sp} . Therefore only their low-frequency phase contributions were important and they could be approximated by a time delay. In this equivalent system analysis, the numerators of the n/δ_e and $\dot{\theta}/\delta_e$ transfer functions were unchanged from the values of the T-33. For each airplane configuration evaluated, the pilot ratings and PIO ratings were then correlated with a delay parameter which was the ratio of the equivalent time delay to the period of the equivalent short-period mode.

Since the control system dynamics studied in the present experiment significantly alter the shape of the airplane response to pilot inputs, determining an equivalent system is a more difficult proposition. For the configurations with simulated control system dynamics, the normalized transfer function is:

$$\left.\frac{\dot{\theta}}{F_s}\right|_{norm} = \frac{(\tau_{\theta_2} s+1)(\tau_1 s+1)}{\left(\frac{s^2}{\omega_{sp}^2}+\frac{2\zeta_{sp}}{\omega_{sp}}s+1\right)\left(\frac{s^2}{\omega_3^2}+\frac{2\zeta_3}{\omega_3}s+1\right)(\tau_2 s+1)}$$

The $\dot{\theta}$ step responses from the above expression were generated for each of the 51 basic FCS/short-period configurations. As described in more detail in Appendix II, these time histories were then analog matched using the following equivalent system:

$$\frac{\dot{\theta}}{F_S} = e^{-a_E s} \frac{(\tau_E s + 1)}{\left(\frac{s^2}{\omega_E^2} + \frac{2\zeta_E}{\omega_E} s + 1\right)}$$

In most cases τ_E was held fixed near the appropriate T-33 value of τ_{θ_2}. However, in a few cases τ_E had to be significantly varied, in addition to a_E, ω_E and ζ_E, to achieve a reasonable match of the $\dot{\theta}$ time history. This usually occurred for those configurations with appreciable values of τ_1 in the simulated control system.

Attempts to correlate the pilot rating data with the delay parameter used in the HOS program, $\frac{a_E}{\rho_E}$, where $\rho_E = \frac{2\pi}{\omega_E}$, were not successful. However, reasonable correlation was achieved by plotting the product $\omega_E \cdot \tau_E$ against the time delay a_E. These efforts are documented in Appendix II and compared with similar results from the HOS program. Several authors, Hall (Reference 7) and the Shomber and Gertsen (Reference 16) for example, have suggested the use of $\omega_{sp} \cdot \tau_{\theta_2}$ as a longitudinal flying qualities parameter.

Although the correlation of the PR data with this equivalent system approach is reasonable, several limitations should be noted. There is considerable artistry involved in certain parts of the analog matching process. Accurate determination of the time delay, a_E is often difficult; and for time delays greater than 0.1 sec, small variations in a_E can mean significant changes in PR. In the region of low $\omega_E \tau_E$ values (say $\omega_E \tau_E <$ 2.5), large trade-offs between τ_E and ω_E, or in some cases between ζ_E and ω_E, can be made with little discernible difference in the accuracy of the analog match achieved. In the present experiment, this problem occurred for those configurations having $\dot{\theta}$ responses with little or no overshoot (configurations with low ω_{sp} or large control system lags). In a few cases, $\omega_E \cdot \tau_E$ could be changed by factors of 2 or more and, with compensating changes in ζ_E and a_E, equally good analog matches could be obtained (see Appendix II). The important point to note is that this lack of precision occurs in an area of primary practical importance, since the lower $\omega_E \tau_E$ boundary would represent a design limit on aft center-of-gravity travel for many airplanes.

Note that the $\omega_E \tau_E$ versus a_E boundaries of Appendix II apply only for $\zeta_E > 0.4$. Limits on damping ratio must be handled separately, as is done in MIL-F-8785B.

In view of the practical difficulties associated with the equivalent system approach, and the lack of correlation with MIL-F-8785B requirements on control-system dynamics or with the C* criterion, the pilot-in-the-loop analysis described in the next section was undertaken.

SECTION VI

PILOT-IN-THE-LOOP ANALYSIS

From the brief discussion of the pilot comments presented in Section 5.1, it is obvious that the pilots weighted very heavily their ability to acquire a target quickly and track it precisely. As a matter of fact, most of the pilot ratings given during the program appeared to be primarily determined by how precisely the pilot could control the airplane's pitch attitude. Because of this, it was decided to see what could be learned through pilot-in-the-loop analysis of pitch-attitude control.

The first step in this study was to examine the results of previous attempts to apply pilot-in-the-loop analysis to pitch-attitude tracking tasks. Considerable work of this nature has been performed by Systems Technology Inc. (STI), and some of the basic principles of their approach are given in References 17 through 20. After studying a number of STI reports, it became apparent that there are certain basic elements which must be defined in a pilot-in-the-loop analysis:

(1) A mathematical model of the closed-loop tracking task.

(2) A series of performance measures describing a "standard of performance" which the pilot tries to achieve when he adjusts his characteristics to the airplane.

(3) A method for converting open-loop characteristics to closed-loop characteristics.

(4) A method for determining how the pilot is likely to apply compensation to achieve the "performance standards".

(5) A method for relating tracking performance and pilot compensation to pilot opinion.

All these elements are treated in STI's work, and their methods provide interesting insights into various types of flying qualities problems. However, the methods are not specific enough to allow direct application to the development of control-system design criteria. Thus, the analysis described below has the same basic elements as STI's approach, but differs considerably in the specific methods used.

The following subsections describe the mathematical model used, the development of closed-loop performance "standards", use of the Nichols chart in the analysis, and how the pilot compensation is obtained. The analysis techniques are then applied to two example configurations, and the various parameters from the analysis are related to pilot opinion.

6.1 The Mathematical Model

The form of the mathematical model used in the present analysis to describe pitch-attitude tracking was taken from Reference 17. This model is shown in Figure 16.

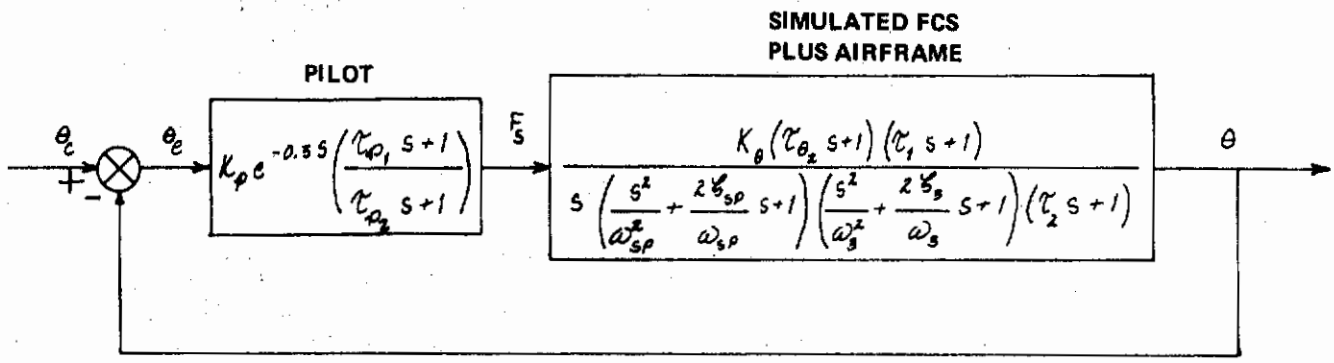

Figure 16. Mathematical Model of Pitch Attitude Tracking

The model of the pilot consists of a variable gain (K_p), a time delay, and a variable first-order compensation network. The time delay includes the time required for the pilot to sense a change in θ_e , the time required to decide what to do, and the neuromuscular lags. STI's work suggests that this time delay may vary with the airplane's dynamics and will usually lie between 0.2 and 0.4 seconds. For simplicity, a fixed value of the time delay is used in the present analysis. The value of 0.3 seconds chosen is an average time delay measured from records of the discrete-error tracking task discussed in Section 4.3.

It should be noted that the block diagram of Figure 16 is known as a compensatory tracking model, which means that the pilot operates only on the difference (θ_e) between the airplane's pitch attitude and the commanded pitch attitude. In real life, of course, the pilot also derives information from θ , θ_c , and various motion cues. In a crude sense, however, the compensatory model does describe what the pilot is trying to do with the airplane, and it has the advantage that it is relatively simple to analyze. In addition, it appears adequate to explain the more important aspects of attitude tracking, as will be shown in Section VII.

With the form of the tracking model chosen, the objective of the analysis will be to determine the pilot model parameters (K_p , τ_{p_1} , τ_{p_2}) and the closed-loop θ/θ_c characteristics which represent how the pilot actually flew each configuration evaluated in the experiment. To aid the reader in understanding the terminology used in the remaining subsections, the following should be noted:

(1) $\frac{\theta}{F_s}$ is the open-loop transfer function of the airplane plus control system.

$\frac{\theta}{\theta_e}$ is the open-loop transfer function of the airplane plus control system plus pilot.

$\frac{\theta}{\theta_c}$ is the closed-loop transfer function of the airplane plus control system plus pilot.

(2) The terms "open-loop" and "closed-loop" are meant to apply to the block diagram shown in Figure 16. Any FCS loops around the airframe are always assumed to be closed when computing the θ/F_s characteristics.

6.2 The Pilot's View of Good Tracking Performance

The first step in the analysis is to identify the performance which the pilot is trying to achieve when he "adapts" to an airplane configuration. The pilot comments indicate quite clearly that he wants to acquire the target quickly and predictably, with a minimum of overshoot and oscillation. The question that remains is how to translate this observation into mathematical terms.

References 17 and 18 express tracking performance in terms of the following open-loop and closed-loop parameters:

(1) The pilot tries to achieve a particular value of the open-loop gain-crossover frequency, ω_c (the frequency at which $|\theta/\theta_e|$ = 0 dB).

(2) The pilot tries to minimize any low-frequency, closed-loop "droop" (hold $|\theta/\theta_c|$ as near 0 dB as possible, for $\omega \leq \omega_c$)

(3) The pilot tries to maintain good high-frequency stability by keeping the damping ratio of any closed-loop oscillatory modes greater than 0.35, and by maintaining a phase margin of 60 to 110 degrees.

These criteria are shown on the Bode plot of Figure 17.

The performance parameters of References 17 and 18 are well accepted performance measures in servo analysis. For flying qualities analyses, however, it seems more direct to express all the performance measures in terms of what the pilot sees, i.e., in terms of closed-loop parameters.

The pilot's desire to "acquire the target quickly and predictably" seems to be related to low-frequency performance (the Bode characteristics in the frequency range from 0.5 to 3 rad/sec, roughly). In the terminology of References 17 and 18, the pilot is trying to achieve some minimum value of ω_c, while minimizing the closed-loop droop for frequencies below ω_c.

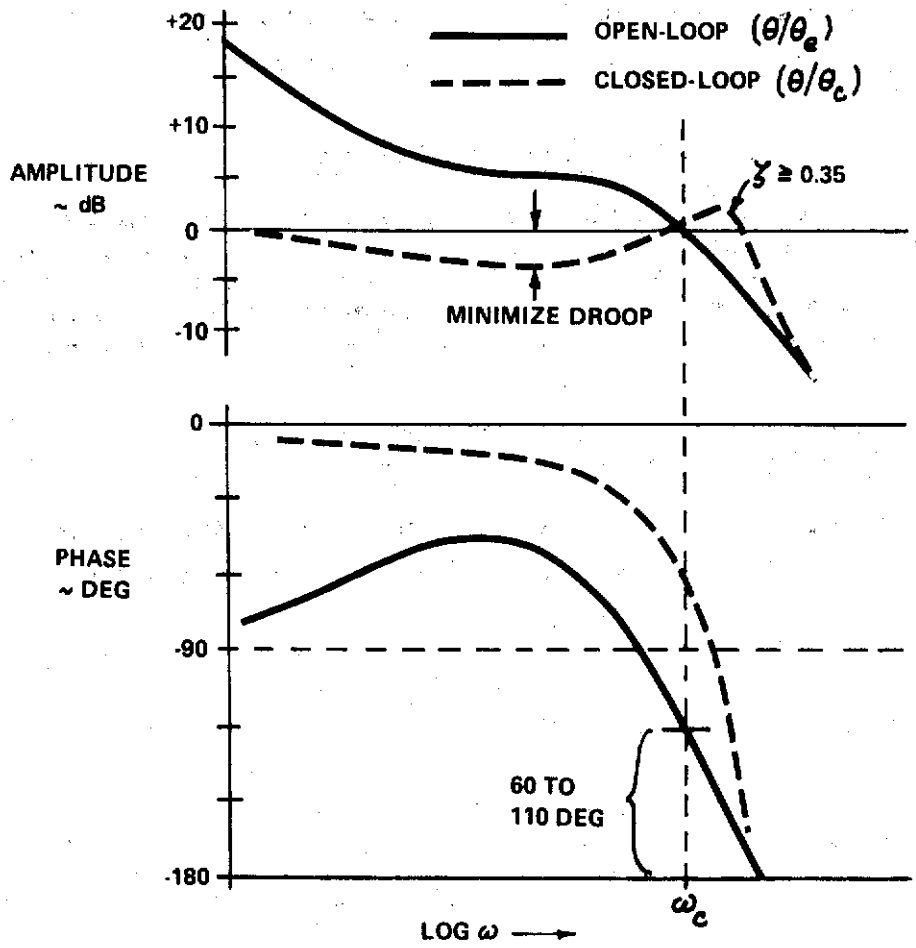

Figure 17. Tracking Performance Parameters of References 17 and 18.

To express low-frequency performance completely in terms of closed-loop parameters for the present analysis, a parameter called closed-loop bandwidth (BW) is first defined: the frequency at which the closed-loop phase ($\angle \theta/\theta_c$) is -90 degrees. (For a simple second-order closed-loop system, BW would be equal to the system's undamped natural frequency.) Using this terminology, it is hypothesized that the pilot is trying to achieve some minimum value of BW. For frequencies below BW, he wants to minimize the closed-loop droop. Figure 18 shows these parameters applied to the closed-loop Bode plots of Figure 17.

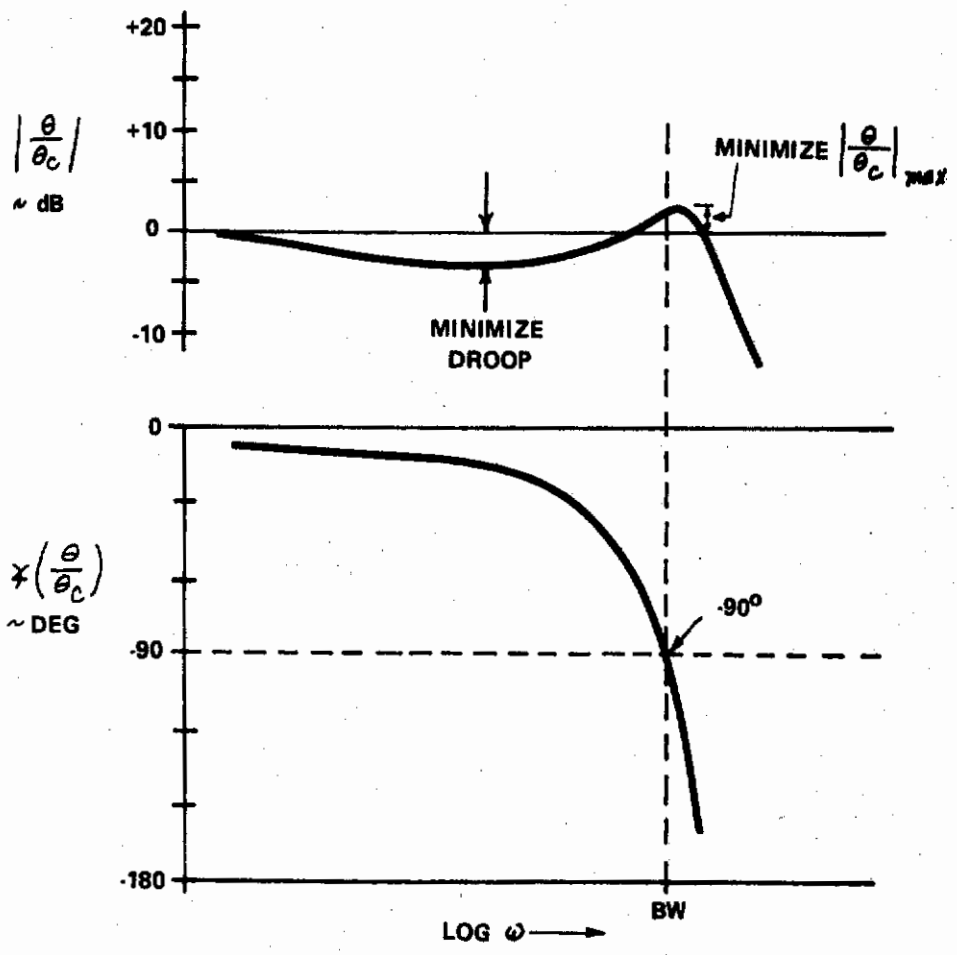

Figure 18. Tracking Performance Parameters Used in the Analysis.

The pilot's desire to acquire the target "with a minimum of overshoot and oscillation" seems to be related to high-frequency stability. In the terminology of References 17 and 18, the pilot is trying to maintain a minimum damping ratio of 0.35 for any closed-loop oscillatory modes (see Figure 17). Because the closed-loop θ/θ_c responses are at least third-order, however, the amount of oscillation which the pilot sees is a function of more than closed-loop damping ratio alone. This can be seen in the following sketches of closed-loop attitude response.

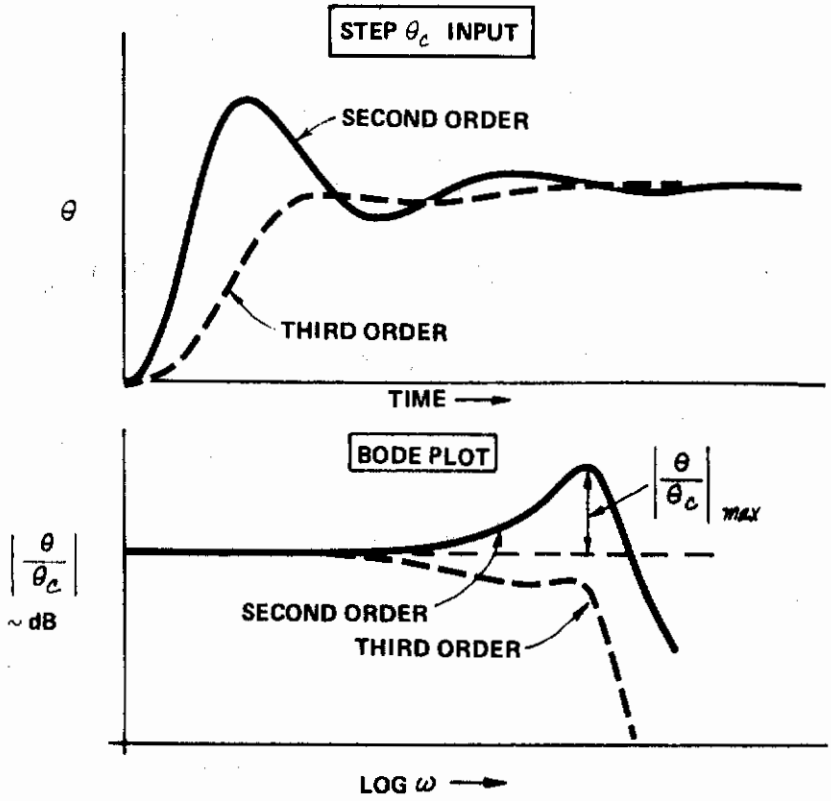

The oscillatory modes in both responses have the same natural frequency and damping ratio (ζ = .28), but the oscillation in the third-order response is smoothed by the presence of a first-order pole (τ = 0.5 sec). Thus, it would appear that the amount of oscillation which the pilot sees is better described by the magnitude of the closed-loop Bode resonance, $|\theta/\theta_c|_{MAX}$, than by damping ratio alone. For purposes of the present analysis, therefore, it is hypothesized that the pilot is trying to minimize the resonant peak, $|\theta/\theta_c|_{MAX}$ (see Figure 18).

To summarize, it is hypothesized that the pilot is trying to achieve good low-frequency performance (a reasonable bandwidth, with a minimum of low-frequency droop), plus good high-frequency stability ($|\theta/\theta_c|_{MAX}$ as small as possible).

6.3 Tracking Performance Standards

Section 6.2 described the various closed-loop performance parameters which are of importance to the pilot. The next step in the analysis is to put numerical limits on these parameters, which describe the "standard of performance" the pilot is trying to achieve in performing the required tracking tasks.

A helpful guide in determining the performance standards lies in the pilot comments concerning what the pilot does when he cannot achieve good low frequency performance without causing oscillatory tendencies. The pilot typically complains that if he flies the airplane as aggressively as the task demands (i.e., keeps the bandwidth up), he gets overshoots or PIO tendencies. If he backs off and flies the airplane smoothly, he can reduce the oscillatory tendencies, but his performance is not adequate for the task. When faced with such a trade-off, the pilot's ratings seem to be primarily a function of the compensation required to achieve good low frequency performance, and the oscillatory tendencies that result. In view of these considerations, the following performance standards are assumed for purposes of the present analysis:

(1) A minimum bandwidth $(BW)_{min}$ of 3.5 rad/sec ($\angle \theta/\theta_c \geq -90°$ at $\omega = 3.5$). This value was determined by trying a few values of BW in the analysis of a cross-section of configurations, until the resulting values of $|\theta/\theta_c|_{max}$ correlated qualitatively with the pilot comments concerning PIO tendencies. It should be noted, however, that certain limitations of the experiment apparently caused the pilot to use $(BW)_{min} = 3.0$ rad/sec for the 250 knot configurations, as will be explained in Section 7.1.

(2) A maximum low-frequency droop of -3 dB was selected somewhat arbitrarily ($|\theta/\theta_c| \geq -3$ dB for $\omega \leq BW$). (For a simple second-order closed-loop system with $\zeta = 0.7$, $|\theta/\theta_c| = -3$ dB at $\omega = BW$.)

These performance standards are summarized in Figure 19.

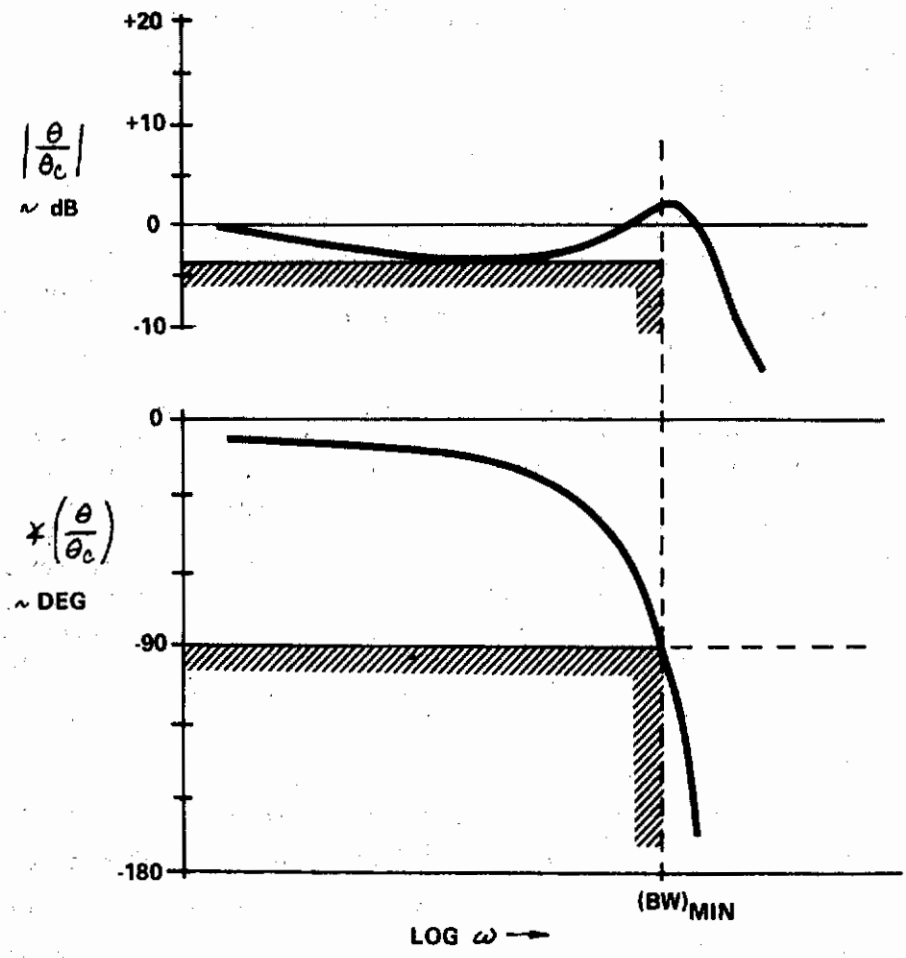

Figure 19. Tracking Performance Standards Used in the Analysis.

The remainder of the analysis is devoted to determining specific values of K_ρ , τ_{ρ_1} , τ_{ρ_2} which will achieve the performance standards of Figure 19, with a minimum of high-frequency resonance (low values of $|\theta/\theta_c|_{max}$). The pilot ratings for each configuration should then be functions of K_ρ , τ_{ρ_1} , τ_{ρ_2} and $|\theta/\theta_c|_{max}$.

6.4 Use of the Nichols Chart

To apply the performance standards of Section 6.3 in the closed-loop analysis, it is necessary to have a method to convert the open-loop (θ/θ_e) Bode characteristics into the closed-loop (θ/θ_c) characteristics. The (θ/θ_c) transfer function is really nothing more than a transformation of (θ/θ_e) according to the following equation.

$$\frac{\theta}{\theta_c} = \frac{(\theta/\theta_e)}{1+(\theta/\theta_e)}$$

One of the simplest and most illustrative methods for effecting this transformation is to plot the (θ/θ_e) amplitude versus phase on a Nichols chart. A Nichols chart is simply a plot showing lines of constant closed-loop amplitude and phase on a grid of open-loop amplitude versus phase. Figure 20 shows a Nichols chart, with the performance standards of Figure 19 transformed onto it.

6.5 Form of the Required Compensation

To determine specific values of K_p , τ_{p_1} , τ_{p_2} for a given configuration, it is first necessary to determine the form of the compensation which the pilot will employ (i.e., whether lead compensation or lag compensation is required).

To determine the form of the required compensation, it is logical to see first what can be accomplished by adjusting the pilot gain alone, without lead or lag compensation. The pilot's transfer function (see Figure 16) then simplifies to:

$$\frac{F_s}{\theta_e} = K_p e^{-0.3s}$$

If a transfer function or a Bode plot is available which describes the dynamics of the complete FCS/airframe configuration, the open-loop Bode characteristics of θ/θ_e (using the simplified pilot) can be obtained from the following transfer function:

$$\left(\frac{\theta}{\theta_e}\right)^* = K_p e^{-0.3s} \left(\frac{\theta}{F_s}\right)$$

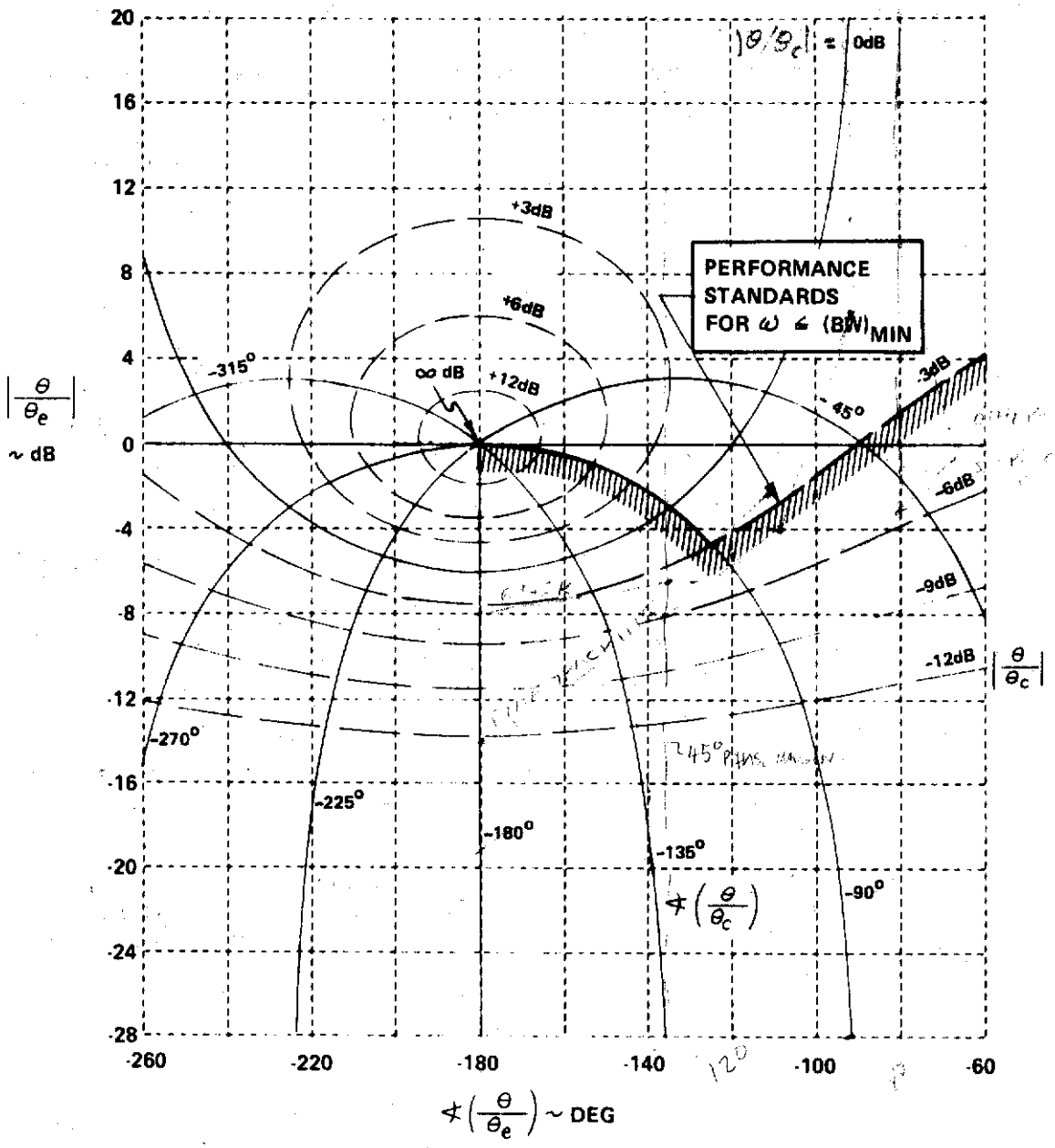

Figure 20. Nichols Chart Showing Performance Standards Used in the Analysis

(The star (*) will be used throughout the rest of the report to signifiy θ/θ_e characteristics of the form shown here, i.e., no pilot lead or lag compensation. All θ/θ_e characteristics without the star will be assumed to include pilot compensation.)

If the Bode amplitude $|\theta/\theta_e|^*$ is plotted versus the Bode phase $\measuredangle(\theta/\theta_e)^*$ on a piece of transparent paper, the resulting curve can be overlayed on the Nichols chart of Figure 20. The effects of changing K_p can then be seen by sliding the amplitude-phase overlay vertically on the Nichols chart. The value of K_p should be chosen so that the performance standards are just barely met (the overlay should be positioned vertically so that the amplitude-phase curve is just barely above the hatched boundaries of Figure 20, for all frequencies less than $(BW)_{min}$). If this is done, there are three basic types of amplitude-phase overlays which can result, as shown in Figure 21.

The form of the pilot's compensation for each curve in Figure 21 is discussed below:

Curve A (limited by the bandwidth requirements alone).
In this case, the closed-loop resonance (+12 dB for this example) can be reduced by using lead compensation:

$$\frac{F_s}{\theta_e} = K_p e^{-0.3s}\left(\frac{\tau_{p_1}s+1}{\tau_{p_2}s+1}\right), \quad \tau_{p_1} > \tau_{p_2}$$

Lead compensation will cause the lower part of the curve to shift upward and to the right, and may cause it to flatten somewhat (curve A will become shaped more like curve C). The compensated curve can now be shifted downward to reduce the resonance without reducing the bandwidth below $(BW)_{min}$. The droop will increase, however. The amount of lead resulting in the least resonance will occur when the bandwidth can be made exactly equal to $(BW)_{min}$ and the droop exactly equal to -3 dB simultaneously (see discussion of curve C).

Curve B (limited by the droop requirements alone).
In this case, the closed-loop resonance (+ 12 dB for this example) can be reduced by using lag compensation:

$$\frac{F_s}{\theta_e} = K_p e^{-0.3s}\left(\frac{\tau_{p_1}s+1}{\tau_{p_2}s+1}\right), \quad \tau_{p_2} > \tau_{p_1}$$

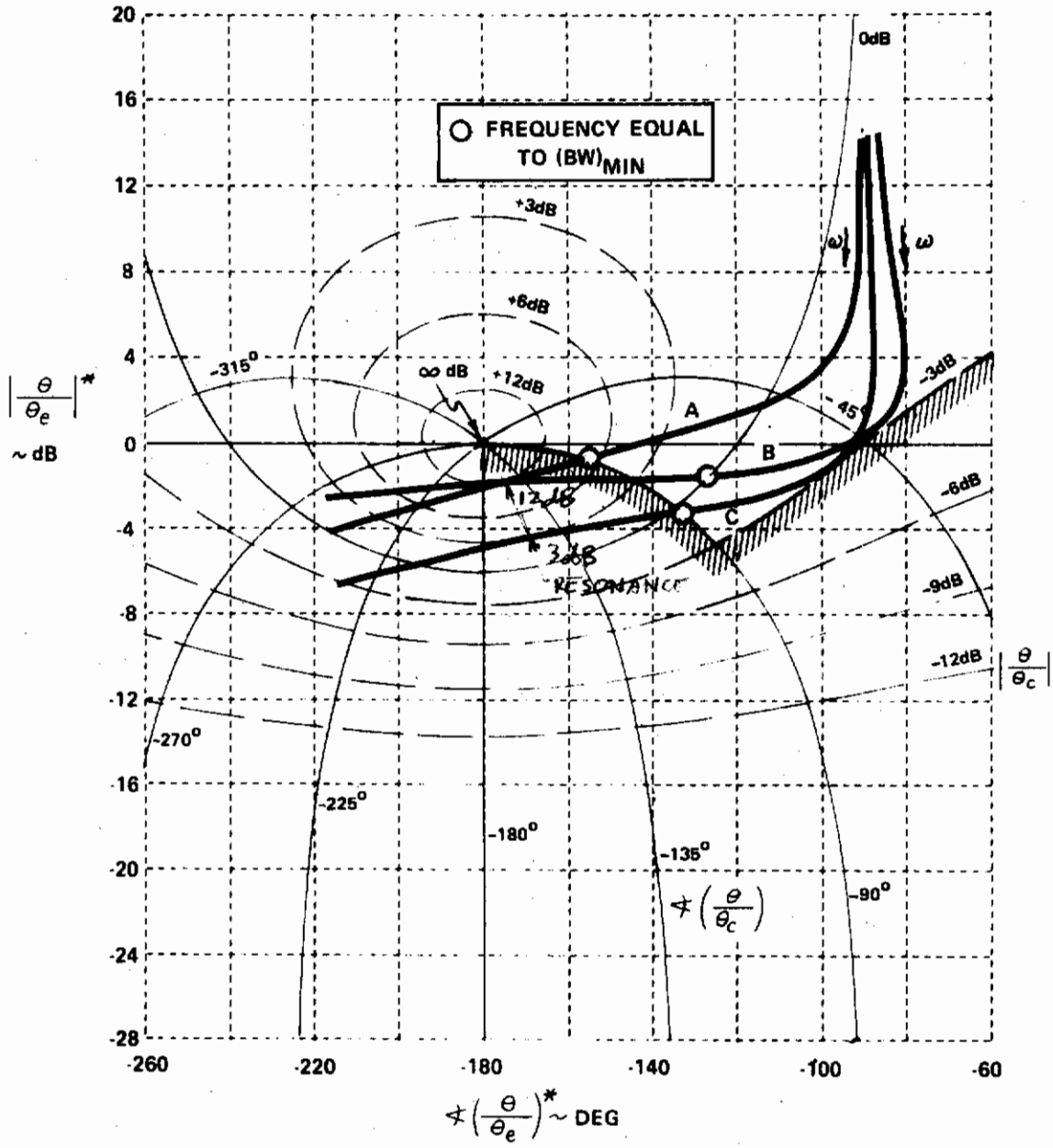

Figure 21. Typical Overlays of $|\theta/\theta_e|^*$ Versus $\angle(\theta/\theta_e)^*$ on a Nichols Chart

Lag compensation will cause the lower part of the curve to shift downward and to the left, and will also cause it to steepen (curve B will become shaped more like curve C). This will result in a reduction in the resonance. The amount of lag resulting in the least resonance will occur when the bandwidth can be made exactly equal to $(BW)_{min}$ and the droop exactly equal to -3 dB simultaneously (see discussion of curve C).

Curve C (limited by the bandwidth and droop requirements simultaneously). No value of the pilot's compensation in the assumed form will reduce the closed-loop resonance (in this case, + 3 dB) without either increasing the droop or decreasing the bandwidth. For example, lead compensation will cause curve C to become shaped more like curve B. In this case, the resonance will be increased if the droop is held at - 3 dB. Lag compensation will cause curve C to become shaped more like curve A. Again, the resonance will be increased if the bandwidth is held at $(BW)_{min}$. Thus, for curve C, the pilot can be expected to use no compensation at all:

$$\frac{F_s}{\theta_e} = K_p e^{-0.3s}$$

Note that the pilot would probably not use lead or lag compensation for any curve having a resonance of less than 0 dB, using K_p alone.

With the form of the compensation determined for a given configuration, it remains to determine the "optimum" choice of τ_{p_1} and τ_{p_2}.

6.6 The "Optimum" Pilot Compensation

To determine the value of τ_{p_1} and τ_{p_2} for a given configuration, it is first necessary to define what is meant by the "optimum" compensation. In general terms, it is the compensation which will minimize the closed-loop resonance, while still meeting the performance standards. The following discussion defines it more specifically.

The "optimum" lead compensation will provide the most positive increase in $\measuredangle (\theta/\theta_e)$ for the least flattening of the amplitude-phase curve, in the general vicinity of $\omega = (BW)_{min}$. (Refer to discussion of curve A, Section 6.5.) The flattening tendency is primarily related to the fact that the increment in open-loop amplitude contributed by lead compensation, $\left|\frac{j\omega\tau_{p_1}+1}{j\omega\tau_{p_2}+1}\right|$, is positive and increases with ω along the curve.

That is, $d\left|\frac{j\omega\tau_{\rho_1}+1}{j\omega\tau_{\rho_2}+1}\right| \Big/ d(\log\omega)$ is positive for lead compensation, as can be seen from Figure 22. Thus, the "optimum" lead compensation is that which will provide the most positive $\angle\left(\frac{j\omega\tau_{\rho_1}+1}{j\omega\tau_{\rho_2}+1}\right)$ for the least positive value of $d\left|\frac{j\omega\tau_{\rho_1}+1}{j\omega\tau_{\rho_2}+1}\right| \Big/ d(\log\omega)$, in the vicinity of $\omega = (BW)_{min}$.

Referring again to Figure 22, the variations in amplitude slope and phase with frequency can be seen, for any given value of $\tau_{\rho_2}/\tau_{\rho_1}$. For both lead compensation ($\tau_{\rho_2}/\tau_{\rho_1} < 1$) and lag compensation ($\tau_{\rho_2}/\tau_{\rho_1} > 1$), the |amplitude slope| and |phase| are shown to increase to maximum values at some intermediate frequency, then decrease again as ω increases to infinity. The frequency at which both maxima occur is centered (logarithmically) between $1/\tau_{\rho_1}$ and $1/\tau_{\rho_2}$, i.e., $\omega = (\tau_{\rho_1}\tau_{\rho_2})^{-1/2}$. These trends can be seen more readily if the amplitude slope is plotted versus the phase for various values of $\tau_{\rho_2}/\tau_{\rho_1}$, as in Figure 23. From Figure 23, it can be seen that the most positive phase for a given positive slope will always be obtained when ($\tau_{\rho_2}/\tau_{\rho_1}$) is zero. Thus the "optimum" lead compensation is pure lead ($\tau_{\rho_2} = 0$).

The "optimum" lag compensation will provide the most steepening of the amplitude-phase for the least negative increase in $\angle\,\theta/\theta_e$, in the general vicinity of $\omega = (BW)_{min}$. (Refer to discussion of curve B, Section 6.5.) The steepening tendency is primarily related to the fact that $d\left|\frac{j\omega\tau_{\rho_1}+1}{j\omega\tau_{\rho_2}+1}\right| \Big/ d(\log\omega)$ is negative for lag compensation (see Figure 22). Thus, the "optimum" lag compensation is that which will provide the most negative value of $d\left|\frac{j\omega\tau_{\rho_1}+1}{j\omega\tau_{\rho_2}+1}\right| \Big/ d(\log\omega)$ for the least negative $\angle\left(\frac{j\omega\tau_{\rho_1}+1}{j\omega\tau_{\rho_2}+1}\right)$, in the vicinity of $\omega = (BW)_{min}$. Referring again to Figure 23, it can be seen that the most negative slope for a given negative phase will always occur at the center frequency, $\omega = (\tau_{\rho_1}\tau_{\rho_2})^{1/2}$. Since the primary area of interest is $\omega = (BW)_{min}$, the following expression will be used to define the "optimum" lag compensation:

$$(\tau_{\rho_1}\tau_{\rho_2})^{-1/2} = (BW)_{min}$$

This means that the lead and lag frequencies ($1/\tau_{\rho_1}$ and $1/\tau_{\rho_2}$) should always be chosen so that $(BW)_{min}$ is centered (logarithmically)

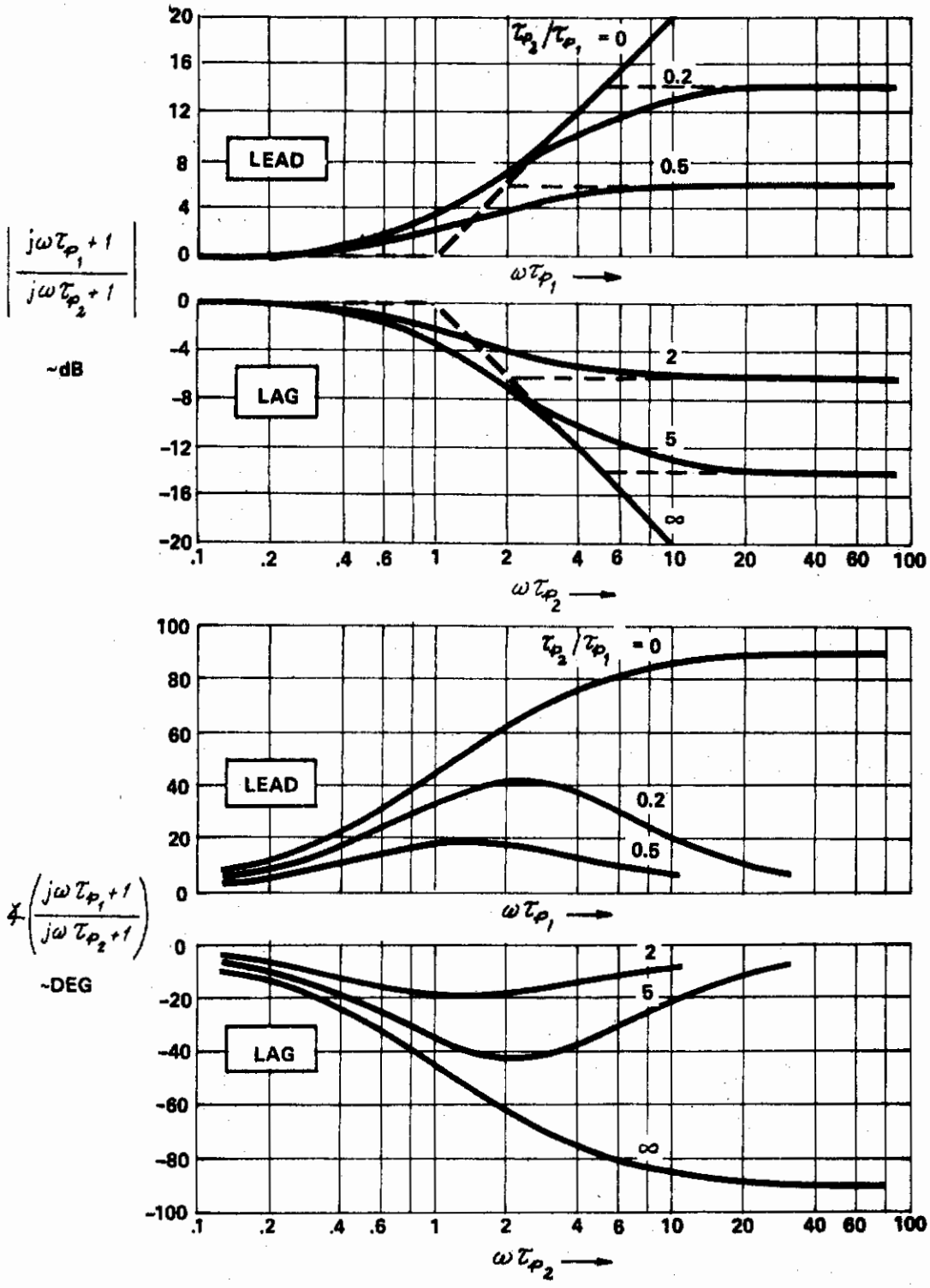

Figure 22. Amplitude and Phase Contributed by Pilot Compensation

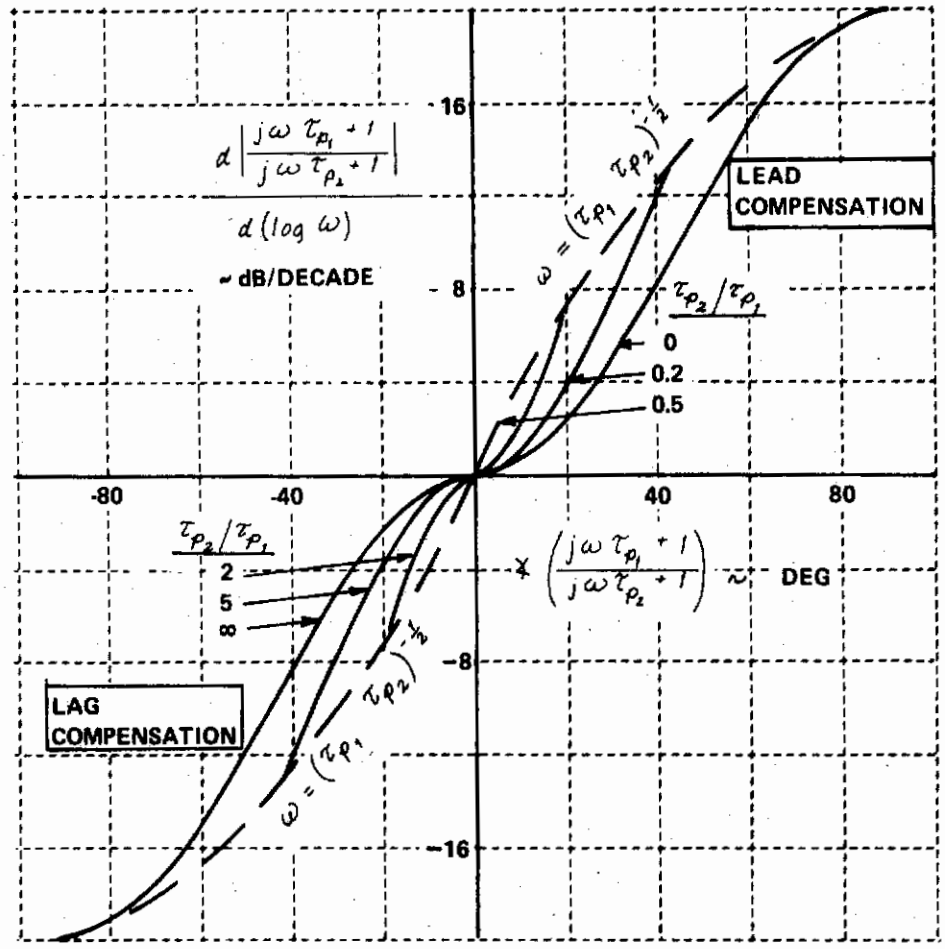

Figure 23. Amplitude Slope and Phase Contributed by Pilot Compensation.

between them, as shown in Figure 24.

Amplitude-phase curves for the "optimum" lag compensation discussed above are shown in Figure 25, for various values of $(\tau_{\rho_2}/\tau_{\rho_1})$. Also shown in this figure is the amplitude-phase curve for "optimum" lead compensation ($\tau_{\rho_2}=0$).

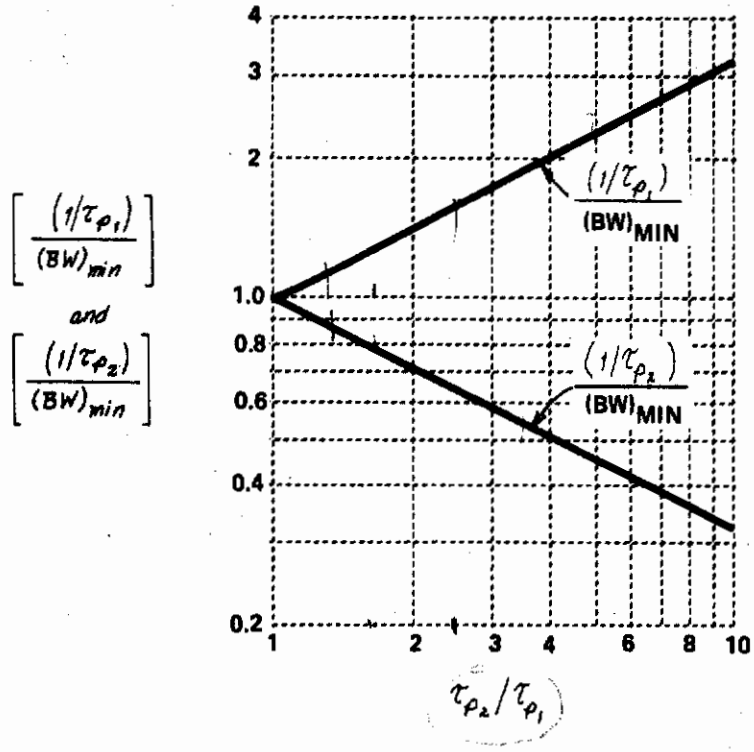

Figure 24. "Optimum" Lag Compensation

Using Figure 25, the pilot compensation can be determined by choosing the value of τ_{p_1} or (τ_{p_2}/τ_{p_1}) which will cause the bandwidth to exactly equal $(BW)_{min}$ and the maximum droop to exactly equal - 3 dB. This will result in the smallest resonance, while still meeting the performance standards. The process can be accomplished very quickly by trial and error, if the amplitude-phase curve of Figure 25 is graphically added to the uncompensated amplitude-phase overlay $(\theta/\theta_e^* = K_p e^{-0.3s} \frac{\theta}{F_s})$ for a few trial values of τ_{p_1} or (τ_{p_2}/τ_{p_1}).

It should be mentioned that the compensation described by Figure 25 is "optimum" in a crude sense, so that it may be possible to find a different combination of τ_{p_1} and τ_{p_2}, for a given configuration, which would result in a slightly smaller closed-loop resonance. The differences will be small, however, and Figure 25 has the advantage of providing a consistent and reasonably simple method for applying the compensation, as will be shown in the examples of Sections 6.7 and 6.8.

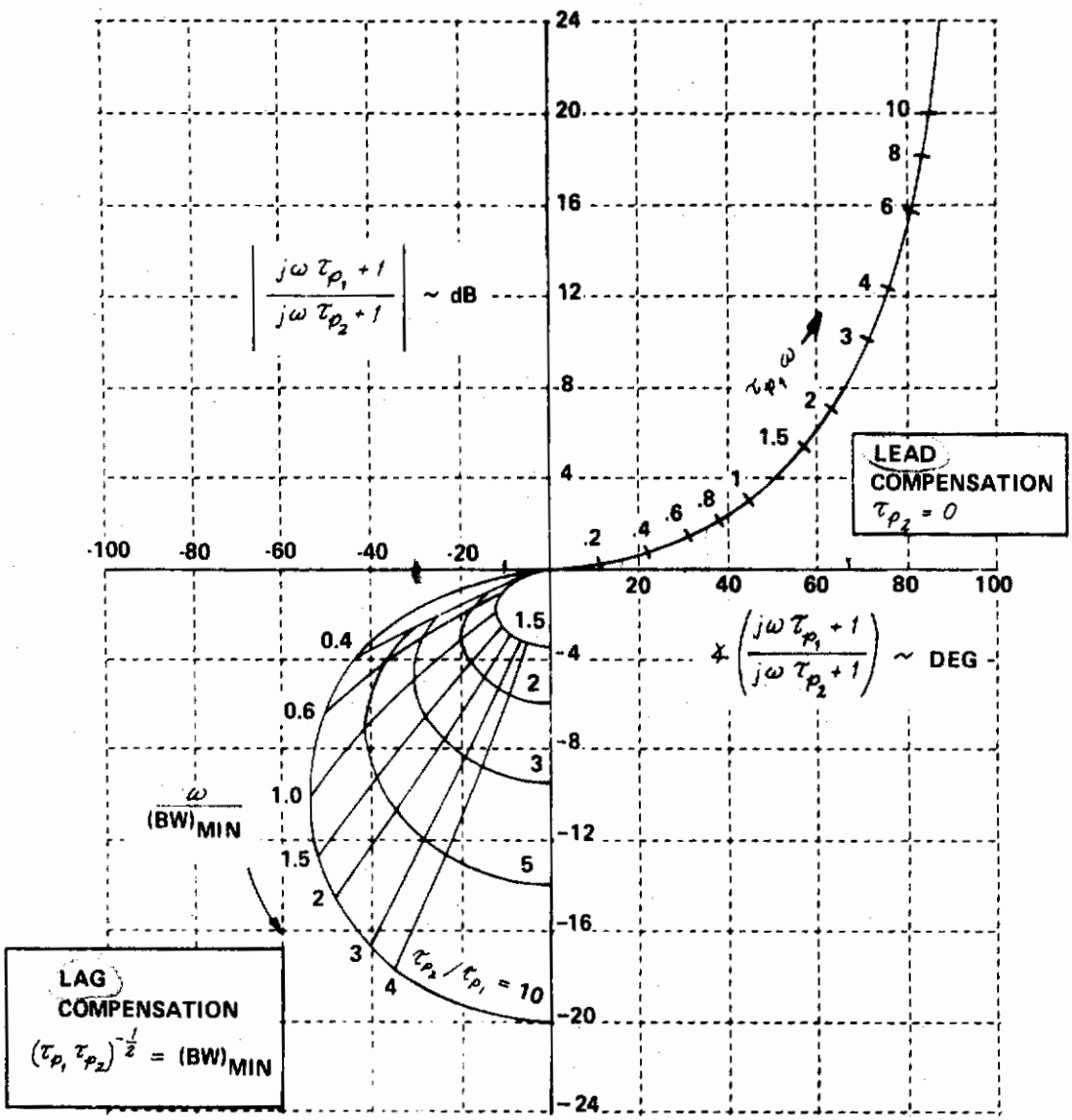

Figure 25. Amplitude-Phase Curves for "Optimum" Pilot Compensation

6.7 Example of a Configuration Having Low ω_{sp}

The first example chosen is a 250 kt configuration with a low short-period frequency and good damping (ω_{sp} = 2.2 rad/sec, ζ_{sp} = 0.69), with negligible control system dynamics (1D). A nominal elevator gearing was used, so that F_s/n = 5 lb/g and K_θ = .77 $\frac{\text{deg/sec}}{\text{lb.}}$.

The first step in the analysis is to adjust the pilot gain alone, without lead or lag compensation. The pilot's transfer function (see Figure 16) then simplifies to:

$$\frac{F_s}{\theta_e} = K_p e^{-0.3s}$$

The open-loop Bode characteristics for the example configuration plus the simplified pilot are shown in Figure 26 (for K_p = 1.0 lb/deg).

The effects of changing K_p can be seen by overlaying a plot of $|\theta/\theta_e|^*$ versus $\angle(\theta/\theta_e)^*$ on a Nichols chart. Such an overlay is shown in Figure 27, positioned on the Nichols chart in an attempt to meet the performance standards.

It is obvious from Figure 27 that a bandwidth of 3 rad/sec can never be achieved using K_p alone, without driving the system unstable. $((BW)_{min}$ is 3 rad/sec for the 250 kt configurations, as will be explained in Section VII.) In this case, the pilot must use lead compensation to increase the bandwidth.

Using Figure 25, the "optimum" pilot compensation can be determined by choosing the value of τ_{p_1} which will cause the bandwidth to exactly equal 3 rad/sec and the maximum droop to exactly equal -3 dB. This will result in meeting the performance standards with the smallest resonance. An initial guess at the optimum value of τ_{p_1} can be made from the following observations. Figure 21 shows that if the compensated amplitude-phase curve is to have a low resonance, the compensated $\angle\,\theta/\theta_e$ at ω = 3 rad/sec will have to be somewhere near -130 degrees (e.g., curve C). Figure 27 shows that the uncompensated $\angle(\theta/\theta_e)^*$ at ω = 3 is roughly -190 degrees. Thus, the pilot's compensation should provide about 60 degrees of phase lead at ω = 3. Figure 25 shows that

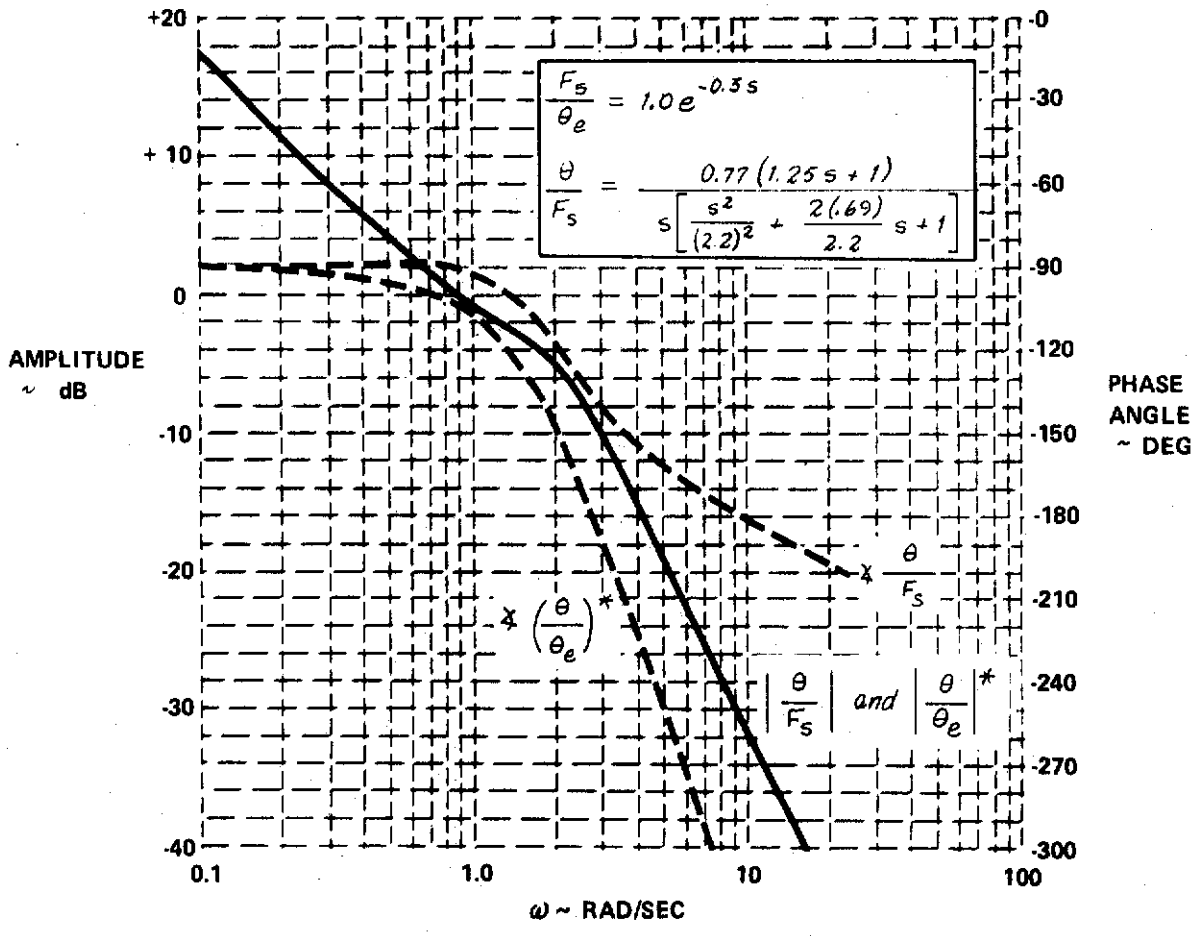

Figure 26. Open-Loop Bode Characteristics for a Configuration Having Low ω_{sp}

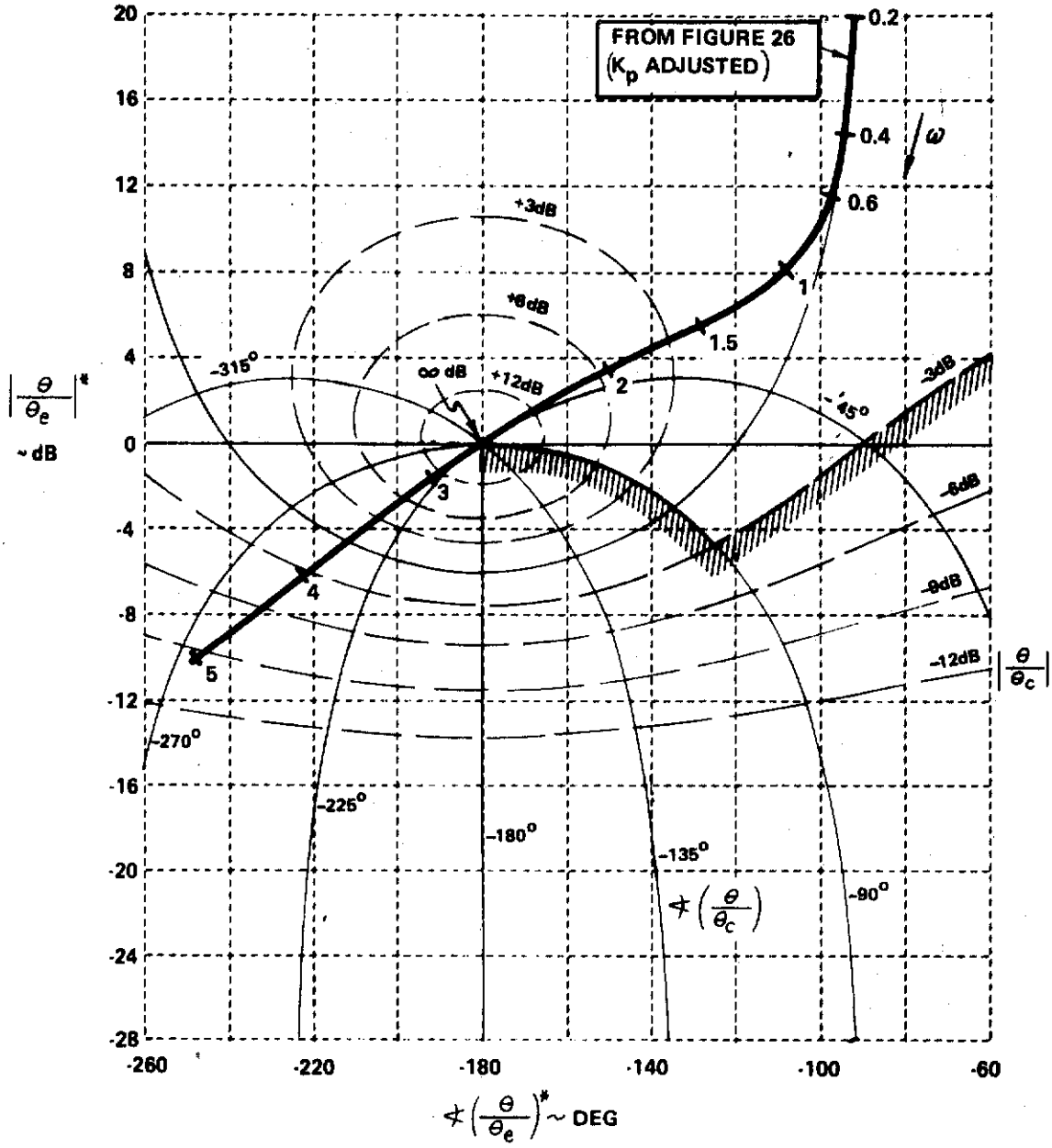

Figure 27. Overlay of $|\theta/\theta_e|^*$ Versus $\not\left(\theta/\theta_e\right)^*$ on a Nichols Chart (Configuration with Low ω_{sp})

60 degrees of lead corresponds to $\tau_{p_1}\,\omega = 1.77$ or $\tau_{p_1} = .59$ sec. Using this value of τ_{p_1}, the compensated amplitude-phase curve can be determined by graphically adding the amplitude and phase of Figure 25 to the uncompensated curve of Figure 27.

The graphical addition process is illustrated in Figure 28. In applying the process, the uncompensated amplitude-phase overlay of Figure 27 is positioned on the "optimum" compensation plot of Figure 25 so that each of several frequencies, in turn, is located at the origin (the particular position illustrated in Figure 28 is for $\omega = 3$ rad/sec. After the compensated amplitude and phase are determined for each frequency, the complete amplitude-phase curve from Figure 28 can be positioned on a Nichols chart so that the performance standards are met for $\omega \leq 3$ rad/sec, as in Figure 29. Normally, an educated guess at a modified value of τ_{p_1} must be made and the process must be repeated to simultaneously achieve a bandwidth equal to 3 rad/sec and a droop equal to -3dB. In this example, however, the initial estimate of τ_{p_1} has achieved the desired result without modification (as shown in Figure 29).

Comparison of Figure 29 with Figure 27 shows that the use of lead compensation has allowed the pilot to reduce the resonance to a negligible value, while maintaining a bandwidth of 3 rad/sec and a droop of -3 dB. A summary of the open-loop and closed-loop characteristics for this configuration is shown on the Bode plots of Figure 30.

6.8 Example of a Configuration Having High ω_{sp}

The second example chosen is a 250 kt configuration with a high short-period frequency and good damping ($\omega_{sp} = 9.7$ rad/sec, $\zeta_{sp} = 0.63$), with negligible control system dynamics (3A). Again, $F_s/n = 5$ lb/g and $K_\theta = .77 \frac{\text{deg/sec}}{\text{lb}}$.

The first step in the analysis is to see what can be accomplished by adjusting the pilot gain alone, without lead or lag compensation. The open-loop Bode characteristics for the example configuration plus the simplified pilot model ($\frac{\theta^*}{\theta_e} = K_p e^{-.3s} \frac{\theta}{F_s}$) are shown in Figure 31 (for $K_p = 1.0$ lb/deg).

The effects of changing K_p can then be seen by overlaying a plot of $|\theta/\theta_e|^*$ versus $\angle (\theta/\theta_e)^*$ on a Nichols chart. Such an overlay is shown in Figure 32, positioned on the Nichols chart so that K_p is just large enough to meet the performance standards.

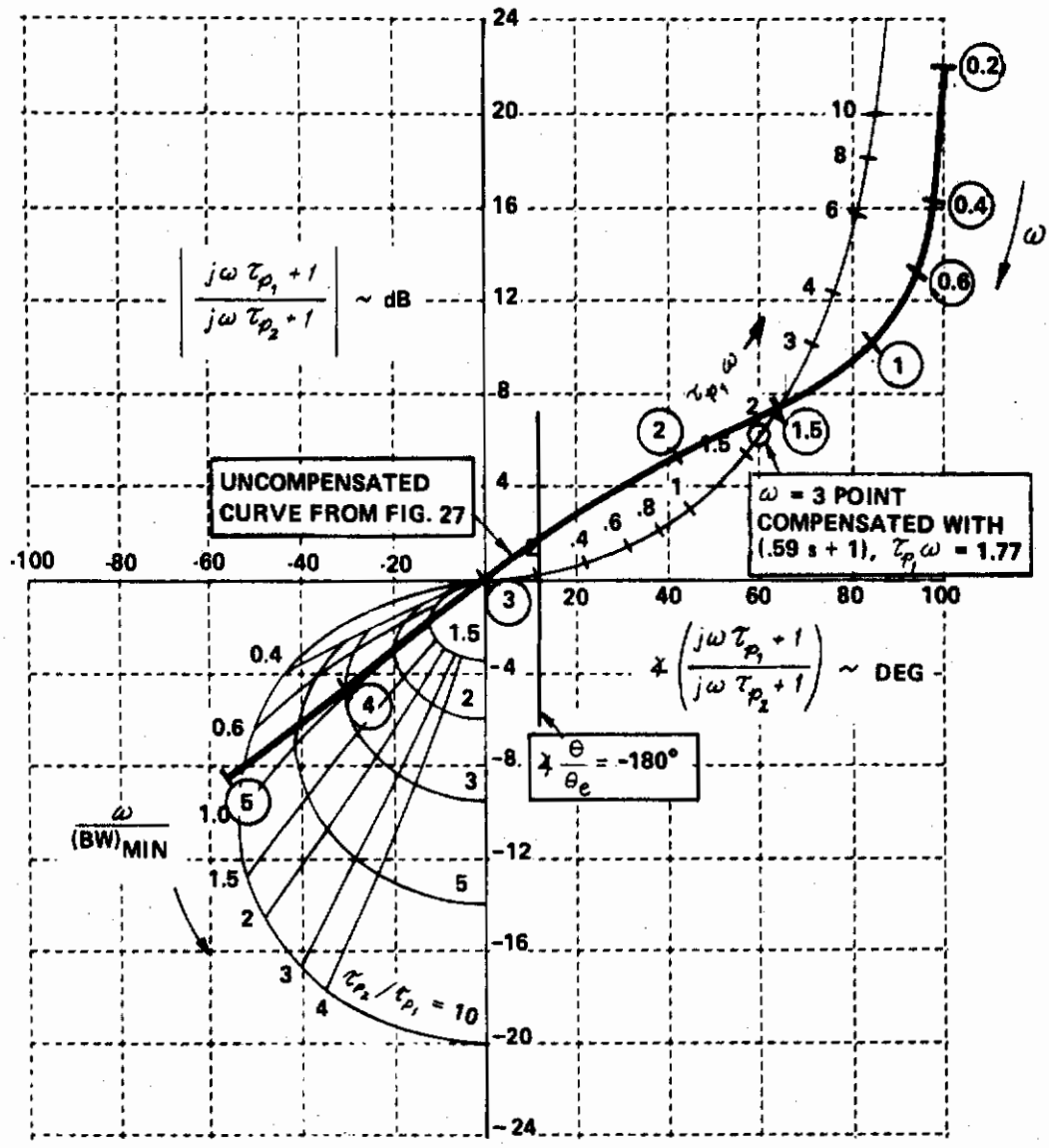

Figure 28. Effects of Pilot Lead Compensation on the Uncompensated Amplitude-Phase Curve (Configuration with Low ω_{SP})

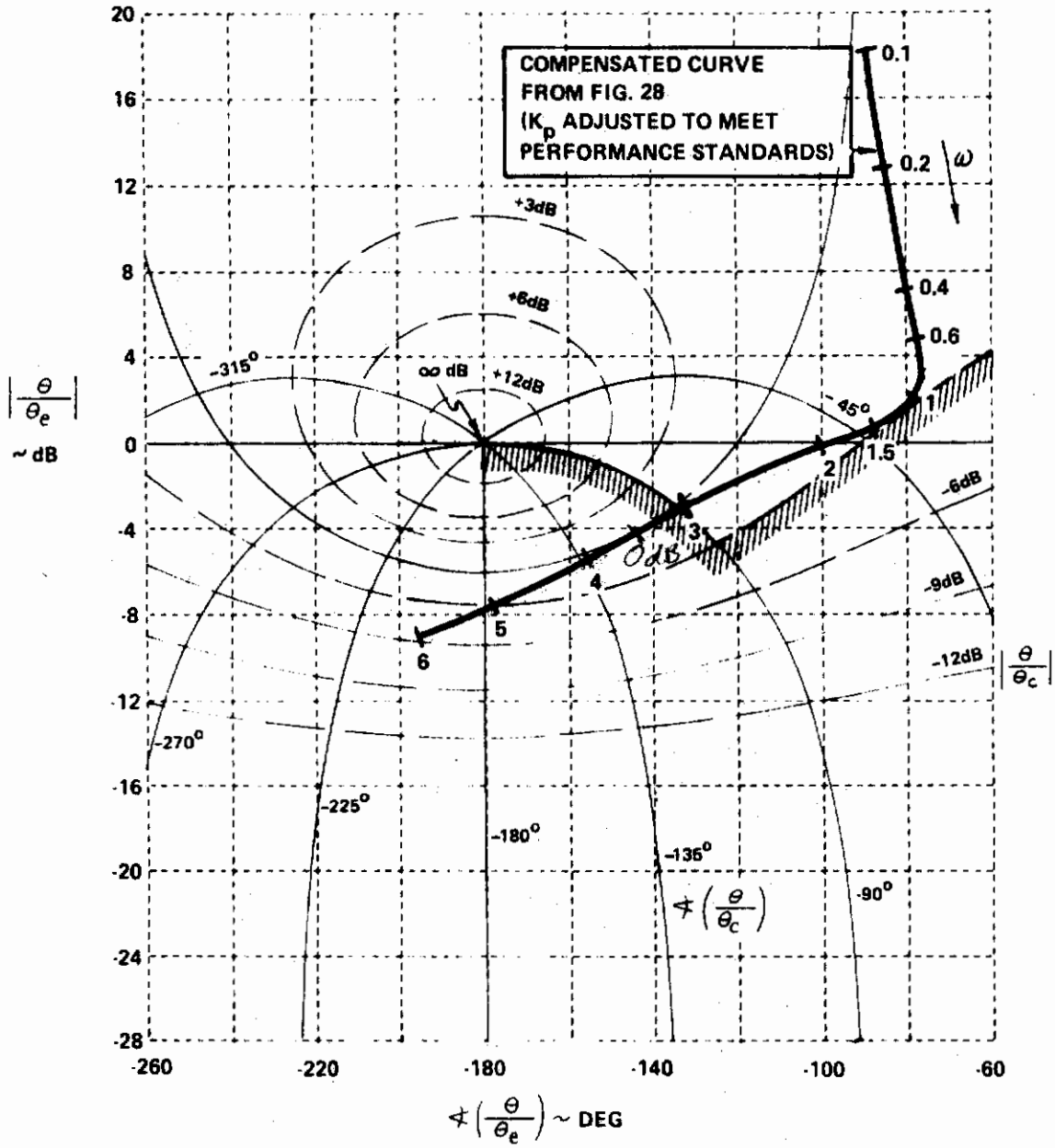

Figure 29. Lead-Compensated Amplitude-Phase Curve Overlayed on a Nichols Chart (Configuration with Low ω_{SP})

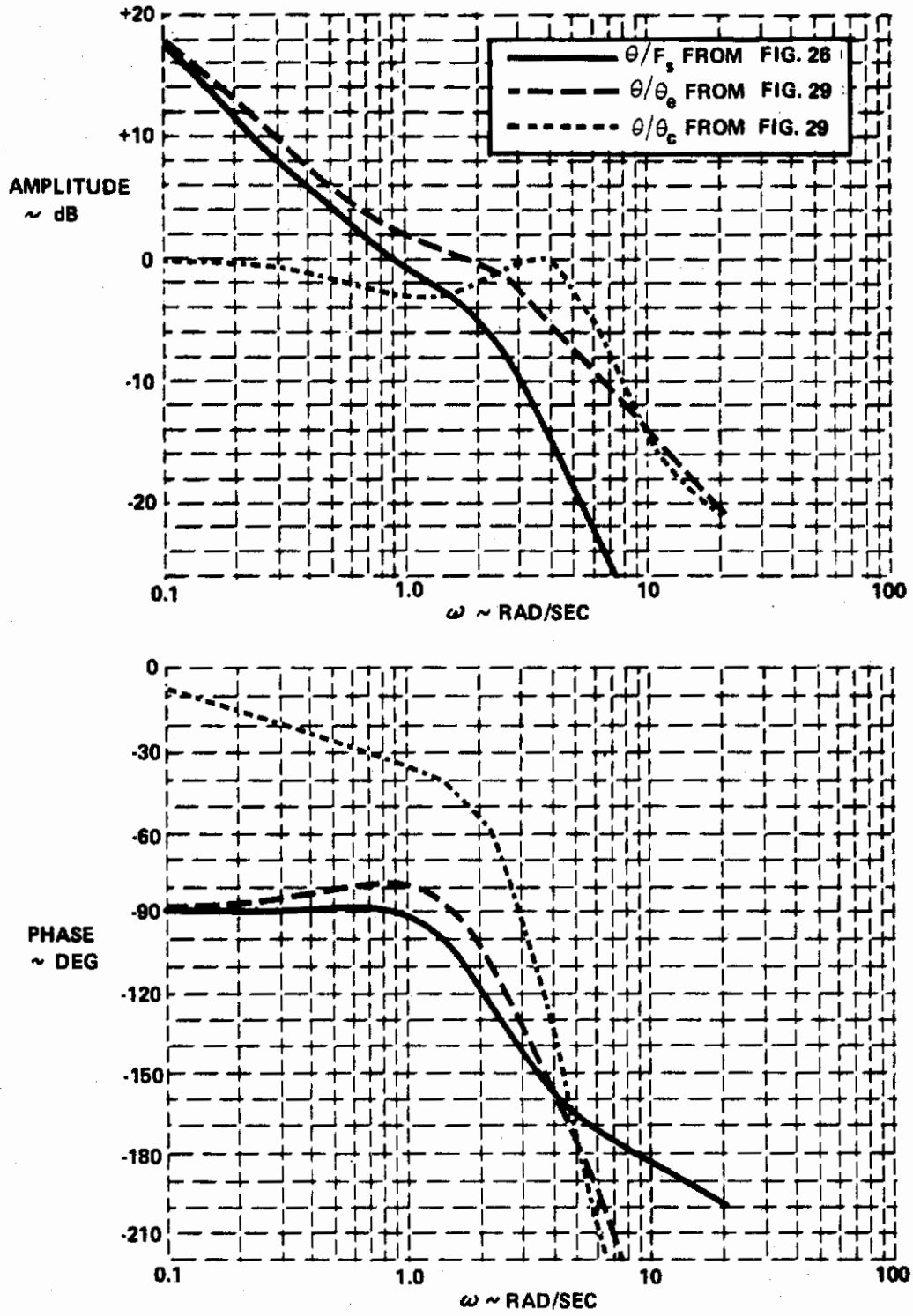

Figure 30. Open-Loop and Closed-Loop Bode Plots for Configuration with Low ω_{sp}

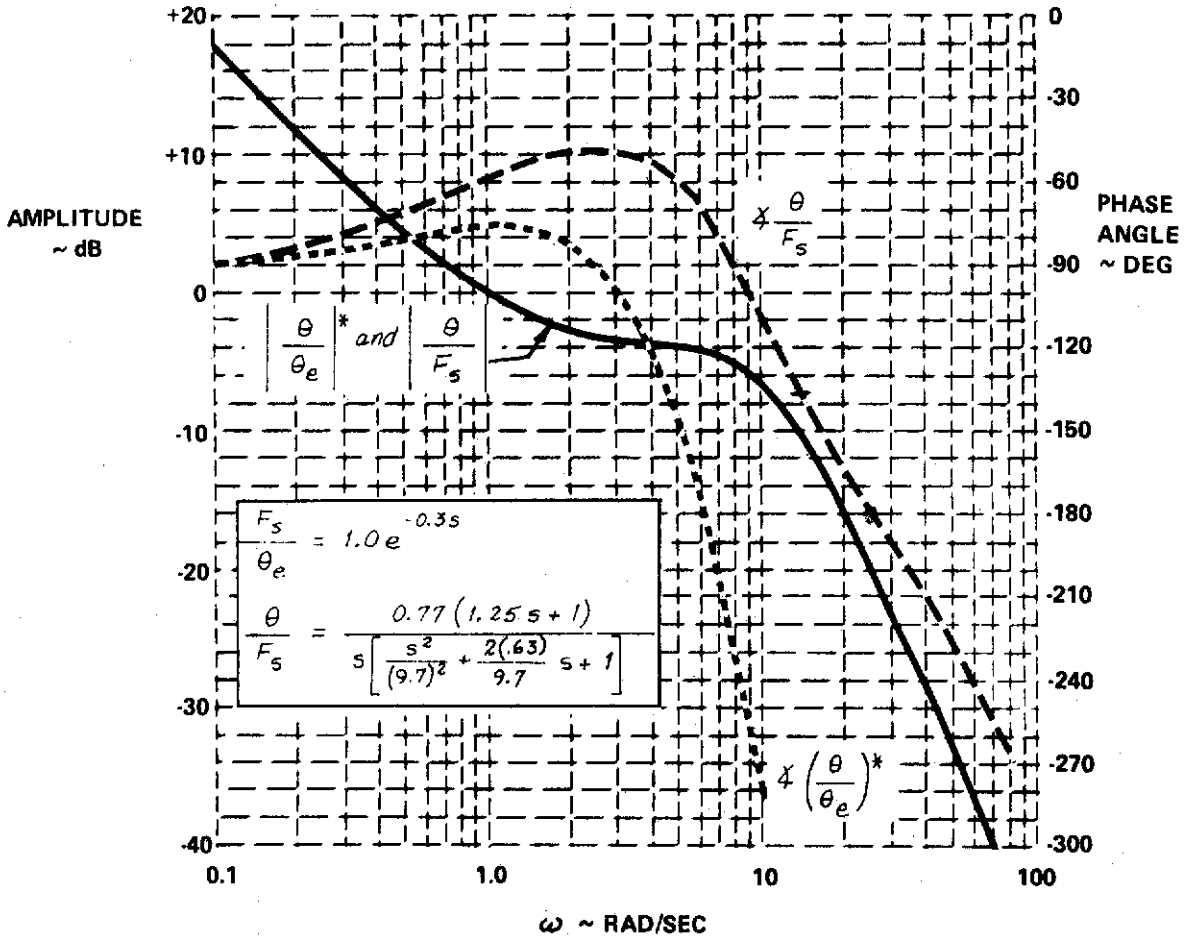

Figure 31. Open-Loop Bode Characteristics for a Configuration Having High ω_{sp}

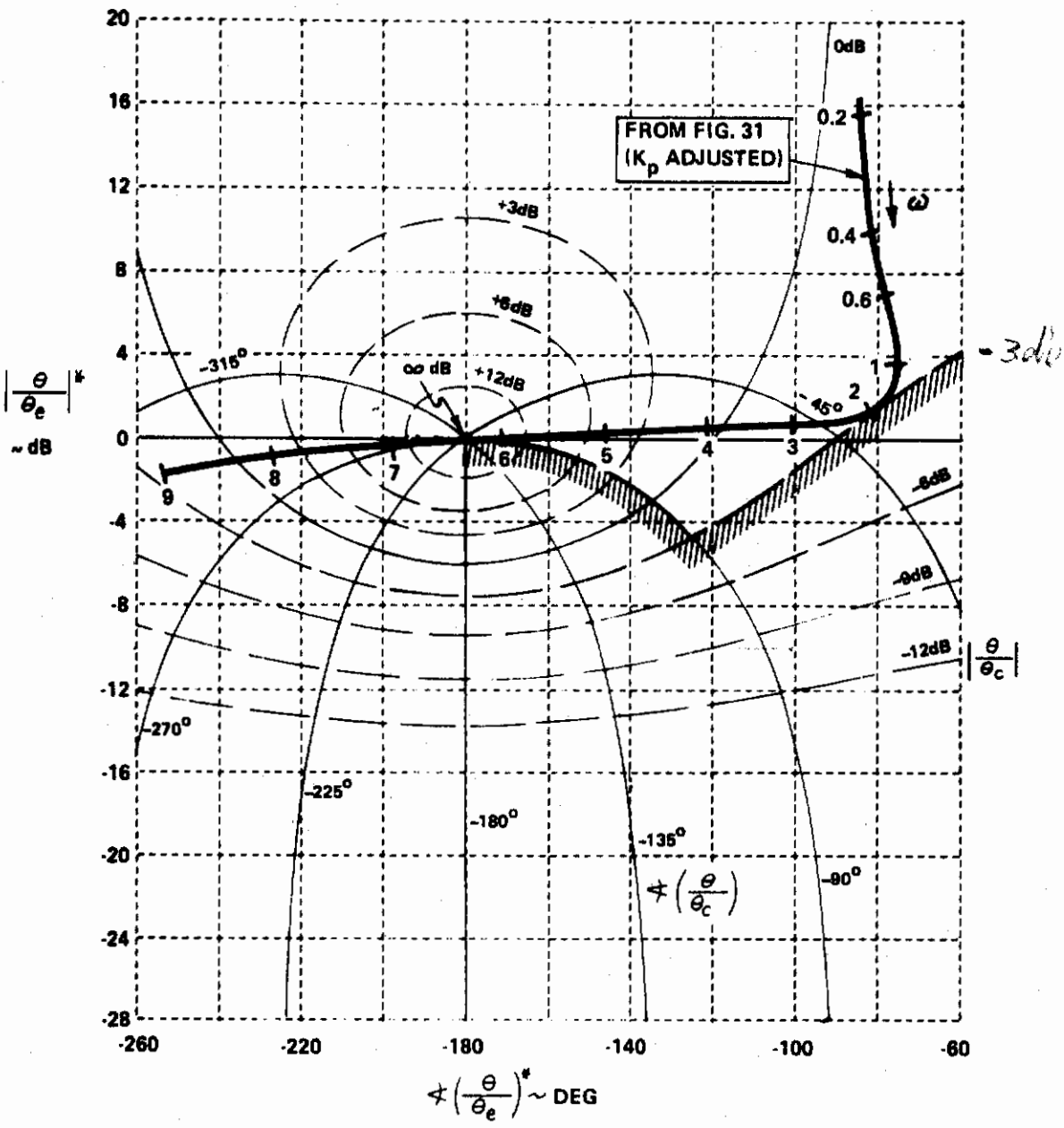

Figure 32. Overlay of $|\theta/\theta_e|^*$ Versus $\angle(\theta/\theta_e)^*$ on a Nichols Chart (Configuration with High ω_{sp})

Notice that in limiting to a droop of -3 dB, a resonance (which is almost zero damped) occurs at ω = 6.3 rad/sec. Also notice that the bandwidth is 6 rad/sec. Obviously lag compensation can be used to reduce the resonance, while still meeting the performance standards.

Using Figure 25, the "optimum" pilot lag compensation can be determined by choosing the value of $\tau_{\rho_2}/\tau_{\rho_1}$ which will cause the bandwidth to exactly equal 3 rad/sec and the maximum droop to exactly equal -3 dB. An initial guess at the optimum value of $\tau_{\rho_2}/\tau_{\rho_1}$ can be made by observing that the uncompensated $\angle (\theta/\theta_e)^*$ at ω = 3 rad/sec is roughly -100 degrees (see Figure 32). By analogy to the example of Section 6.7, about 30 degrees of phase lag at ω = 3 can be used. Figure 25 shows that this corresponds to $\tau_{\rho_2}/\tau_{\rho_1}$ = 3.0. Using this value of $\tau_{\rho_2}/\tau_{\rho_1}$, the compensated amplitude-phase curve can be determined by graphically adding the amplitude and phase of Figure 25 to the uncompensated curve of Figure 32. Overlaying the compensated curve on a Nichols chart, an educated guess at a modified value of $\tau_{\rho_2}/\tau_{\rho_1}$ can be made which will simultaneously achieve a bandwidth equal to 3 rad/sec and a droop of -3 dB. The graphical addition process is illustrated in Figure 33, for the final value of $\tau_{\rho_2}/\tau_{\rho_1}$ = 2.5 (τ_{ρ_1} and τ_{ρ_2} can be found from Figure 24). In applying the process, the uncompensated amplitude-phase overlay of Figure 32 is positioned on Figure 25 so that each of several frequencies, in turn, is located at the origin. (The particular position shown in Figure 33 is for ω = 6 rad/sec).

Figure 34 shows the compensated amplitude-phase curve from Figure 33 positioned on a Nichols chart so that the performance standards are met for $\omega \leq 3$ rad/sec. Comparison of Figure 34 with Figure 32 shows that the use of lag compensation has allowed the pilot to reduce the closed-loop resonance to a negligible value, while maintaining a -3 dB droop and a minimum bandwidth of 3 rad/sec. A summary of the open-loop and closed-loop characteristics for this configuration is shown on the Bode plots of Figure 35.

6.9 Factors Influencing Pilot Opinion

The parameters K_ρ , τ_{ρ_1} , τ_{ρ_2} which the pilot would choose in "adapting" to a particular configuration, together with the resulting closed-loop performance characteristics, can be determined from the preceding analysis. It now remains to relate the primary pilot opinion factors, discussed in Section 5.1, to the various parameters determined from the analysis. Based on a detailed study of the pilot comments (Appendix I), the following relationships are offered:

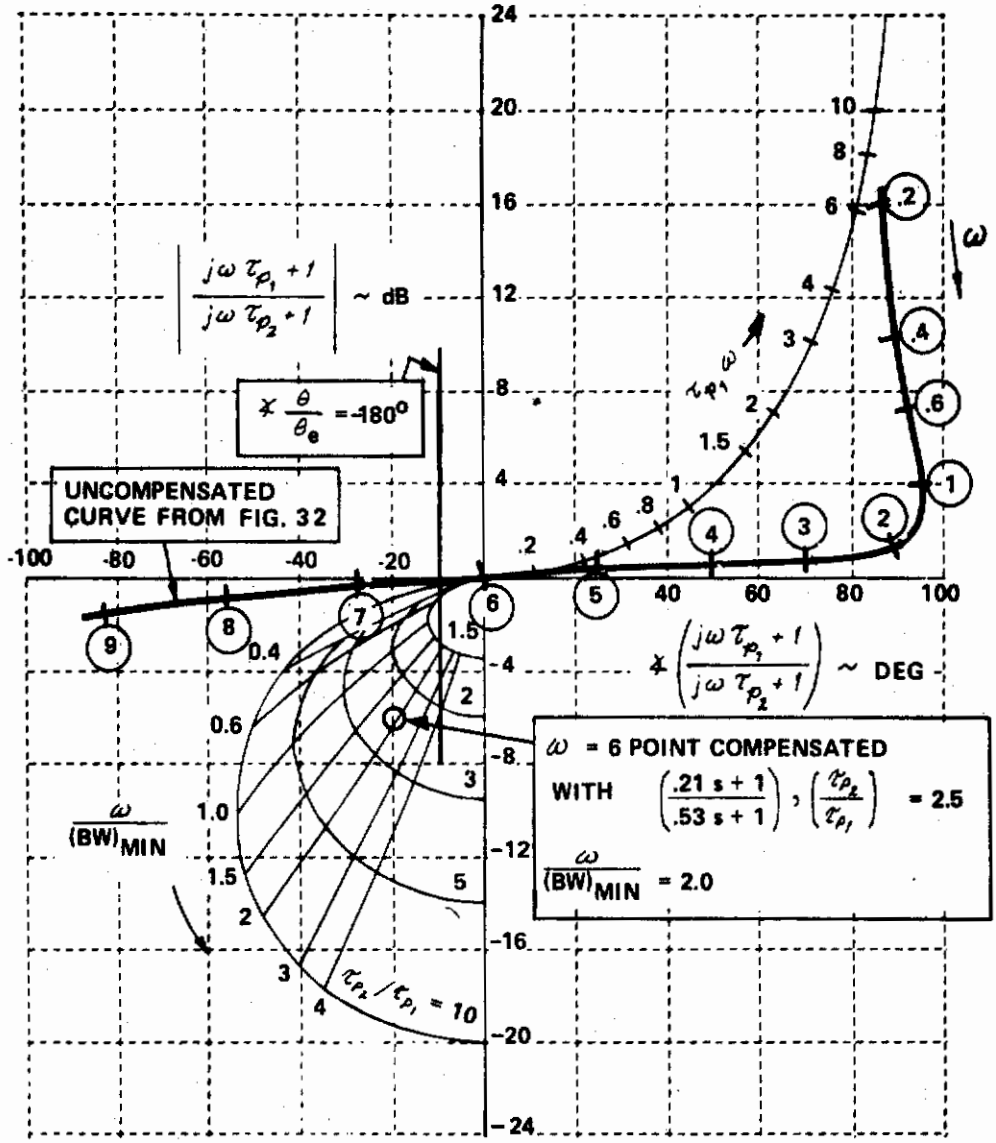

Figure 33. Effects of Pilot Lag Compensation on the Uncompensated Amplitude-Phase Curve (Configuration with High ω_{sp})

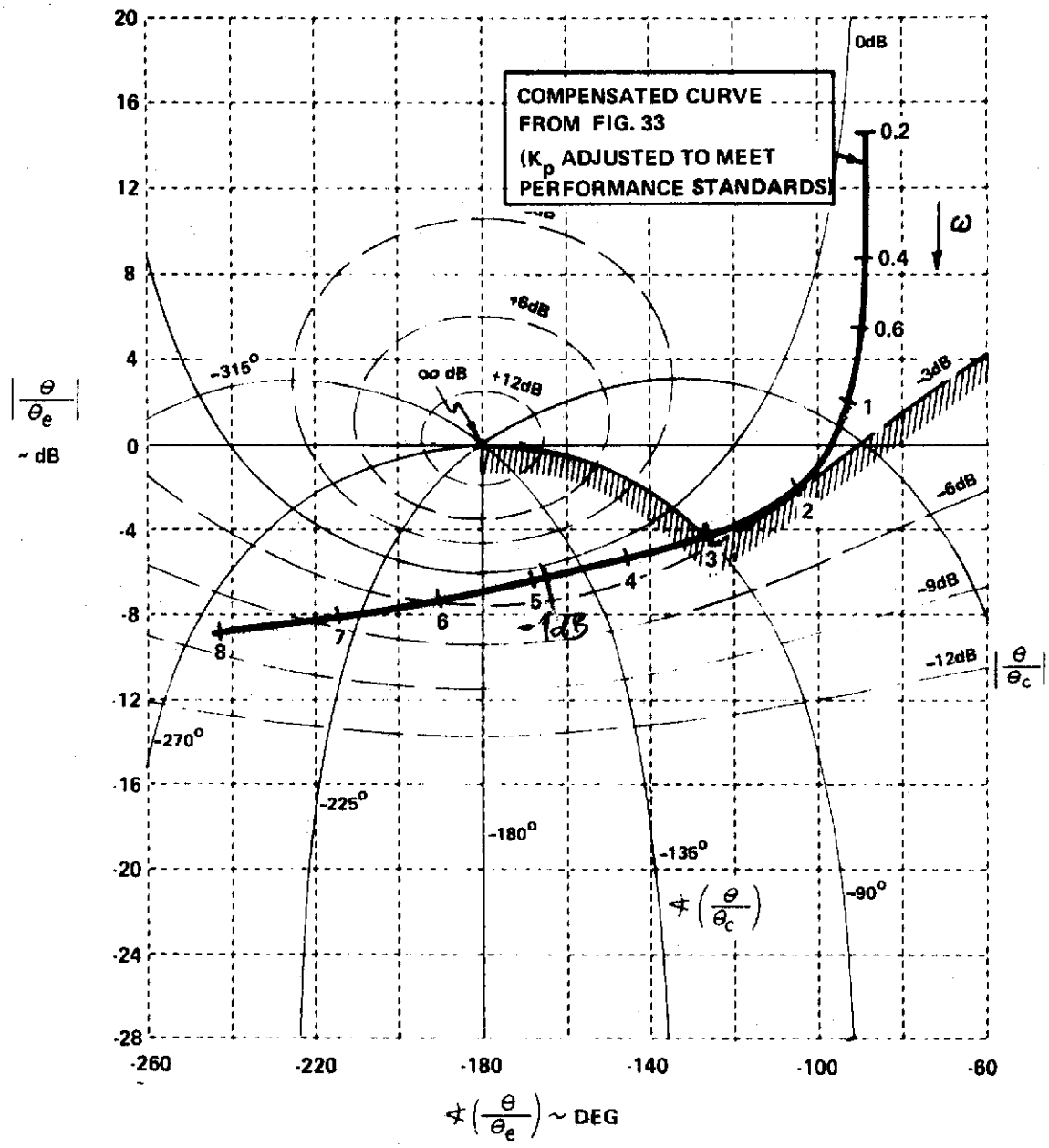

Figure 34. Lag-Compensated Amplitude-Phase Curve Overlayed on a Nichols Chart (Configuration with High ω_{sp})

Need at least BW = 3, $|\theta/\theta_c|_{DC}$ = 0dB with droop < 3dB ?

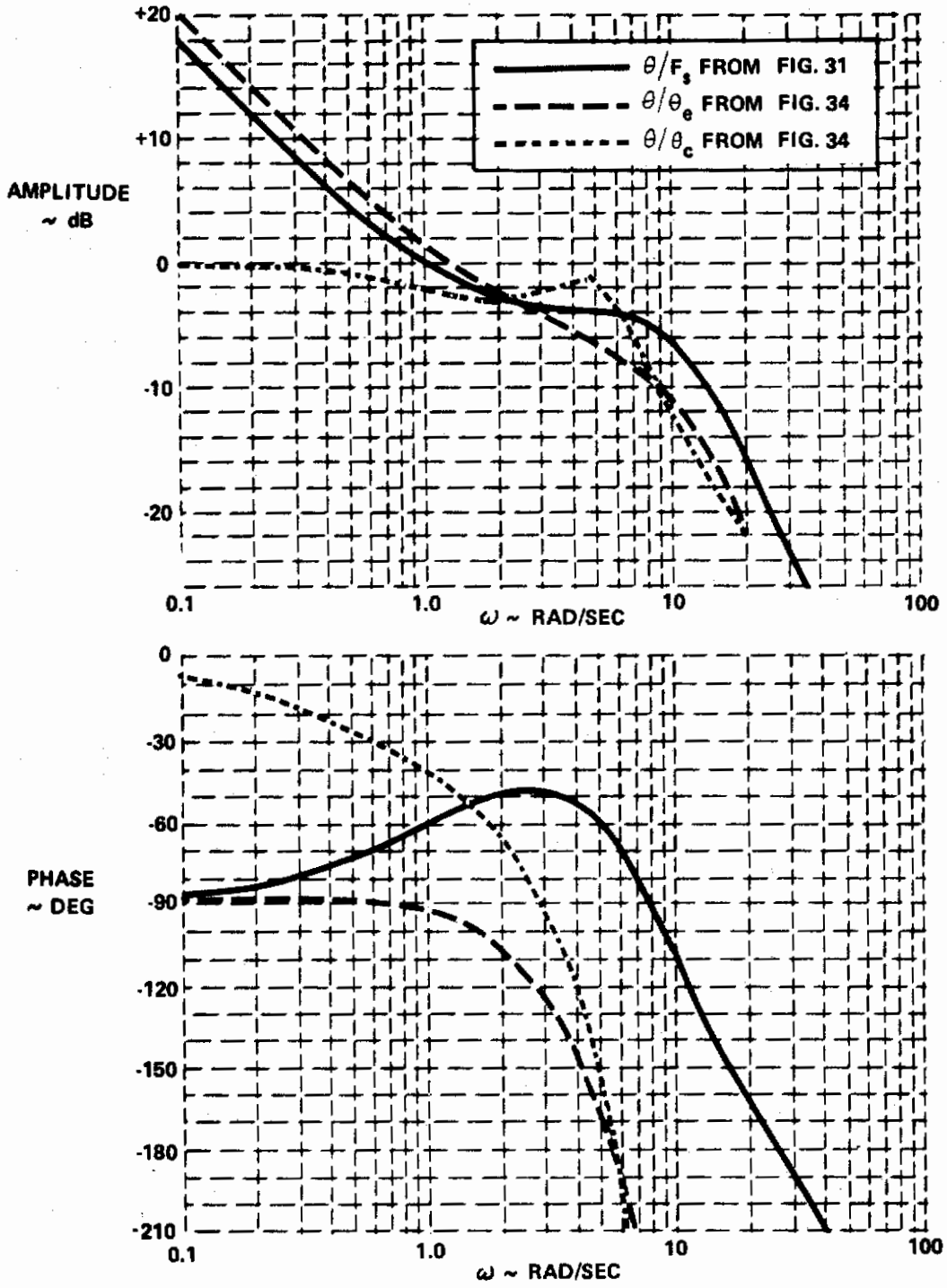

Figure 35. Open-Loop and Closed-Loop Bode Plots for Configuration with High ω_{sp}

(1) PIO Tendencies It seems straightforward to relate the pilot's complaints of oscillatory tendencies to the closed-loop resonance $|\theta/\theta_c|_{max}$

(2) Pilot Compensation It would seem that the pilot's comments concerning his compensation are closely related to whether he has to generate phase lead or phase lag (over and above the phase lag caused by his 0.3 second time delay). Since the phase characteristics are most important for frequencies in the vicinity of the bandwidth, it seems logical to describe the pilot's compensation in terms of the following phase angle:

$$\angle_{pc} = \angle \left(\frac{j\omega \tau_{p_1} + 1}{j\omega \tau_{p_2} + 1} \right)_{\omega = (BW)_{min}}$$

This phase angle can be determined from Figure 25 for the particular value of (τ_{p_2}/τ_{p_1}) or τ_{p_1} used. For the example of Section 6.8, Figure 25 shows that $\angle_{pc}$ is -25 degrees at $\omega = 3$ ($\tau_{p_2}/\tau_{p_1} = 2.5$). For the example of Section 6.7, $\angle_{pc}$ is + 60 degrees ($\tau_{p_1} = .59$, $\tau_{p_1}\omega = 1.77$ at $\omega = 3$). $\angle_{pc}$ will be positive for lead compensation and negative for lag compensation. Thus, when the pilot complains of having to "overdrive" the airplane, $\angle_{pc}$ will probably be positive. When he complains of having to "fly it smoothly", $\angle_{pc}$ will probably be negative.

(3) Stick Forces During the experiment, the pilots often complained of the incompatibility between the steady stick forces and the initial forces (or forces required for tracking). It is clear, from the comments, that the steady forces referred to are related to the steady-state stick force per g (F_s/n). The comments concerning tracking forces are probably related to the pilot's gain; but since the pilot uses the term "initial" forces, K_p is clearly not the gain in question since it is a steady-state gain. Because of this, it would seem logical to use the pilot's gain at some intermediate frequency (say, at $\omega = (BW)_{min}$) as a measure of the tracking forces. To this end, the following gain is defined:

$$K_{BW} = |F_s/\theta_e|_{\omega = (BW)_{min}}$$

where $\left|F_s/\theta_e\right| = \left|K_\rho \left(\frac{j\omega\tau_{\rho_1}+1}{j\omega\tau_{\rho_2}+1}\right)\right|$

The easiest way to compute K_{BW} is from the following compensated open-loop characteristics:

$$\left|\theta/\theta_e\right|_{\omega=(BW)_{min}} = \underbrace{\left|\frac{F_s}{\theta_e}\right|_{\omega=(BW)_{min}}}_{K_{BW}} \times \left|\frac{\theta}{F_s}\right|_{\omega=(BW)_{min}}$$

$$K_{BW} = \frac{\left|\theta/\theta_e\right|_{\omega=(BW)_{min}}}{\left|\theta/F_s\right|_{\omega=(BW)_{min}}}$$

For the example of Section 6.8, Figure 34 shows that:

$$\left|\theta/\theta_e\right|_{\omega=3} = -4.5 \text{ dB} = 0.60$$

and Figure 31 shows that (Figure 31 is based on F_s/n = 5 lb/g):

$$\left|\theta/F_s\right|_{\omega=3} = -3.5 \text{ dB} = 0.67 \text{ deg/lb}$$

so that

$$K_{BW} = 0.90 \text{ lb/deg}$$

As will be shown in Section 7.2, K_{BW} appears to have been a strong factor in only a few configurations evaluated in the present experiment.

If the value of K_ρ is desired, it can be computed from K_{BW} as follows:

$$K_p = K_{BW} \left| \frac{j\omega\tau_{p_1} + 1}{j\omega\tau_{p_2} + 1} \right|^{-1}_{\omega = (BW)_{min}}$$

For the present example, the magnitude of the compensation at $\omega = 3$ is -4 dB (determined from Figure 25 with α_{pc} = - 25 degrees), or 0.64 in linear magnitude . Thus,

$$K_p = 0.90\ (0.64)^{-1} = 1.4\ \text{lb/deg}$$

The purpose of Section VII is to correlate $|\theta/\theta_c|_{max}$, α_{pc}, K_{BW} with the detailed pilot comments and ratings.

SECTION VII

APPLICATION OF THE ANALYSIS TO THE EXPERIMENTAL RESULTS

Each configuration evaluated in the present experiment was analyzed using the techniques presented in Section VI. For each configuration, the various parameters resulting from the analysis are presented in Appendix I, along with the pilot comments. Appendix I also presents open-loop and closed-loop time histories and Bode plots for each configuration. In addition, Tables II and III summarize the more important parameters from the analysis.

The purpose of Section VII is to discuss the results of the analysis, beginning with a discussion of the importance of closed-loop bandwidth. Next, the pilot comments are explained in light of the analysis and the pilot ratings are correlated with the analysis parameters. Finally, the analysis is applied to the results of some special T-33 flights and to the HOS data.

7.1 Effect of Bandwidth

One of the first things which became apparent during the analysis was the importance of $(BW)_{min}$. To illustrate its importance, consider configuration 6E. This configuration has a low short-period frequency(ω_{sp} = 3.4 rad/sec) with good damping, and considerable lag in the control system ($1/\tau_2$ = 3.3 rad/sec).

If the analysis of Section VI is applied to this configuration, lead compensation is required to achieve any reasonable bandwidth. A value of $\angle_{pc}$ equal to + 71 degrees is needed to achieve a $(BW)_{min}$ of 3 rad/sec, and the resulting resonance ($|\theta/\theta_c|_{max}$) is + 6 dB. (This would correspond to $\zeta \approx .25$ for a simple second-order system.) If $(BW)_{min}$ is 3.5 rad/sec, however, $\angle_{pc}$ of + 78 degrees is required, and the resonance becomes very large (+ 12 dB). This appears to be a rather dramatic change in the closed-loop resonance for a rather small change in $(BW)_{min}$. Before concluding that this is unrealistic, however, consider two separate evaluations of the same configuration by Pilot M.

On Flight No. 1040, Pilot M complained of some tendency to PIO during attitude tracking tasks, but the PIO's were not full-blown. He gave the airplane a PR of 5.5, with a PIO rating of 2.5. On Flight No. 1071, Pilot M complained that the airplane was PIO prone, with large amplitude oscillations. He observed that any aggressive tracking or maneuvering led to PIO's. He assigned the airplane a PR of 8.5 and a PIO rating of 5.

It is clear that Pilot M was not striving for the same standard of performance for both evaluations. The comments give the impression that the pilot flew the configurations more aggressively on Flight 1071 than on 1040. This could be interpreted as meaning that he was striving for a higher $(BW)_{min}$. With these ideas in mind, a resonance of 6 dB (for BW = 3) seems consistent with the PIOR of 2.5 on Flight 1040, while a resonance of + 12 dB (for BW = 3.5) appears to explain the PIOR of 5 on Flight 1071.

The pilot comments for the two flights also indicate differences in the IFR tracking tasks. On Flight 1040, Pilot M commented that he never got into anything that approached a full-blown PIO during the IFR tracking tasks. During Flight 1071, however, he said that he could get into beautiful PIO's when he tried to do the job. Typical IFR tracking records for the two flights are shown in Figure 36. The discrete error records show that the airplane initially reached the target sooner on Flight 1071, clearly indicating a higher closed-loop bandwidth. A price is paid for reaching the target sooner, however, in the form of more pronounced oscillations. The random-error records show the same trend: Flight 1040 shows decreased oscillations, but the low frequency performance is poor.

On the basis of the above considerations, it can be seen that the closed-loop bandwidth the pilot is trying to achieve, $(BW)_{min}$, is a very important flying qualities parameter, for two reasons:

(1) It has a very strong effect on PIO tendency (closed-loop resonance), as well as the pilot compensation required.

(2) It is a very difficult parameter for the pilot to quantify. The reason for this is that BW is simply a measure of how aggressively the pilot feels he must initially move the nose up to the target, and is based on his experience and the task being evaluated. (The importance of defining the task precisely in a flying qualities experiment is obvious.)

It is felt that these two considerations may be the major factors responsible for the scatter in pilot comment and rating data which is characteristic of many flying qualities experiments. In fact, it is remarkable that pilots are able to perform evaluations as consistently as they do, in view of the strong effects of $(BW)_{min}$.

Aside from the influence of $(BW)_{min}$ on scatter in the data, there is one other effect in the present experiment which should be mentioned. One of the evaluation limitations discussed in Section 4.5 is that the buffet boundary of the T-33 at 250 knots apparently caused the pilots to fly the 250 knot configurations somewhat less aggressively than the 350 knot configurations. This would suggest that the pilots decreased $(BW)_{min}$ for the

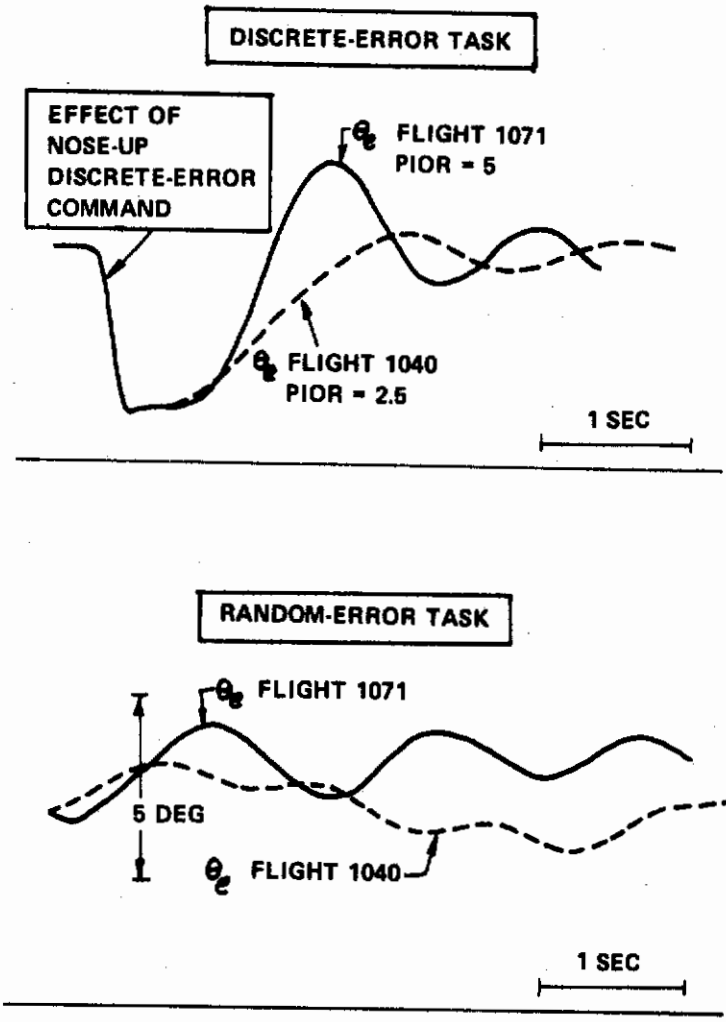

Figure 36. Typical IFR Tracking Records for Configuration 6E

low-speed cases. Analysis of the 350 knot data, using a $(BW)_{min}$ of 3.5 rad/sec, resulted in values of χ_{pc} and $|\theta/\theta_c|_{max}$ which correlated very well with the pilot comments. The pilot comments for the 250 knot configurations, however, were not as severe as the results of using $(BW)_{min} = 3.5$ would indicate. A value of $(BW)_{min}$ equal to 3 rad/sec was then tried for the low speed cases, which resulted in good correlation with the comments.

Therefore, to account for the fact that the pilots flew the low speed configurations somewhat less aggressively, the following values of $(BW)_{min}$ were used in analyzing the results of this experiment.

V_{ind}	$(BW)_{min}$
250 kt	3.0 rad/sec
350 kt	3.5 rad/sec

7.2 Correlation with Pilot Comments

The purpose of this subsection is to interpret the pilot comment data of Appendix I in terms of the various parameters resulting from the pilot-in-the-loop analysis. The various comment categories from Appendix I will be handled in the following way:

Stick Forces — Stick forces, per se, and the selection of elevator gearing will be discussed in detail only when the forces appear to be a strong factor in the overall pilot opinion. A more detailed discussion of stick forces will be given in Section 7.4.

Predictability of Response and Attitude Control/Tracking Capability — The comments under these two headings are the primary pilot opinion factors for virtually every configuration evaluated. They form the core of the following discussions and will normally be correlated with the parameters $\not\angle_{pc}$ and $|\theta/\theta_c|_{max}$.

Normal Acceleration Control — This will not normally be mentioned because the difficulties in g control are usually similar to those of attitude control, but are less severe. In a few cases, however, g control seems to be equally as difficult as attitude control; these cases will be discussed.

Effect of Random Disturbances — This will not be discussed unless it appears to be a strong factor.

IFR Problems — These comments usually deal with problems encountered during the IFR tracking tasks. If important, these comments will be incorporated into the discussions of attitude control/tracking capability.

Good Features and Objectionable Features These comments summarize the specific comments above, and will be incorporated into the specific discussions.

To aid the reader in following the discussion of the pilot comments, Figure 37 relates $|\theta/\theta_c|_{max}$ to the damping ratio of a second-order system having the same $|\theta/\theta_c|_{max}$.

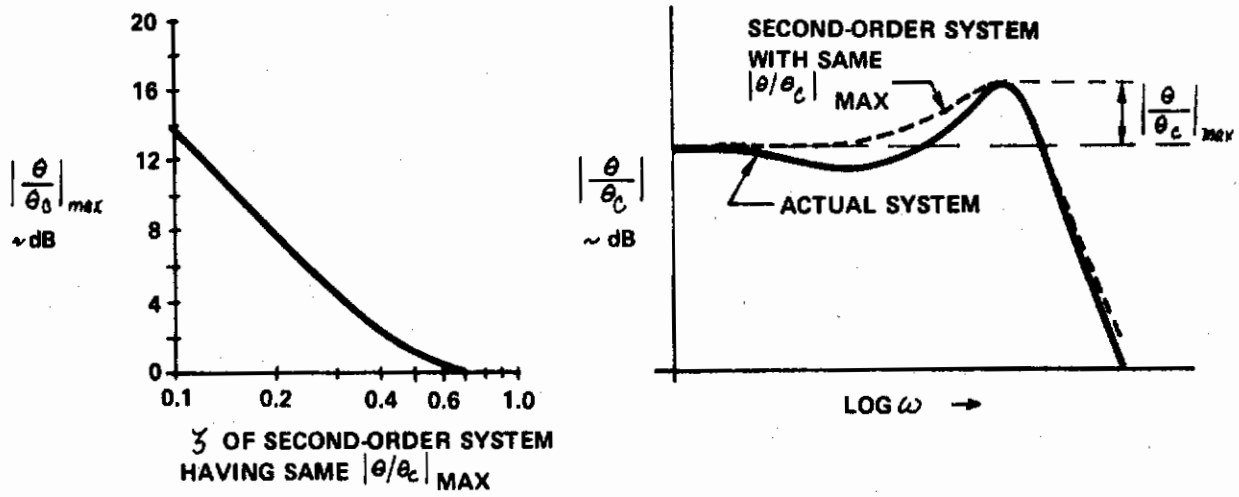

Figure 37. Damping Ratio of Simple Second-Order System as a Function of $|\theta/\theta_c|_{max}$

This is a crude relationship at best because the actual system is not second order, but it should give the reader some physical feeling for the parameter $|\theta/\theta_c|_{max}$. Perhaps a better appreciation for the physical significance of $|\theta/\theta_c|_{max}$ can be obtained by referring to the closed-loop time histories shown in Appendix I for each configuration.

Configuration 1 (A to G), ω_{sp} =2.2, ζ_{sp} =0.69, n/α =18.5

The pilot-in-the-loop analysis predicts pilot lead compensation, τ_{pc} = + 60 degrees, for the base configuration for this group (Configuration 1D) with no tendency to oscillate in pitch attitude tracking, $|\theta/\theta_c|_{max}$ = 0 dB. According to the pilot comments, the principal problem with this configuration is centered around the slow initial response. The pilot must learn to "overdrive" the airplane to achieve the desired initial response, then quickly take out the input as the response develops in order to stop the airplane on a target. He often describes the control inputs required as pulse-like. In this situation, the final response is difficult to predict and some pilot effort is required to learn the correct control inputs to quickly and accurately acquire a target. The initial forces appear heavy to the pilot and lighten up dramatically as the response develops. The pilot must learn to anticipate the airplane's response; in other words, he must introduce lead compensation. Pilot W's comments indicate that he can learn to generate the required lead compensation but only with some effort. Pilot M, on the other hand, expresses difficulty in predicting the final response and complains of overcontrolling or overshooting tendencies in g control, as well as in pitch attitude control. The pilots refer to overcontrol in g as a "digging-in" tendency which is bothersome. In summary, the pilot comments make no mention of oscillations, which is consistent with the predicted resonance of 0 dB. However, there are complaints about overcontrolling tendencies. It is apparently difficult for the pilot to consistently generate the considerable lead compensation required to achieve the desired performance. This difficulty leads to poor precision of control, as shown by the pilot comments.

The closed-loop analysis indicates that the addition of moderate control-system lead to the base configuration is beneficial. For example, in Configuration 1B, reduced lead compensation (τ_{pc} = + 35 degrees) is predicted and the resonance is still very small (+ 0.5 dB). The pilot comments are, in general, consistent with these values. There are no oscillatory tendencies noted and Pilot W comments that a fast-pulse technique was used with success, confirming that some lead compensation is needed. Minor complaints are made about the airplane's tendency to "dig in" or overshoot, which reflects the difficulty that the pilot has in accurately generating the required lead, particularly in gross maneuvers.

With further increase in control-system lead, as in Configuration 1A, the analysis indicates a + 7 dB resonance and the requirement for some pilot lead compensation, τ_{pc} = + 20 degrees. The pilot comments indicate that the main problem is in pitch attitude control, although considerable scatter exists in the pilot ratings and comments for this configuration. The comments show that it is difficult to acquire a target, the response takes off, and the final response is oscillatory with some PIO tendency in the IFR tracking tasks. These comments are consistent with the trend predicted in the analysis, although the + 7 dB resonance is perhaps more severe than the

comments indicate. Rapid pulse-type inputs are used, correlating with the predicted requirements for pilot lead compensation. The problems noted for g control are similar to the pitch attitude control problems. The pilot comments also indicate a problem with the stick forces which may have influenced the pilot ratings. A discussion of the possible reasons for this problem will be made in Section 7.4.

For Configuration 1C, which has the same control-system lead characteristics as 1B but with ω_s = 16 rad/sec, the closed-loop analysis predicts a + 2 dB resonance and the requirement for more lead compensation than for 1B (χ_{pc} = + 42 degrees). The pilot comments for Configuration 1C do show increased problems with pitch attitude control and confirm the requirement for lead compensation.

The addition of control-system lag to the base configuration, as in Configurations 1E, F and G, results in increased problems with oscillations in precision tracking and increased pilot lead compensation. In Configuration 1G, for example, the pilot says the tracking capability is poor, practically nil, with PIO's occurring in tight tracking and that pulse-like inputs are required. The closed-loop analysis adequately predicts the trend toward large oscillations in pitch attitude when tracking, as well as the large lead compensation required to get the desired performance. For example, the analysis predicts a zero damped oscillation for Configuration 1G, $\left|\theta/\theta_c\right|_{max}$ = ∞, and χ_{pc} = + 80 degrees.

Figure 38 shows the θ_e, F_s, and n time histories from the flight records for the discrete-error tracking task for Configuration 1G. These records clearly show the pitch attitude tracking problems that the pilot has in trying to follow the step change in pitch attitude commanded by the tracking needle. The frequency of the zero damped oscillation in θ_e is 3 rad/sec (±0.2) which corresponds well with the resonance frequency of 2.7 rad/sec predicted in the analysis. The very large, rapid F_s inputs substantiate the predicted requirement for pilot lead compensation.

Configurations 2 (A to J), ω_{sp} = 4.9, ζ_{sp} = 0.70, n/α = 18.5

The base configuration for this group, Configuration 2D, is described as a nice airplane with good maneuvering characteristics, but with a slight tendency to overshoot the target. The predicted resonance of + 2 dB and χ_{pc} = -5 degrees is certainly consistent with the pilot comments for this configuration.

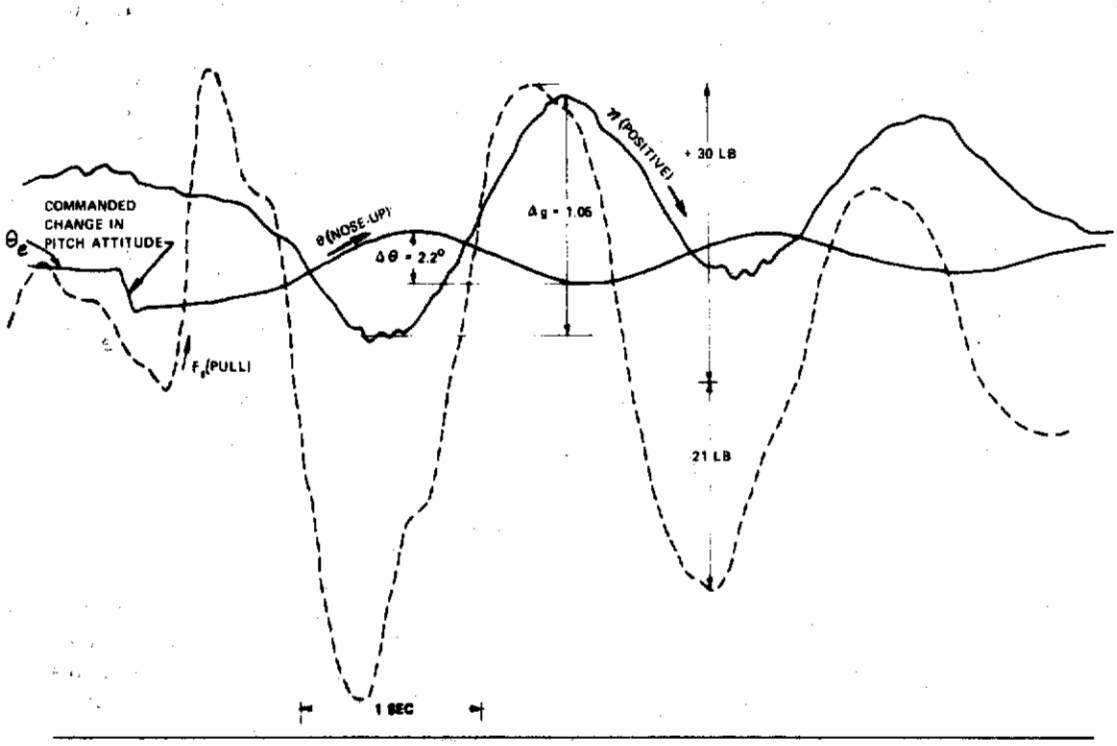

Figure 38. In-Flight Record of a PIO Occurring During Discrete Error Tracking Task. (Configuration 1G, Flight 1061)

For Configuration 2A, which has considerable lead in the control system, the pilots comment on a tendency to overshoot when flown aggressively. Pilot W notes that with smooth inputs (lag compensation) the pitch attitude control becomes quite accurate. The pilot comment that the forces go from light to heavy is typical of configurations that require lag compensation and further evidence of the type of compensation used in this case. The analysis predicts a + 3 dB resonance and $\measuredangle_{pc}$ = -26 degrees, which are consistent with the pilot comments.

The effect of reducing the value of ω_3 from 63 rad/sec in Configuration 2A to 16 rad/sec in Configuration 2B, is to increase the resonance to + 7 dB and leave $\measuredangle_{pc}$ nearly unchanged at -20 degrees. The pilot comments for the last 3 evaluations of Configuration 2B, show increased concern with overshooting the target and occasionally getting out of phase with the airplane response. The comments also describe the need for smooth inputs

(lag compensation). These observations tend to correlate with the results of the analysis.

When first-order lags are introduced into the control system of the base configuration, as in Configurations 2E, F, H, and J, the analysis predicts a resonance which is approximately constant at + 3 dB and the requirement for increasing pilot lead compensation as the lag effects are increased. The pilot comments describe similar trends. As the control system lag is increased, the pilot comments describe the heavy initial forces and the need to "overdrive" the airplane with greater regularity and emphasis, confirming the need for increasing pilot lead compensation. The comments on the pitch-attitude control describe tendencies to oscillate, gradually changing to complaints of overcontrolling as the control system lag is increased. This indicates that the pilots' preoccupation with the closed-loop resonance is giving way to poor predictability of the response due to increased lead compensation.

For the two configurations with ω_3 = 16 rad/sec, in addition to a first-order lag in the control system (Configurations 2G and 2I), the analysis predicts increased resonances and more pilot lead compensation than for the same configurations with ω_3 = 63 rad/sec (2F and H). The + 6 dB resonance and $\angle_{pc}$ = + 35 degrees predicted for Configuration 2G are consistent with the pilot comments, which complain of the tendency toward PIO's and the heavy initial forces. For Configuration 2I, a resonance of + 7 dB and $\angle_{pc}$ = + 59 degrees is predicted. The pilot comments indicate PIO problems and complain about heavy initial forces, confirming that pilot lead compensation is used. The PIO tendencies for both configurations appear to be somewhat more severe than predicted by the analysis.

Configurations 3 (A to E) ω_{sp} = 9.7, ζ_{sp} = 0.63, n/α = 18.5

The analysis predicts that the base Configuration (3A) will require lag compensation ($\angle_{pc}$ = -25 degrees) and the resonance will be negligible ($|\theta/\theta_c|_{max}$ = - 1dB). The pilots comment that the airplane is initially very abrupt and that it must be flown smoothly. This is consistent with $\angle_{pc}$ = -25 degrees. However, there are comments that indicate overshoots or "bobbling" tendencies on target, which are not consistent with a resonance of -1 dB. Much of this tendency to oscillate is explainable in terms of the lag compensation required, which pilots apparently do not like to use. The problem with lag compensation is related to the fact that it is difficult to apply smooth inputs consistently in the context of the fighter mission. For Configuration 3A, the 25 degrees of lag compensation is necessary to prevent oscillations, so that oscillations will obviously result whenever the

pilot inadvertently applies an abrupt input. Figure 39 illustrates the extreme effect of removing the lag compensation entirely (for constant pilot gain K_p). It is important to note that this effect does not occur with lead compensation, since the removal of lead compensation will not cause the lower part of the amplitude-phase curve to flatten appreciably (it may even cause it to steepen).

In addition to the difficulty of consistently applying lag compensation, the "bobbling" tendencies seem to be related to light initial stick forces. The pilots complain that the airplane is sensitive, that the light initial forces lead to unwanted inputs, and that the stick must be held rather lightly. The effects of light initial forces will be described in more detail in Section 7.4. The tendencies to oscillate and bobble are accentuated by the random noise disturbances (simulated turbulence), which cause the pilot to continually force the nose back onto the target.

It should be mentioned that when Configuration 3A was evaluated early in the program (Flights 1023 and 1024), there were problems with coupling between the variable-stability system and the T-33's wing bending modes. Other than to cause the pilots to select unusually high stick forces, this coupling did not appear to have a strong effect. The coupling was reduced on later flights by evaluating this configuration at lighter fuel weights.

As control-system lag is added to the base configuration, the analysis indicates that the required lag compensation lessens significantly, and the resonance increases very slightly. For Configuration 3C, no compensation is predicted, and the resonance is + 2.5 dB. The comments indicate some improvement over the base configuration, in that it is no longer necessary to use smooth inputs, and the initial forces are more reasonable. The bobbling tendencies due to light initial forces for the base configuration, however, are now replaced with slight overshooting due to the + 2.5 dB resonance.

As the control-system lag continues to increase, the analysis predicts that the resonance will become insignificant again, but lead compensation will be needed. For Configuration 3E, considerable lead compensation is predicted ($\not\phi_{pc}$ = + 55 degrees), along with a negligible resonance ($\left|\theta/\theta_c\right|_{max}$ = -2 dB). The primary complaints for this configuration center around having to pulse the airplane and the fact that the stick forces are initially heavy but lighten up as the response develops. This clearly indicates the use of lead compensation. The comments indicate very little tendency to oscillate, which is compatible with the small resonance. The pilot also complains of some tendency to overshoot, which is probably related to problems with the predictability of the response due to having to use lead compensation.

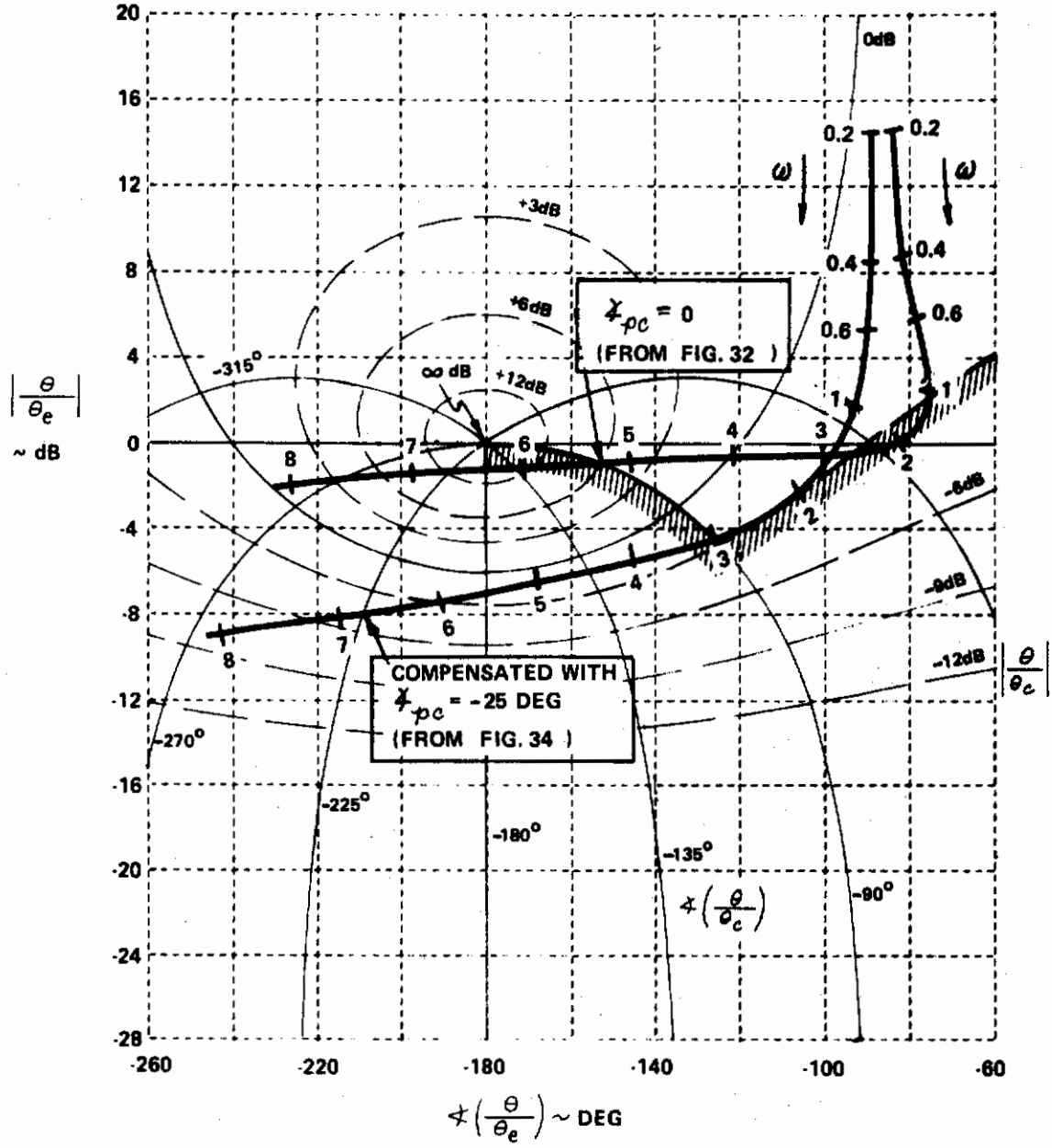

Figure 39. Effects of Removing Pilot Lag Compensation for Configuration 3A (at Constant K_p)

Configurations 4 (A to E, and P) ω_{sp} =5.0, ζ_{sp} =0.28, n/α =18.5

The analysis predicts large resonances (greater than 10 dB) for all the configurations in this group, with Configurations 4A, B and C requiring pilot lag compensation, while Configurations 4D and E require pilot lead compensation. The pilot comments for the configurations with appreciable lag in the control system, 4B to E, all indicate serious problems with pitch-attitude control, including full PIO's, and are therefore compatible with the results of the analysis. However, the pilot comments for the base configuration, 4A, seem to indicate that the oscillatory tendencies are not quite as severe as predicted by the analysis (a resonance of + 10 dB).

A range of pilot compensation from $\angle_{pc}$ = - 28 degrees for Configuration 4A to $\angle_{pc}$ = + 57 degrees for Configuration 4E, is predicted by the analysis. The pilot comments support this trend in general, although specific correlations are not possible in every case. For example, in Configuration 4A, the pilot describes the forces as going from light to heavy, a consistent comment for $\angle_{pc}$ = - 28 degrees. In Configuration 4E, $\angle_{pc}$ = + 57 degrees is predicted, and the pilot complains of very heavy initial forces, which dramatically lighten as the response develops. In all the configurations of this group, the response to random disturbances is a problem, but the tracking characteristics of these configurations are generally so poor that this factor is not critical.

A sample of the in-flight discrete-error tracking records for Configuration 4D is shown in Figure 40 to illustrate the pitch-attitude tracking difficulties experienced by the pilot. The analysis predicts a resonance of + 10 dB with $\angle_{pc}$ = + 31 degrees. The oscillation of θ_e in Figure 40 appears to be close to zero-damped, which seems worse than a resonance of + 10 dB would indicate. It must be understood, however, that the analysis is intended only to predict PIO tendencies, and that the pilot's technique will change when a PIO becomes fully developed. It is interesting to note, however, that the frequency of the oscillation is between 4.5 and 4.8 rad/sec, which is reasonably close to the predicted resonant frequency of 4.3 rad/sec. After studying Figure 40, the reader will find it interesting to refer back to the C* response given for this configuration in Section 5.3, which falls completely inside the "satisfactory" C* envelope.

On Flight 1049, an electrical failure occurred, which caused the T-33's variable-stability system to switch from stick force commands to stick position commands. Thus, the base configuration (4A) was evaluated with the feel system in series with the rest of the control system (as described in Section 3.2). This configuration is designated 4P. Analysis of Configuration 4P shows that the introduction of the feel-system dynamics

into the θ/F_s transfer function causes the required pilot lag compensation to decrease from $\angle_{pc}$ = - 28 degrees to - 20 degrees and the resonance to increase from + 10 dB to + 12 dB. The pilot comments indicate that the oscillatory tendencies of Configuration 4A become more severe with Configuration 4P (in fact, they are now called PIO tendencies). The pilot rating increases from a 5 to a 7.

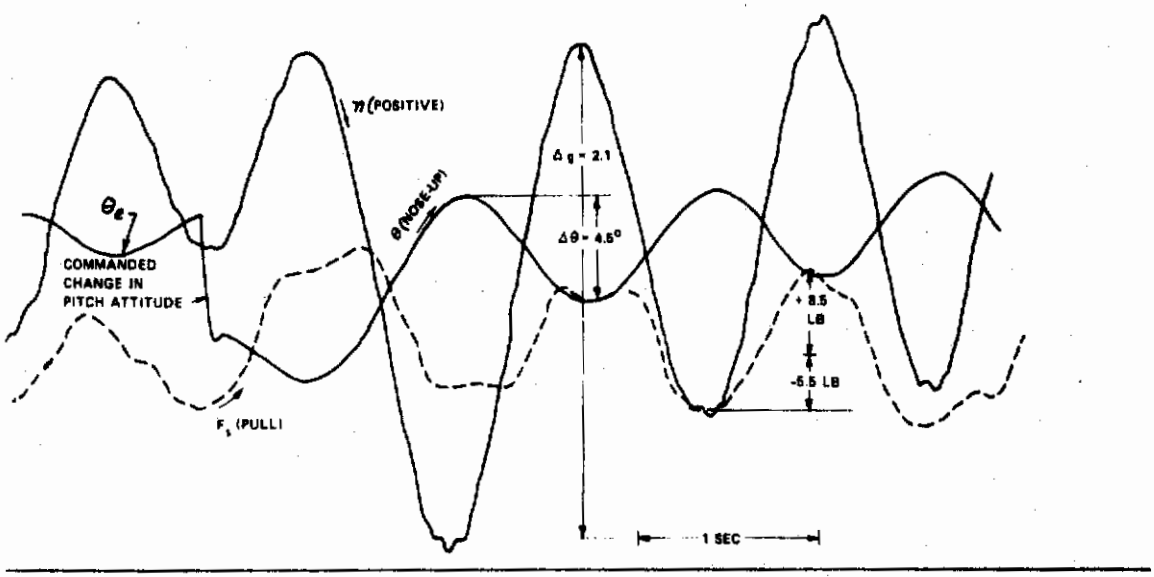

Figure 40. In-Flight Record of a PIO Occurring During Discrete-Error Tracking Task (Configuration 4D, Flight 1057)

Configurations 5 (A to E) ω_{sp} = 5.1, ζ_{sp} = 0.18, n/α = 18.5

The analysis predicts severe tracking problems for all the configurations in this group, i.e., resonances greater than + 12 dB. Pilot comments for all the configurations indicate PIO problems when tight tracking is attempted. However, the comments on Configuration 5A do not seem to indicate PIO tendencies quite as severe as predicted by the analysis. Pilot lag compensation is predicted for Configurations 5A, B, and C and lead compensation for 5D and E. The pilot comments confirm these trends

in pilot compensation required. For example, in 5A the pilot comments on the need for smooth control inputs (lag compensation), while in 5E the pilot had to try to anticipate the response (lead compensation). The pilots consistently complain about the effects of the random disturbances, but in the words of one pilot, they just make a bad configuration worse.

Configurations 6 (A to F) $\omega_{sp} = 3.4$, $\zeta_{sp} = 0.67$, $n/\alpha = 50$

The analysis predicts that considerable lead compensation ($\lambda_{pc} = +57$ degrees) will be required for the base Configuration (6C), but the closed-loop resonance will be small ($\left|\theta/\theta_c\right|_{max} = +1.5$ dB).

The primary complaints are the sluggish initial response, having to "overdrive" the airplane, having to use pulse-like inputs, and the fact that the stick forces go from heavy to light as the response develops. These comments certainly indicate that considerable lead compensation is being used. There is no mention of oscillations, which is consistent with the resonance of + 1.5 dB. There are complaints of overcontrolling tendencies, however, which appear in g control, as well as in attitude control. The pilots refer to overcontrol in g as a "digging-in" tendency, which is quite bothersome. The overcontrolling tendencies are felt to be a direct result of the requirement for considerable lead compensation, which seems to be difficult to generate accurately. Thus, the final response is difficult to predict with any degree of precision.

The analysis shows that the addition of a small amount of control-system lead to the base configuration is beneficial. For example, the predicted lead compensation for Configuration 6B is considerably reduced ($\lambda_{pc} = +38$ degrees), and the resonance becomes very small (+0.5 dB). The pilot comments indicate only minor problems. There was no indication of oscillatory tendencies in tracking, which is consistent with a resonance of + 0.5 dB. Pilot W mentions that the initial response seems a little bit slow, which indicates that some lead compensation is needed.

If more control-system lead is added to the base configuration, the analysis predicts that the effects will be degrading. For Configuration 6A, the compensation required becomes negligible ($\lambda_{pc} = +11$ degrees), but the resonance increases to + 9 dB. Pilot W complains that the attitude control is "bad" for large attitude changes, and that there is a tendency to overcontrol in the IFR tracking tasks. These comments certainly indicate some resonance, although the comment data is sufficiently sparse that it is difficult to judge whether a + 9 dB resonance is reasonable (Pilot M's comments were lost due to a malfunction in the voice recorder). Pilot W also complains of a very abrupt initial response, which indicates that the initial stick forces might be a little light. This latter effect will be explained in more detail in Section 7.4.

When control-system lag is added to the base configuration, the analysis predicts that the required lead compensation will rapidly increase, as will the closed-loop resonance. The pilot comments clearly substantiate this trend. For example, the analysis shows Configuration 6E to have $\chi_{p\alpha}$ = + 78 degrees and a resonance of + 12 dB. The pilots comment that the stick forces go from heavy to light as the response develops and that a pulsing technique helped, clearly indicating the use of lead compensation. In addition, the pilots complain of strong PIO tendencies.

Figure 41 shows a special record made during the evaluation of Configuration 6E on Flight 1071 . It documents a classic PIO which resulted when Pilot M tried to acquire a distant target and track it. The first cycle of the PIO has a frequency of about 4.4 rad/sec; the + 12 dB resonance predicted by the analysis occurs at about 3.9 rad/sec. After the PIO is fully developed, the frequency increases to over 5 rad/sec. It is also interesting to note the rather large stick forces required to move the nose of the airplane rapidly. This is further evidence that the pilot is "overdriving" the airplane, i.e., using considerable lead compensation. It should be understood that the exact nature of a PIO obtained from a given configuration is

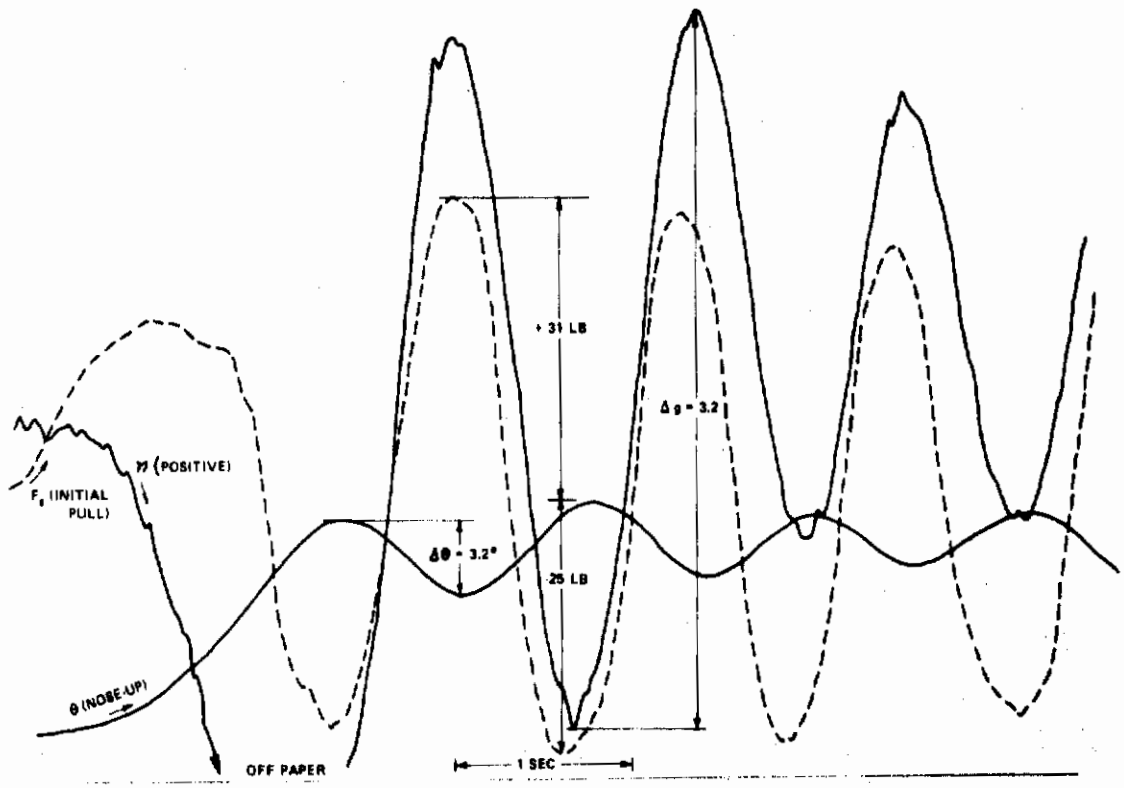

Figure 41. In-Flight Record of a PIO Occurring During Visual Tracking (Configuration 6E, Flight 1071)

somewhat dependent on how the pilot is flying the airplane, e.g., on the bandwidth he is trying to achieve. For example, Figure 36 shows PIO's obtained for Configuration 6E (also on Flight 1071) during the IFR tracking tasks. The frequency of the PIO's shown on those records varies from 3.5 to 4.5 rad/sec.

Configurations 7 (A to H) $\omega_{sp} = 7.3$, $\zeta_{sp} = .73$, $n/\alpha = 50$

The base Configuration (7C) should be a good airplane, based on the analysis ($\phi_{pc} = +13$ degrees, $\left|\theta/\theta_c\right|_{max} = 0$ dB). The pilot comments indicate a slight tendency to bobble on target. This may be partially related to light initial forces, but seems to be minor. Overall, the response was judged to be snappy -- good but a little abrupt.

As control system lead is added to the base configuration, the analysis shows that the required compensation will change from lead to lag and the resonance will increase somewhat. For example, the analysis predicts $\phi_{pc} = -10$ degrees and a resonance of + 3 dB for Configuration 7A. Thus, Configuration 7A should be a reasonably good airplane, with a slight tendency to oscillate. The comments indicate some inconsistency between the two pilots for this configuration. Pilot W says that the airplane is a little too snappy, but is quite good overall. He makes no mention of overshooting tendencies. Pilot M, on the other hand, complains of some overshooting in acquiring a target, and says that the light initial forces tend to make the airplane sensitive to unwanted inputs. The light initial forces will be discussed in more detail in Section 7.4. On the average, comments seem to be compatible with the analysis.

As increasing amounts of control-system lag are added to the base configuration, the analysis predicts that the resonance will gradually increase to + 5.5 dB and the required lead compensation will rapidly increase to + 80 degrees (for Configuration 7H). The pilot comments for Configurations 7D through 7H do show an increasingly sluggish response, with tendencies to dig in and complaints of having to overdrive the airplane, all of which indicate that more lead compensation is required. The comments do not indicate any increased tendency to oscillate as the control system lag is increased. In fact, there is a gradual transition in the comments from complaints of "oscillatory tendencies" for Configuration 7D to "overcontrolling tendencies" for Configuration 7H. This may indicate that the poor precision of control resulting from the large amount of lead required for Configuration 7H overshadows the oscillatory tendencies. It is difficult to understand, however, why the overall pilot opinion suddenly changes from satisfactory (for the base configuration) to a pilot rating of 5.5 when a small amount of control system lag is added (Configuration 7D), and then remains between a pilot rating of 5 and 6 when large amounts of lag are added (Configurations 7E, 7G, 7H).

In addition to the somewhat peculiar pilot ratings for Configurations 7D, 7E, 7G, and 7H, the comments and ratings for Configuration 7F seem to defy explanation, except to say that the two pilots were flying the airplane differently. Each pilot evaluated Configuration 7F three times. Pilot M complained of having to overdrive the airplane somewhat and tendencies to overshoot. His pilot ratings were very consistent: 3, 4, and 4. Pilot W complains of having to use pulse-like inputs and PIO tendencies during tight tracking. His pilot ratings were also very consistent: three 7's. Pilot W does comment that the PIO tendencies occur when he flies the airplane aggressively. This may indicate that he is striving for a higher bandwidth than Pilot M, but why? Perhaps the explanation of all the peculiarities in Configurations 7D through 7H is related to the frequent pilot comments that the responses for these configurations are "peculiar" and difficult to describe.

The electrical failure on Flight 1049 caused Configuration 7C to be evaluated with stick position commands to the elevator (designated Configuration 7P). Analysis of Configuration 7P shows that the required lead compensation has increased from + 13 degrees for 7C to + 22 degrees for 7P. In addition, the resonance increases from 0 dB to + 2 dB. The comments for 7P show that the pilot has to "take out some of the initial input in order to achieve the desired response" and that there is an initial hesitation in the response, which indicates that he is using noticeable lead compensation. The comments for 7C, on the other hand, indicate that the initial response is snappy, with no indication of having to consciously overdrive the airplane. In addition 7P shows some tendency to bobble in tracking, while 7C does not.

Configurations 8 (A to E) $\omega_{sp} = 16.5$, $\zeta_{sp} = 0.69$, $n/\alpha = 50$

The analysis predicts a resonance of 0 dB with a small amount of lag compensation ($\angle_{pc}$ = - 10 degrees), for the base Configuration (8A). Thus, the base configuration should be a good airplane. Pilot W indicates that it is basically a pretty good airplane, but he complains that the initial response is too abrupt and the airplane is sensitive to inadvertent small inputs. Pilot M comments that the stick forces are initially very light, then heavy up as the response develops. He also complains that the airplane is "nervous" and bobbles on target. Certainly the comments indicate the type of problems to be expected when lag compensation is needed, but the complaints seem more severe than a pilot lag of - 10 degrees would indicate. Much of the problem appears to be related to the light initial forces per se, as will be discussed in more detail in Section 7.4. Pilot M also points out that control in the presence of random disturbances is no good, although Pilot W does not mention this characteristic.

When control system lag is added to the base configuration, the analysis indicates that the closed-loop resonance remains small (less than + 1.5 dB), which seems consistent with the comments. When moderate

amounts of control-system lag are present (Configurations 8B and 8C), the analysis shows that very little pilot compensation is required ($\angle_{pc}$ = 0, + 14 degrees, respectively). Thus, Configurations 8B and 8C should be good airplanes. The comments indicate that this is the case, although there are still minor complaints of light initial forces and bobbling tendencies.

As large amounts of control system lag are added to the base configuration, the analysis predicts that the required pilot lead compensation will become large ($\angle_{pc}$ = + 38 degrees for Configuration 8D, and + 70 degrees for Configuration 8E). The comments for these configurations do indicate a definite trend toward the use of lead compensation. The comments on Configuration 8E , for example, describe the response as sluggish with a necessity to overdrive the airplane. There is also an indication of overshooting tendencies and problems with precision of control, which are normally related to the difficulty of generating large lead compensation accurately. However, the two pilots do not agree very well on the severity of the problems for Configurations 8D and 8E. Pilot M considers the problems minor, while Pilot W feels that the problems are severe enough to make both configurations unsatisfactory. Thus, the pilots appear to be flying the airplane differently, e.g., Pilot M may not be keeping his bandwidth up.

Six Additional Configurations (9 to 14)

The six additional short-period configurations were evaluated primarily by Pilot M, using stick position commands to the elevator. The heavily damped, low frequency short-period configurations (9, 10, and 11) were also evaluated with stick force commands, and neither the analysis nor pilot opinion seem to indicate any significant effects of the feel system dynamics on these configurations. It should also be mentioned that during some of the repeat evaluations of these configurations, limits were imposed on the elevator-to-stick-force gearing. However, these limits were incorrectly set, so that the minimum stick force per g allowed was too large (approximately 8 lb/g). The pilot complained that the stick forces were too high, but the high forces did not appear to have any major effect on the overall evaluation.

For the heavily damped, low frequency configurations (9, 10, 11) at n/α = 18.5, the analysis predicts no oscillatory tendencies and the requirement for moderate to large pilot lead configuration. Configuration 9 (ω_{sp} = 2.3, ζ_{sp} = 1.7) and 10 (ω_{sp} = 2.3, ζ_{sp} = 1.2) have a resonance of -1 dB and $\angle_{pc} \approx$ + 60 degrees. The pilot comments emphasize the need to "overdrive" the airplane, with the resulting heavy initial forces, and are therefore consistent with the predicted requirement

for pilot lead compensation. The pilots do not comment on any oscillatory characteristics but do complain that the airplane tends to "dig in" when maneuvering, which causes problems in predicting the final response. It is apparently difficult for the pilot to accurately generate the lead compensation required for precise control. For Configuration 11 (ω_{sp} = 3.3, ζ_{sp} = 1.1), the analysis predicts a resonance of - 1.5 dB and $\angle_{pc}$ = + 45 degrees. The comments indicate that the pilot has to "overdrive" the airplane a little to get it moving initially (lead compensation) and that he could acquire a target quite well with no tendency to oscillate (resonance = - 1.5 dB).

For Configuration 12 (ω_{sp} = 10, ζ_{sp} = 0.45, n/α = 50), the analysis predicts a + 4 dB resonance and no pilot compensation. The pilot comments note some difficulty in acquiring a target, with 3 or 4 oscillations about the target. These comments would appear to be a little more severe than the predicted resonance would indicate, but the analysis does point up some difficulty with pitch attitude tracking for this configuration. As far as the pilot compensation is concerned, Pilot M comments that the initial response is abrupt and that the stick forces go from light to heavy, which indicates the use of lag compensation. However, Pilot W also evaluated this configuration and commented that the initial response was pretty good.

For Configuration 13 (ω_{sp} = 13, ζ_{sp} = 0.34, n/α = 50), the analysis predicts a + 2.0 dB resonance and the requirement for pilot lag compensation, $\angle_{pc}$ = - 6 degrees. According to the pilot comments, unless the airplane is flown very smoothly (lag compensation), the tracking capability is not good. For the tight control required during VFR tracking, the pilot notes that it is a different airplane - you just can't track at all. The pilot also notes a high frequency bobble around the target which can eventually be eliminated. The bobbling tendency appears to be related to comments about the airplane being "nervous" and abrupt. These latter characteristics will be discussed further in Section 7.4.

The analysis predicts a resonance of + 1 dB and the requirements for pilot lag compensation, $\angle_{pc}$ = - 10 degrees, for Configuration 14 (ω_{sp} = 15.6, ζ_{sp} = 0.23, n/α = 50). The comments give no clear indication of the pilot compensation used, which probably means that the compensation is slight. However, the comments do indicate difficulties in acquiring a target and oscillations about the target, which are not consistent with the predicted resonance. This can be partially explained by referring to the Bode plots and time histories which accompany the pilot comments for Configuration 14 in Appendix I. The closed-loop Bode plot ($|\theta/\theta_c|$)

shows a second resonance at high frequencies, which is poorly damped. The residue of this additional low-damped mode is large enough that it appears in the closed-loop time history of pitch attitude to a step attitude command. The high frequency resonance is attributable to the high ω_{sp} and low ζ_{sp}, which cause the open-loop Bode amplitude ($|\theta/\theta_e|$) to still be large on the second pass (at high frequencies) of the amplitude-phase curve across the Nichols chart (Figure 42). Other aspects of the oscillatory tendencies will be discussed in Section 7.4.

In all these high frequency Configurations (12, 13, 14) there is evidence from the comments that the response to external disturbances is a problem and, no doubt, is a factor in the pilot rating.

7.3 Summary of Correlation with Pilot Comments

Based on the detailed study of the pilot comments presented in Section 7.2, it is seen that the trends in the pilot comments, for various combinations of short-period and control-system dynamics, can be nicely explained in terms of the parameters χ_{pc} and $|\theta/\theta_c|_{max}$. Of course, there are aspects of the comments for individual configurations which are not completely explained, but it must be remembered that the purpose of the analysis is to explain the causes of the more important piloting difficulties, not to show exactly how the pilot flies the airplane. With these ideas in mind, the following summary is presented of the pilot comments associated with various combinations of χ_{pc} and $|\theta/\theta_c|_{max}$.

$\chi_{pc} \approx 0$ (no pilot compensation)

If $|\theta/\theta_c|_{max}$ is small (e.g., less than + 2 dB), a configuration with small χ_{pc} is normally a good airplane. The pilot describes it as a responsive airplane, which makes it easy to acquire and track a target. Pilots seem to prefer an airplane which requires a small amount of lead compensation to one which requires a small amount of lag compensation. In other words, he prefers to overdrive the airplane somewhat than to fly the airplane smoothly. As the size of the resonance increases, the pilot first complains of overshoots, then tendencies to oscillate, and finally, strong PIO tendencies.

χ_{pc} Positive (pilot lead compensation)

As previously mentioned, small amounts of lead compensation appear to be no problem for the pilot to generate. When χ_{pc} is large

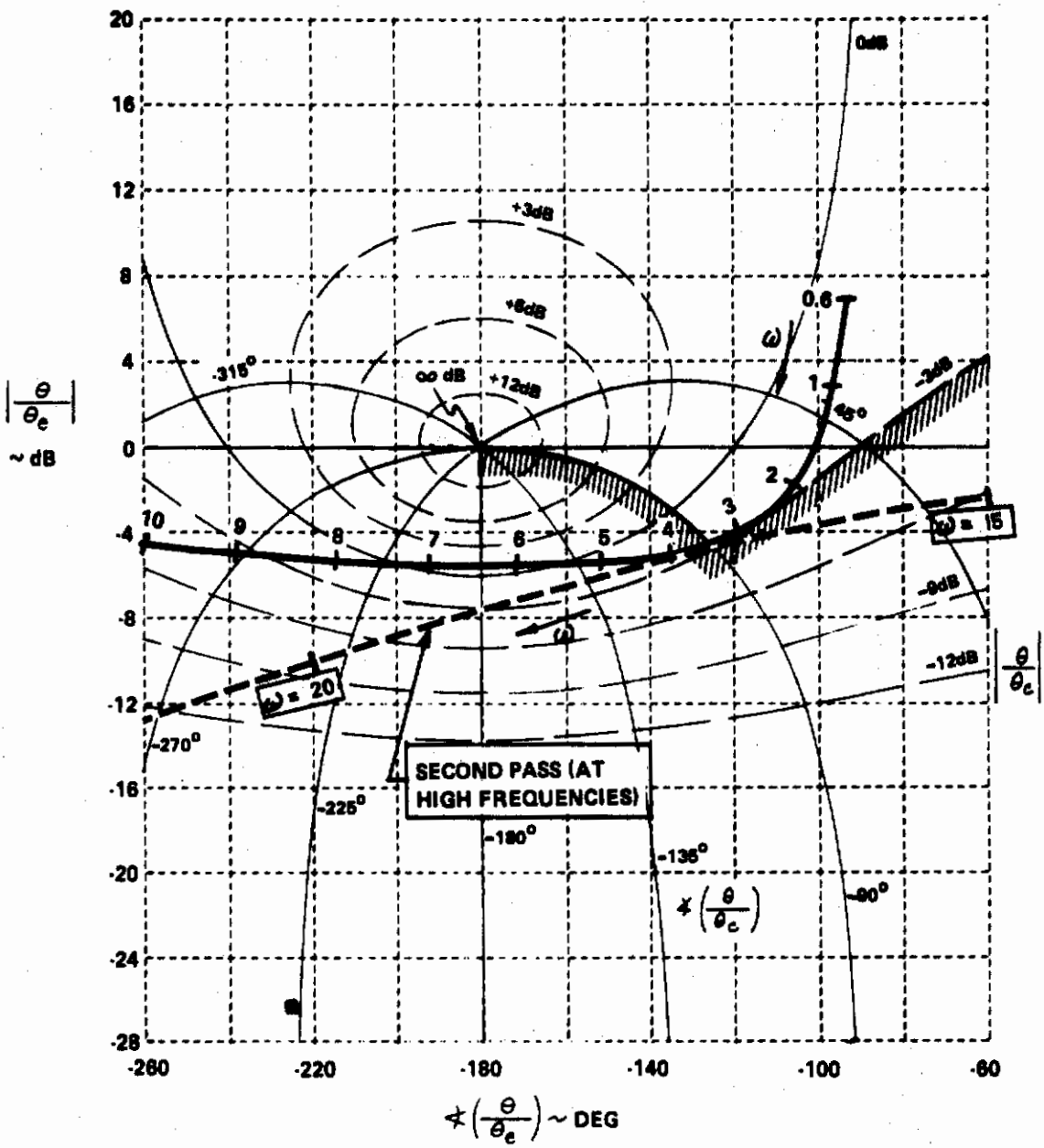

Figure 42. Compensated Amplitude-Phase Plot for Configuration 14, Showing the Cause of the High Frequency Resonance

(and positive), however, the pilot complains that the response is sluggish, which causes him to "overdrive" the airplane or use "pulse-like" inputs. Because he has to overdrive the airplane, the stick forces appear very heavy initially and then lighten up as the response develops. If the closed-loop resonance is small, the pilot will not mention any tendencies to oscillate, but will complain of tendencies to overcontrol and "dig in". The overcontrolling tendencies apparently result from the difficulty of generating large values of lead accurately, so that the pilot has difficulty in predicting or anticipating where the nose will end up. These tendencies are particularly bothersome to the pilot when making large attitude changes or attempting large pullup maneuvers, because of the unexpectedly large g levels which occur. The term " digging in" is descriptive of the unanticipated amounts of g obtained.

As the resonance increases (with $\angle_{pc}$ large), the complaints of overcontrolling tendencies are gradually replaced with tendencies to oscillate, and eventually, with comments on strong PIO tendencies.

$\angle_{pc}$ Negative (pilot lag compensation)

Unfortunately, no configurations were evaluated in this program which required large amounts of pilot lag compensation. However, the values of ω_{sp} and control-system lead which caused pilot lag compensation to be needed were fairly extreme values, so that perhaps practical airplanes are unlikely to require more than moderate amounts of pilot lag.

When pilot lag compensation is required, the pilot comments that the initial response is abrupt, which forces him to fly the airplane smoothly. Because he has to fly it smoothly, the stick forces appear very light initially and then heavy up as the response develops. Even if the closed-loop resonance predicted by the analysis is small, there will quite often be complaints of oscillations or "bobbles" on target. This is largely due to the difficulty of consistently applying smooth inputs, in the context of the fighter mission. As shown in Figure 39, the closed-loop resonance can become quite large if the lag compensation is reduced slightly (the pilot forgets to smooth his inputs).

There are other factors which can contribute to bobbling tendencies. For example, the discussion of Configuration 14 in Section 7.2 (Figure 42), shows that a high frequency resonance can be present. In addition, the large initial abruptness or sensitivity, in itself, can cause inadvertent stick inputs which make the airplane feel "nervous". These latter effects will be discussed in Section 7.4.

As the size of the closed-loop resonance increases, of course, the pilots begin to complain of increasing tendencies to oscillate and PIO. In addition, all the problems associated with configurations requiring pilot

lag compensation can be aggravated by the presence of external disturbances, such as turbulence.

Figure 43 presents the above pilot comment summary in a more compact form. The effects of pilot gain, which have not been discussed in detail, will be explained in Section 7.4.

PIO Tendencies

It is interesting to note that for the reasonably large ranges of ω_{sp} and $1/\tau_{\theta_2}$ evaluated in the present experiment, both the analysis and the pilot comments clearly indicate the lack of any strong PIO tendencies when ζ_{sp} is good and the control-system dynamics are negligible. The reason for this is that some form of the pilot's compensation can be found which allows the performance standards to be met with very slight closed-loop resonance. The flying qualities may be degraded because of the extreme values of τ_{pc}, but not because of strong PIO tendencies.

When ζ_{sp} is reduced, the PIO tendencies rapidly increase, as the pilot comments for Configurations 4A and 5A clearly show. The increase in PIO tendencies with decreased ζ_{sp} is less pronounced when ω_{sp} is high, as can be seen from the comments for Configurations 12, 13, and 14. The results also indicate some PIO tendencies when extreme values of control-system lead are combined with low ω_{sp} (Configurations 1A and 6A), and when low-frequency, second-order control-system modes are present (Configurations 2B, 2G, 2I). The most serious PIO's which occurred during the present experiment, however, are attributable to the addition of large amounts of control system lag (τ_2) to configurations with low ω_{sp} or low ζ_{sp} (Configurations 1F, 1G, 4B to 4E, 5B to 5E, 6E, and 6F).

7.4 Effects of Pilot Gain and Control Sensitivity

As can be seen from the pilot comments of Appendix I, the pilots often comment that the selection of elevator gearing is a compromise between the initial stick forces (i.e., the forces required to initiate a maneuver) and the steady forces (i.e., F_s/n). As explained in Section 6.9, the pilot gain at $\omega = (BW)_{min}$ is a logical parameter to describe the initial forces:

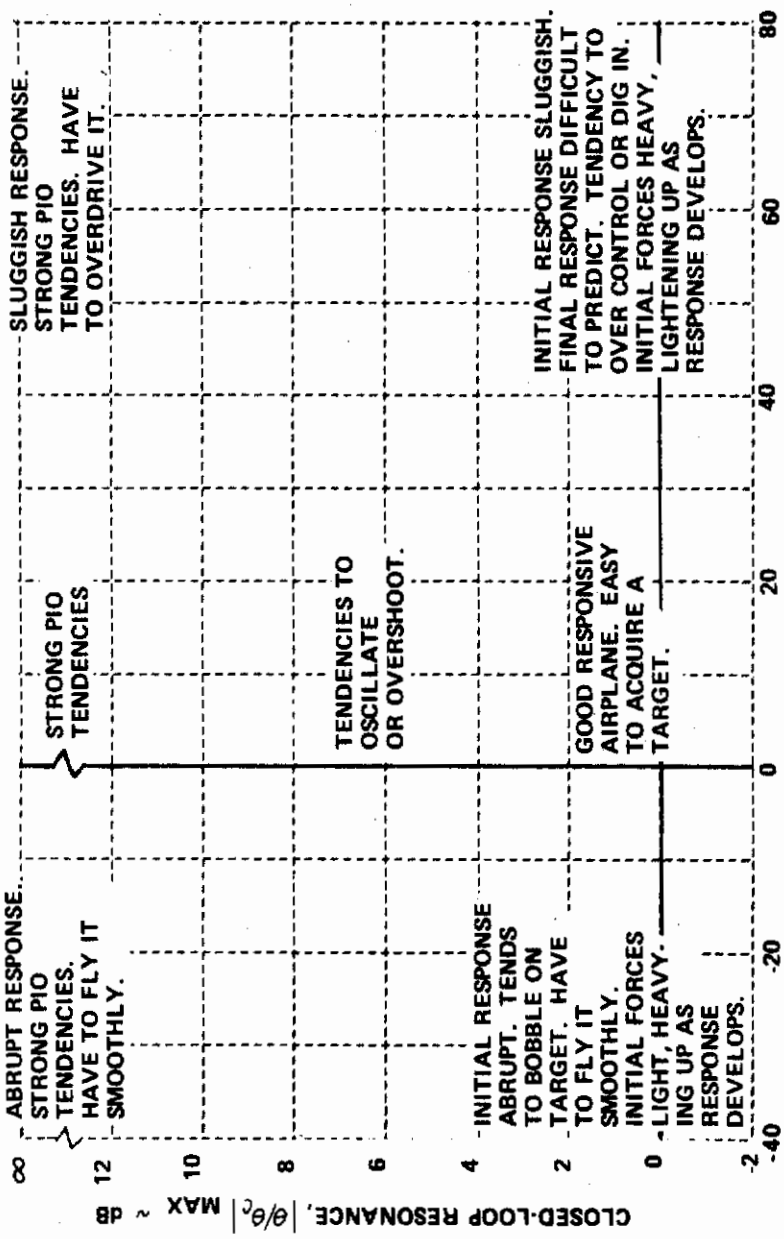

Figure 43. Summary of Pilot Comment Data as a Function of Closed-Loop Parameters

$$K_{BW} = \left| K_p \left(\frac{j\omega \tau_{p_1} + 1}{j\omega \tau_{p_2} + 1} \right) \right|_{\omega = (BW)_{min}}$$

The values of K_{BW} (and K_p) for each configuration evaluated in this experiment are shown with the pilot comments in Appendix I. To determine these parameters, values of K_{BW} and K_p were first calculated for each configuration by the methods described in Section 6.9, using θ/F_s Bode characteristics based on a value of F_s/n equal to 5 lb/g ($K_\theta = \frac{57.3\,g}{V_T (F_s/n)}$ from Appendix IV). The total loop gain, $K_L = K_\theta K_p$, was then computed. To hold the closed-loop characteristics fixed for a given configuration as the pilot changes the elevator-to-stick-force gearing, he must adjust his gain to keep K_L constant (in addition to holding his compensation fixed). Therefore, K_p (and K_{BW}) are inversely proportional to K_θ and directly proportional to F_s/n. Thus, the values of K_{BW} and K_p shown in Appendix I were computed from the $F_s/n = 5$ values for the configuration and the actual F_s/n selected, as follows:

$$K_{BW} = \frac{F_s/n}{5.0} (K_{BW})_{5.0}$$

$$K_p = \frac{F_s/n}{5.0} (K_p)_{5.0}$$

In addition to the values shown in Appendix I, nominal values of K_{BW} (based on the average F_s/n for each flight condition) are shown in Table III. Because K_{BW} is directly proportional to F_s/n, the value of K_{BW} shown in Appendix I for any given flight is related to the value shown for that configuration in Table III, as follows:

$$K_{BW} = \begin{cases} \frac{(F_s/n)}{6.0} (K_{BW})_{\text{Table III}}, & V_{ind} = 250 \text{ KT} \\ \frac{F_s/n}{4.5} (K_{BW})_{\text{Table III}}, & V_{ind} = 350 \text{ KT} \end{cases}$$

To obtain a feeling for the range of satisfactory values of K_{BW}, the pilot comments were again examined. Unfortunately, since the independent variation of elevator-to-stick-force gearing was not part of the present experiment, it is not possible to clearly separate the effects of K_{BW}, per se, from the effects of pilot compensation ($\not\angle_{\rho c}$). The reason for this is that the largest values of K_{BW} are usually associated with large amounts of lead compensation, so that it is difficult to tell whether the pilot is complaining about the heavy initial forces alone (due to large K_{BW}) or the fact that the forces go from heavy to light as the response develops (due to large, positive $\not\angle_{\rho c}$). Conversely, the smallest values of K_{BW} are usually associated with lag compensation, so that it is difficult to separate the pilot comments related to light initial forces alone (due to low K_{BW}) and those resulting from the forces going from light to heavy ($\not\angle_{\rho c}$ negative).

By examining the pilot comment data for small values of $\not\angle_{\rho c}$ (- 5 to + 25 degrees), it would appear that K_{BW}, per se, did not have an important effect on the configurations evaluated in this experiment. However, the pilot does begin to comment on the light initial forces when K_{BW} becomes approximately 1.0 lb/deg. For values of K_{BW} as high as 2.5 lb/deg, the pilot is still describing the stick forces as comfortable.

For a number of configurations, notably 3A, 3B, 8A, 8B, 13, and 14, the pilot comments indicate tendencies to oscillate or bobble on target which are more severe than the analysis predicts($|\theta/\theta_c|_{max}$ less than + 2 dB). In addition, the pilots feel certain that the frequency of the bobble is two or three times that of the larger-amplitude PIO's commonly observed. These comments are usually accompanied by complaints of sensitivity to inadvertent control inputs. One possible explanation of the bobbling tendencies is that the high pitch-acceleration sensitivity of these configurations is causing high-frequency inadvertent inputs. If this control sensitivity is defined in terms of the peak Bode amplitude $|\ddot{\theta}/F_s|_{max}$, it can be computed from the θ/F_s Bode plots of Appendix I for each configuration, using the following expression:

$$\left|\frac{\ddot{\theta}}{F_s}\right| = \omega^2 \left|\frac{\theta}{F_s}\right|$$

The values of $|\ddot{\theta}/F_s|_{max}$ for each configuration are shown in Table III, based on an average value of F_s/n for each flight condition. It can be seen that the control sensitivities for the above mentioned six configurations are all greater than 0.5 $\frac{rad/sec^2}{lb}$.

Whatever the exact cause of the bobbling tendencies and sensitivity to unwanted inputs, values of $|\ddot{\theta}/F_s|_{max}$ greater than 0.5 $\frac{rad/sec^2}{lb}$ seem to contribute to it. Of the configurations having control sensitivities greater than 0.5, the pilot comments indicate that roughly half (3A, 3B, 8A, 8B, 13 and 14) were downrated somewhat because of this tendency.

It is interesting to note that Configurations 8A, 8B, 13 and 14 all have a high frequency "bump" in the closed-loop Bode $|\theta/\theta_c|$ plots shown in Appendix I, indicating a high frequency resonance. The cause of this bump is illustrated in Figure 42 for Configuration 14. For Configuration 14, of course, the bump is large enough to appear as a bobble in the computed closed-loop time history (also shown in Appendix I). The bumps for the other three configurations are not large enough to appear in the computed time histories. The discrete-error tracking records for all four configurations, however, often show bursts of low-amplitude, high-frequency oscillations riding on the pitch attitude traces, which is consistent with the pilot complaints of bobbling tendencies. The frequency of these observed bobbles is close to the frequency of the bump in the Bode plot for each configuration. Thus, it would appear that high control sensitivity somehow causes an increase in high-frequency pilot gain, which increases the size of the bump over that predicted by the present analysis.

7.5 Correlation with Pilot Ratings

The discussion of the pilot comments in Section 7.2 has shown that the two most important factors in determining the pilot rating of a configuration are: the oscillatory tendencies occurring during attitude tracking, represented by $|\theta/\theta_c|_{max}$, and the amount of pilot compensation required to achieve the desired standard of tracking performance, $\mathcal{K}_{pc}$. This section will discuss the correlation of these two parameters with the pilot rating data.

The pilot rating data of Pilot M and Pilot W for the basic FCS/short-period configurations (1A to 8E) are presented in Figures 44 and 45. These plots of pilot rating against $|\theta/\theta_c|_{max}$ and $\mathcal{K}_{pc}$ contain

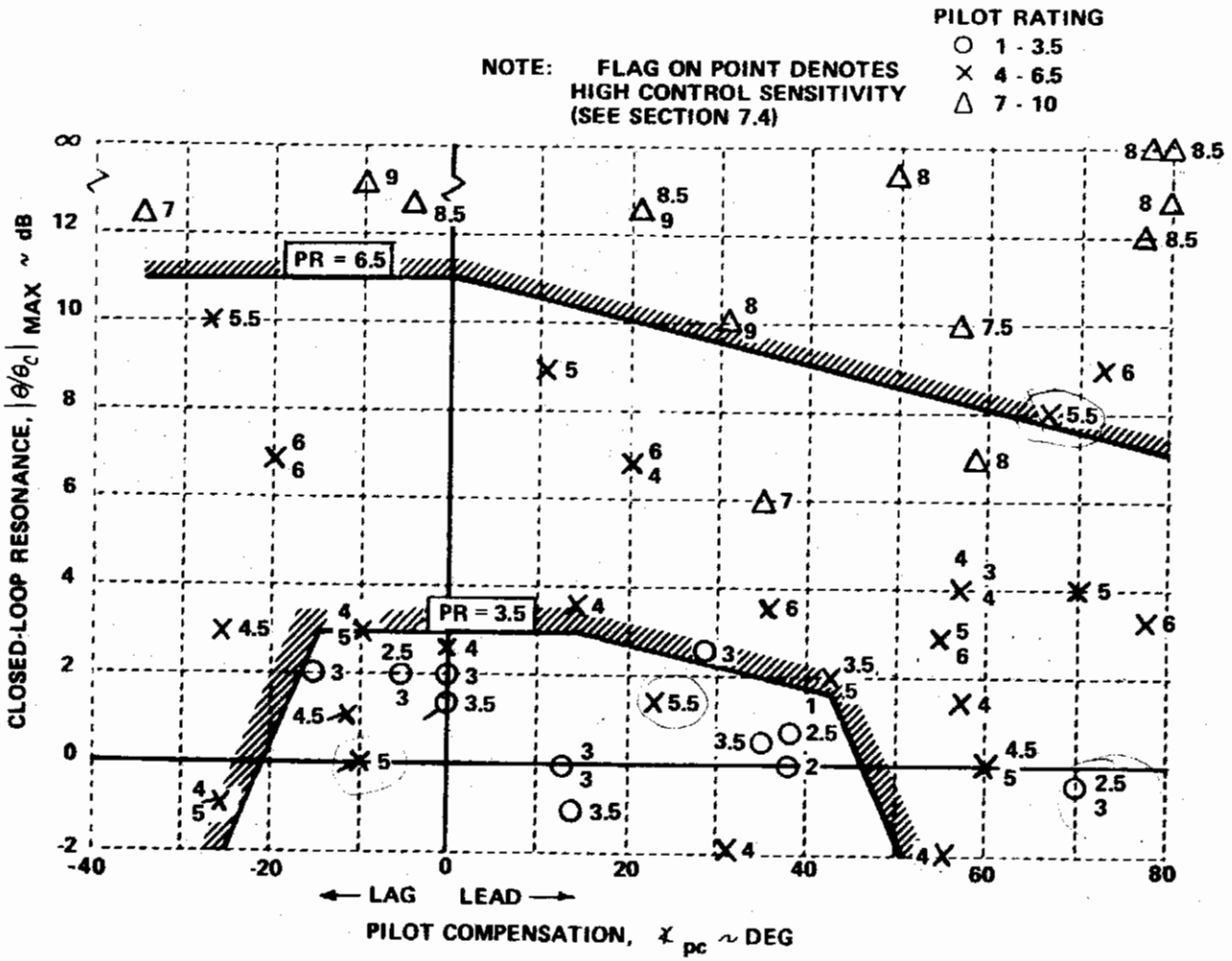

Figure 44. Correlation of Pilot M Rating Data with Closed-Loop Parameters (Configurations 1A to 8E)

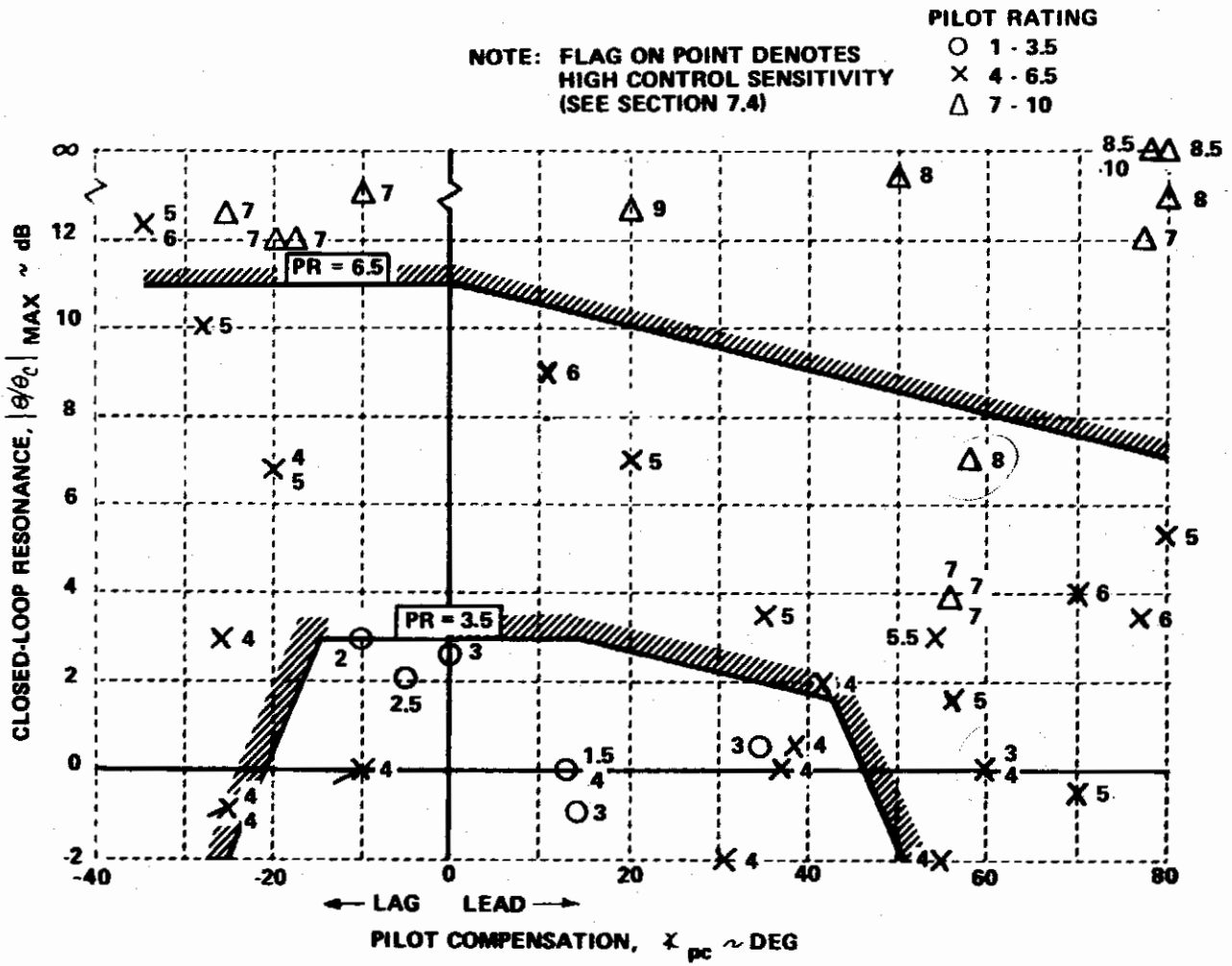

Figure 45. Correlation of Pilot W Rating Data with Closed-Loop Parameters (Configurations 1A to 8E)

all the evaluations performed in this part of the experiment, except for the 7 evaluations not used in the data analysis for reasons noted in Appendix I. The closed-loop parameters for the configurations evaluated at high speed (n/α = 50) are based on $(BW)_{min}$ = 3.5 rad/sec, while those for the low-speed configurations (n/α = 18.5) are based on $(BW)_{min}$ = 3.0 rad/sec (see Section 7.1). For convenience, Figure 46 shows the configuration numbers for each closed-loop-analysis data point.

Note that pilot lead compensation was somewhat arbitrarily limited to $\angle_{pc}$ = + 80 degrees for the analysis because values greater than + 80 degrees do not significantly improve the closed-loop performance. This restriction on $\angle_{pc}$ reduced the BW achieved for Configurations 1G and 6F, and reduced the low-frequency droop for Configurations 1F, 1G, 6F, and 7H.

Also note that the top of the $|\theta/\theta_c|_{max}$ scale in the figures shows a discontinuity between + 12 dB and ∞. Reference to a Nichols chart (e.g., Figure 20) shows that any value of $|\theta/\theta_c|_{max}$ greater than + 12 dB is very close to being unstable and is difficult to measure. Therefore, the data points in the figures were distributed between + 12 dB and ∞ on the basis of open-loop gain margin. Figure 20 shows that $|\theta/\theta_c|_{max} = \infty$ corresponds to a gain margin of 0 ($|\theta/\theta_c| = 0$) and $|\theta/\theta_c|_{max}$ = + 12 dB roughly corresponds to a gain margin of 2 dB ($|\theta/\theta_e| = -2$ dB).

The 3.5 and 6.5 pilot rating boundaries shown on Figures 44 and 45 are based primarily on the ratings of both pilots, although additional factors were considered. In determining the boundaries, for example, more weight was given to those configurations which were evaluated several times and received consistent pilot ratings and comments. Those configurations with additional problems, such as high control sensitivity (flagged symbols), or those rated by only one pilot and seemingly inconsistent relative to the other configurations within the same short-period group, were given less weight. Note that the flagged configurations (3A, 3B, 8A, 8B) $|\ddot{\theta}/F_s|_{max} > 0.5 \frac{rad/sec^2}{lb}$ (Table III) and the pilot comments indicate that major

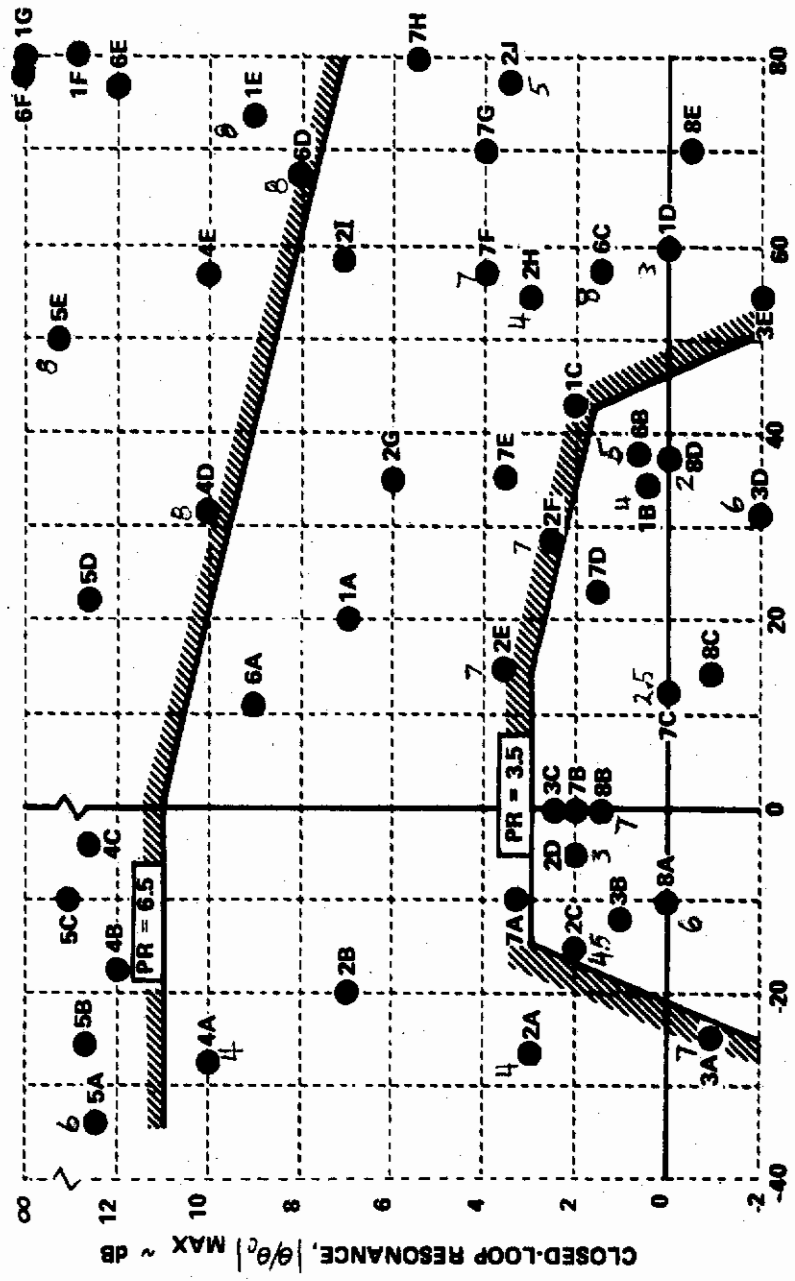

Figure 46. Configuration Numbers for Closed-Loop Data Points (Configurations 1A to 8E)

complaints about the configuration appear to be related to the high pitch sensitivity (see Section 7.4). The pilot rating data separates quite nicely into 3 regions, consistent with the pilot rating boundaries shown, and therefore correlates with the closed-loop parameters, $|\theta/\theta_c|_{max}$ and $\angle_{pc}$. Considering the large variety of configurations represented on these figures, and the potential sensitivity of the data points to the manner in which the pilot performs the required fighter tasks, the correlation of pilot ratings with the closed-loop parameters is considered good.

There are some data points which violate the pilot rating boundaries; but in most cases, the ratings of the other pilot tend to offset any discrepancy with the boundary. For Configuration 7F, with a resonance of + 4 dB and $\angle_{pc}$ = 57 degrees, Pilot W gave a rating of 7 on three separate evaluations, while Pilot M rated it a 3, 4, and 4 on three evaluations. Based on the ratings of both pilots, the location of the data point relative to the boundaries appears reasonable. More discussion of this particular configuration can be found in Section 7.2. Another example of inter-pilot rating differences which are difficult to interpret is Configuration 8E (- 0.5 dB and + 70 deg). Pilot W gave a PR = 5 which agrees well with the pilot rating boundary. However, Pilot M rated the configuration a 2.5 and 3. Configuration 7D (+ 1.5 dB, + 23 deg), which Pilot M rated 5.5, clearly violates the 3.5 boundary. In this instance, the pilot rating seems a bit severe relative to the ratings for Configurations 7C and 7E, as mentioned in the discussion of the pilot comments (Section 7.2).

Aside from these specific observations, comparison of Figures 44 and 45 indicates that Pilot M averages about 1 rating unit better than Pilot W when $\angle_{pc}$ is large and positive. In addition, Pilot M rates configurations with negative $\angle_{pc}$ about 1 rating worse than Pilot W. Thus, it would appear that Pilot W has a slight preference for more responsive airplanes than Pilot M.

The pilot rating data for the six additional configurations are presented in Figure 47 and compared with the closed-loop pilot rating boundaries established in Figures 44 and 45. The three low ω_{sp}, high ζ_{sp} configurations (9, 10, 11) correlate well with the 3.5 boundary. However, of the three high ω_{sp}, low ζ_{sp} configurations (12, 13, 14), only Configuration 12 (+ 4 dB, 0 deg) correlates with the boundaries. The other two configurations (13 and 14) clearly violate the 3.5 boundary. These configurations are flagged since the values of control sensitivity are very high (Table III), and major complaints in the pilot comments appear to be related to the high pitch sensitivity (see Section 7.4).

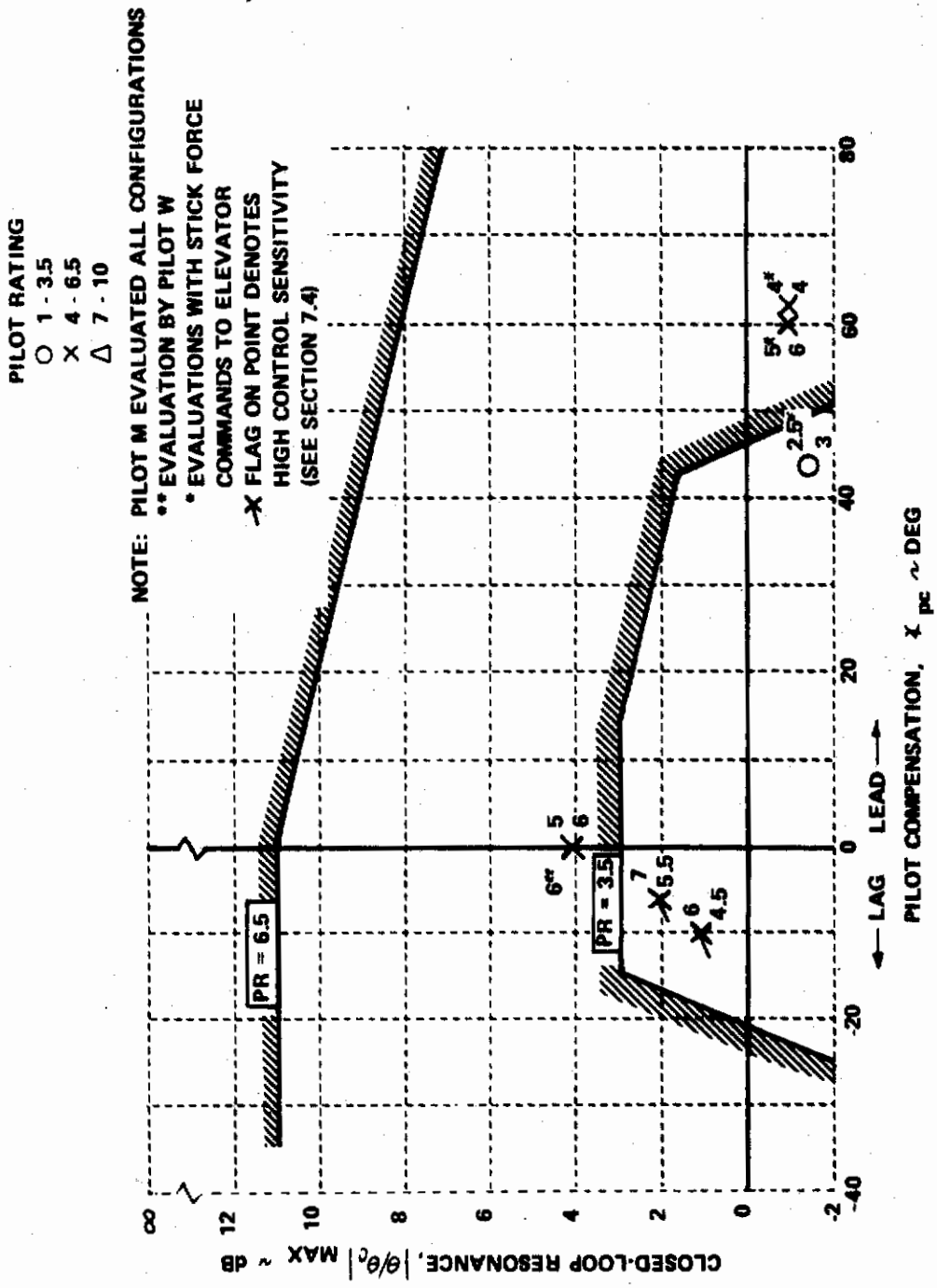

Figure 47. Correlation of Pilot Rating Data for Six Additional Configurations (9 to 14) with Closed-Loop Parameters

In summary, the correlation between the pilot rating data and the closed-loop analysis parameters is generally good. Sections 7.6 and 7.7 will compare the pilot rating boundaries established using the closed-loop analysis with the results of two somewhat similar fighter control-system experiments.

7.6 Application to Data From Special T-33 Flights

The data used to draft the short-period requirements for MIL-F-8785B (Reference 12) were obtained using various types of airplanes, having various types of control-system dynamics. To better understand the influence of the control-system dynamics on the short-period data, two special flights were piggybacked on the T-33 experiment of Reference 8. It is interesting to see how the results of the six configurations evaluated on these flights compare with the present analysis.

The pitch attitude response to pilot inputs for the six configurations can be represented in the following form:

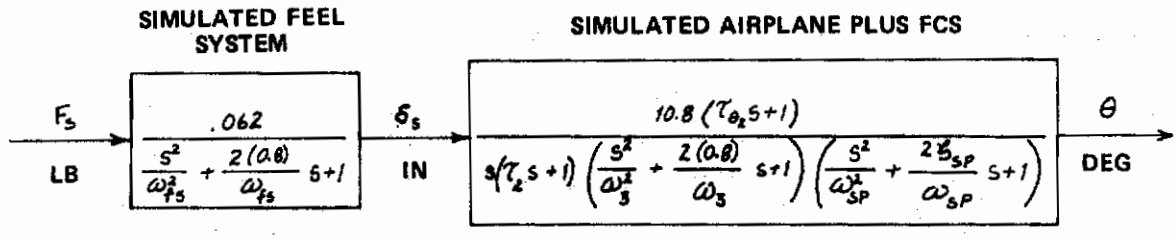

The following parameters were held fixed for all six configurations.

V_T	= 550 ft/sec	ω_{sp}	= 5.5 rad/sec
n/α	= 22 g/rad	ζ_{sp}	= 0.6
$1/\tau_{\theta_2}$	= 1.3 sec^{-1}	F_s/n	= 5 lb/g

Various combinations of ω_{fs}, $1/\tau_2$, and ω_3 were then evaluated by Pilot S of Reference 8. The evaluation tasks performed were those of Reference 8, which are quite similar to those used in the present experiment.

The present analysis was applied to the six configurations, using $(BW)_{min}$ equal to 3 rad/sec. The flight condition for these configurations is similar to the 250 knot condition in the present experiment, with similar limitations on the maximum g available for maneuvering. The results of the analysis and the pilot ratings for each configuration are presented below.

Flt. No.	ω_{sp}	ω_s	$1/\tau_{\theta_2}$	PR	PIOR	γ_{pc}	$\lvert\theta/\theta_c\rvert_{max}$
950	41	6.3	∞	7	4	+30°	+9.5 dB
↓	↓	↓	5	7	3	+50°	>12 dB
↓	↓	↓	2	7.5	4	+68°	>12 dB
951	25	63	∞	3	1	-4°	+4 dB
↓	↓	↓	5	4	1	+26°	+5 dB
↓	↓	↓	2	5	2	+55°	+5 dB

Figure 48 shows that the data agree quite well with the boundaries on γ_{pc} and $\lvert\theta/\theta_c\rvert_{max}$ established using the results of the present experiment.

7.7 Application to the HOS Data

For a comparison of the flying qualities data from different experiments to be meaningful, the tasks performed, as well as the performance standards used by the pilots, must be similar. It is a well known fact of life in flying qualities work that very different pilot ratings and comments can result from two pilots flying the same task with different performance standards. The discussion in Section 7.1, for example, shows the effects of flying the same configuration with different values of BW, the performance measure used in the closed-loop analysis. Before proceeding with the application of the analysis to the results of the HOS program (Reference 6), therefore, some of the differences between that experiment and the present one will be discussed.

The fighter evaluations in the HOS program were performed at a flight condition which is very similar to the low-speed flight condition in this experiment (for the HOS program, n/α = 22 g/rad, $1/\tau_{\theta_2}$ = 1.25 sec^{-1}, and V_T = 565 ft/sec). The fighter evaluation tasks performed in the HOS program are, in general, similar to those performed in this program. There are, however, some indications that high-load-factor maneuvers were not stressed to the same extent as they were in the present experiment. For example, the levels of F_s/n given to the pilot were higher in the HOS program. Excluding those cases where F_s/n was intentionally increased, the average F_s/n values used were 8 to 13 lb/g, depending on the pilot

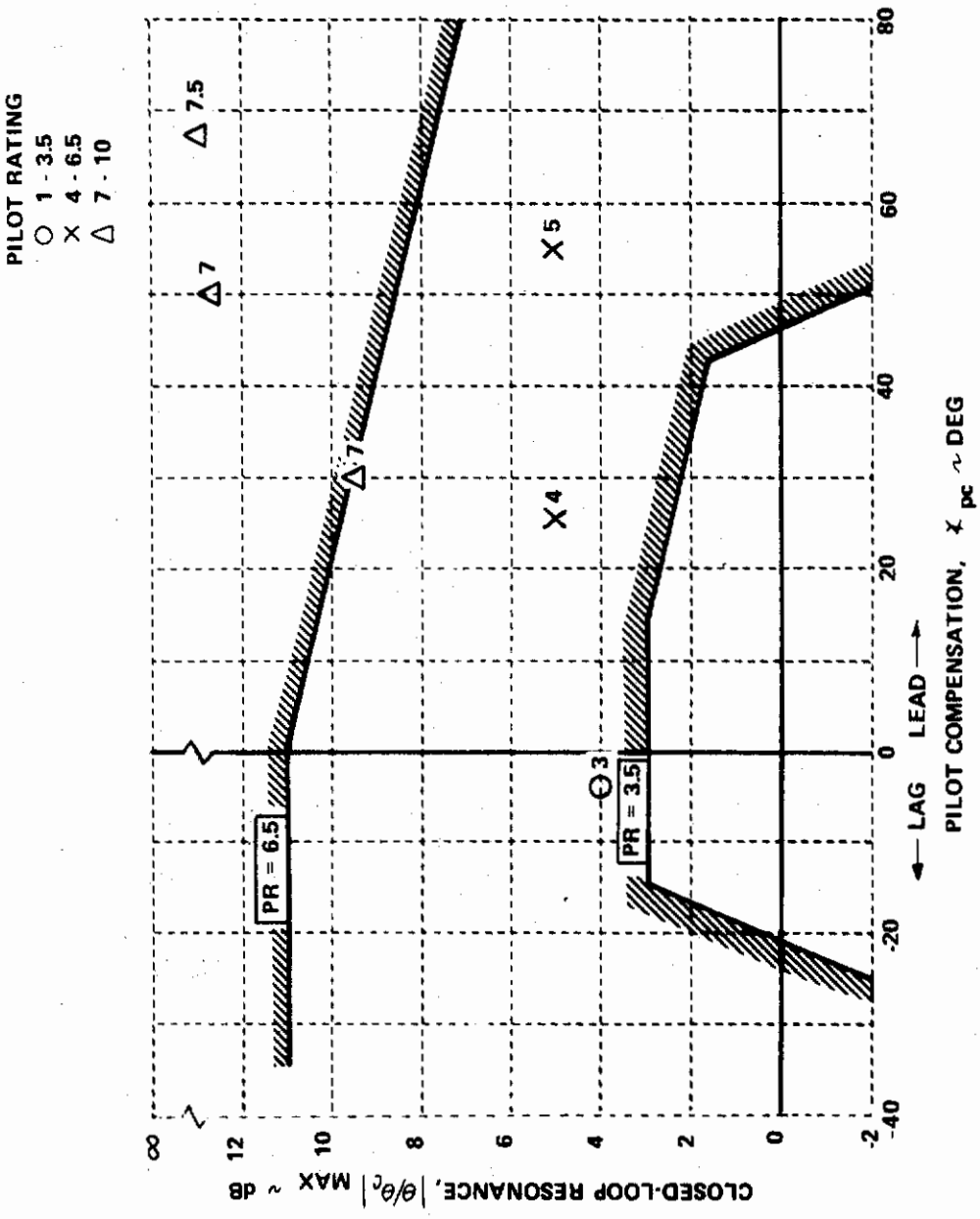

Figure 48. Correlation of Pilot Rating Data for Special T-33 Flights with Closed-Loop Parameters

and the particular configuration. This contrasts with an average F_s/n selected by the pilots in this experiment of 6 lb/g. Perhaps more important than the difference between the average F_s/n values is the fact that pilot ratings better than 6.5 could be obtained for values as high as 17 lb/g; in fact, one configuration was considered satisfactory (PR < 3.5) with 17 lb/g. Such high values of F_s/n are not compatible with good overall fighter maneuverability. These observations tend to indicate that the pilots flew the tasks less aggressively than in the present experiment. Further weight is given to this assumption by the fact that there were very few satisfactory airplanes evaluated in the HOS program. In fact, 60% of the evaluations were rated worse than 6.5. Because of this, the pilots may have become accustomed to not flying the airplane aggressively. In addition, the evaluations were all performed at one flight condition and the pilots did not have the benefit of flying at higher speeds where the T-33 buffet boundary does not restrict maneuverability. In the present experiment, the evaluations at 350 knots served as a constant reminder to the pilots of the desired performance standards for the fighter task.

In the present experiment, a $(BW)_{min}$ of 3 rad/sec was used in the closed-loop analysis for the low-speed flight-condition data, in recognition of the limitations imposed on the low-speed evaluations by the T-33 buffet boundary (see Section 7.1). For the HOS program, however, a $(BW)_{min}$ of 3 rad/sec resulted in values of $|\theta/\theta_c|_{max}$ which were larger than the pilot comments on PIO tendencies indicated. Values of 2.5 and 2.0 rad/sec were also tried. The value of 2.5 rad/sec produced the best correlation with the pilot comments, and was therefore selected as the appropriate value for the HOS experiment. Use of this lower performance standard is felt to be justified in light of the above evidence that the pilots flew the tasks less aggressively than in the present experiment.

The portion of the HOS program related to the "combat" phase of a fighter's mission looked at the effects of adding a variety of higher-order lag dynamics to three combinations of ω_{sp} and ζ_{sp}. To retain a reasonable basis for comparison with the results of the present experiment, only those evaluations having F_s/n values consistent with good overall maneuverability were analyzed. The basis for determining reasonable values of F_s/n was MIL-F-8785B. Thus for configurations with PR < 3.5, only the evaluations with F_s/n < 10 lb/g are used, and for those configurations with a PR between 3.5 and 6.5, only the evaluations with F_s/n < 16 lb/g

are used. The table on the following page summarizes the HOS data selected in this way and lists the closed-loop parameters calculated for each configuration. Figure 49 shows the HOS data compared with the boundaries determined for the present experiment.

The correlation of the rating data with the boundaries is certainly not perfect but, considering all the factors involved, it seems reasonable. The fact that the majority of the configurations evaluated in the HOS program had very poor dynamic characteristics no doubt made it difficult for the pilots to establish a consistent performance standard, which possibly accounts for some of the scatter in the data.

Considering the analysis of the HOS data as a whole, there is an interesting observation which should be made. Referring to the table of HOS data, it can be seen that there is a general trend for a given set of control-system-lag dynamics to degrade configurations with medium ω_{sp} more than configurations with low ω_{sp}. For example, Configuration A(F)-5(2.5) (ω_{sp} = 2.7) has pilot ratings of 5 and 4, while Configuration C(F)-5 (2.5) (same control system dynamics, but ω_{sp} = 5.1) has ratings of 8, 9, 7, 8 and the comments indicate severe PIO problems. The analysis shows $|\theta/\theta_c|_{max}$ = + 8 dB for the A configuration and + 11.5 dB for C, which are consistent with the ratings.

The reverse trend is apparent for the present experiment, i.e., a given first-order control-system lag is more degrading for low ω_{sp} than for medium ω_{sp}. For example, Configuration 1F (ω_{sp} =2.2 rad/sec) has pilot ratings of 8 and 8 and the comments indicate severe PIO problems, while Configuration 2H (same control system dynamics, but ω_{sp} = 4.9) has ratings of 5, 6, 5.5. The analysis shows $|\theta/\theta_c|_{max}$ > + 12 dB for Configuration 1F and only + 3 dB for Configuration 2H, which are consistent with the ratings. Thus, it can be seen that a very fundamental difference between the HOS results and those of the present experiment is accounted for by the analysis.

Config. Number	ω_{sp} (rad/sec)	ζ_{sp}	PR Pilot B/Pilot H	γ_{pc} (deg)	$\lvert\theta/\theta_c\rvert_{max}$ (dB)
A(F)-2(10)	2.7	0.55	4/ 2, 1.5, 4	+ 29	+ 3
A(F)-2(2.5)			3/ 3.5	+ 34	+ 5
A(F)-2(1)			7, 6/ 7.5, 7, 4.5	+ 45	> 12
A(F)-4(2.5)			4, 4/ 6	+ 42	+ 8
A(F)-5(2.5)			5/ 4	+ 45	+ 8
A(F)-5(1)			9/ 10	+ 60	∞
A(M)-2(10)			5/ 2.5, 3.5	+ 37	+ 6
A(M)-2(2.5)			5/ 6	+ 42	+ 8
A(M)-4(2.5)			4/ -	+ 47	+ 12
A(S)-2(10)			5/ 4	+ 45	+ 9
A(S)-2(2.5)			7/ 7.5, 6.5, 10	+ 47	> 12
A(S)-4(2.5)			-/ 8.5	+ 50	> 12
B(F)-2(2.5)		0.24	5/ -	- 6	> 12
B(F)-2(1)			8/ 7	0 *	∞(2.3)
B(F)-4(2.5)			6/ 6	- 6 *	∞(2.4)
B(F)-5(2.5)			7/ 7.5	- 8 *	∞(2.3)
B(F)-5(1)			-/ 10	+ 22 *	∞(2.2)
B(S)-2(10)			-/ 8	- 6 *	∞(2.3)
C(F)-2(10)	5.1	0.43	4, 2/ 4, 4.5	- 17	+ 4
C(F)-2(1)			7, 7, 9/ 7	+ 9	+ 10.5
C(F)-4(2.5)			7, 7/ 7.5	0	> 12
C(F)-5(2.5)			8/ 9, 7, 8	+ 9	+ 11.5
C(F)-5(1)			10/ 10	+ 37	> 12
C(M)-2(10)			-/ 7	- 10	+ 8
C(S)-2(10)			7/ 7	+ 8	+ 11

* For these configurations, a $(BW)_{min} = 2.5$ rad/sec could not be achieved without driving the airplane unstable. The pilot compensation used is that which produces the largest BW for $|\theta/\theta_c|_{max} = \infty$, and the BW achieved is shown in brackets.

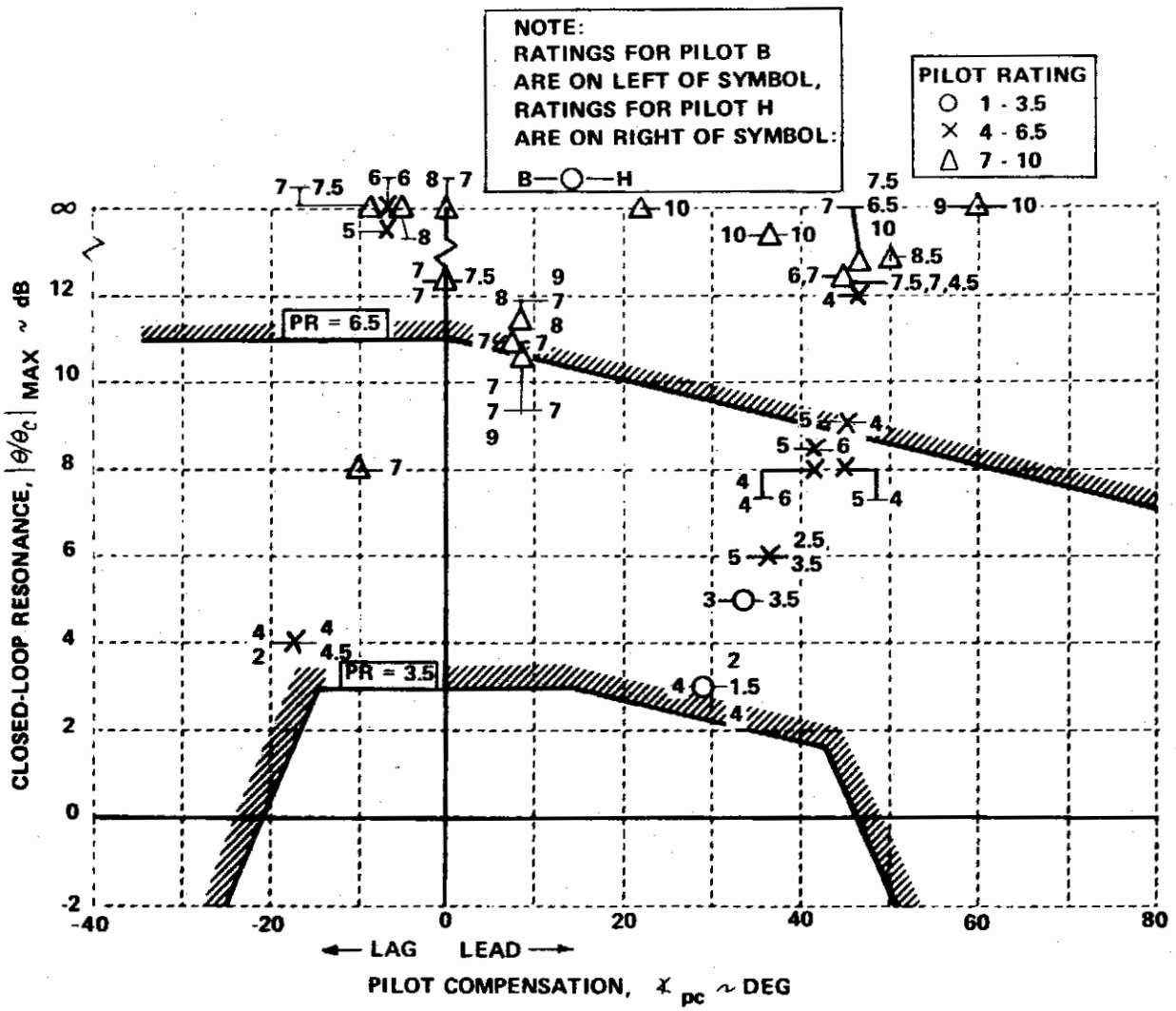

Figure 49. Correlation of Pilot Rating Data from HOS Program (Reference 6) with Closed-Loop Parameters

SECTION VIII

PROPOSED DESIGN CRITERIA

As shown in Section VII, the pilot-in-the-loop analysis technique developed in this report can be used to explain, in considerable detail, the flying-qualities problems associated with a wide variety of short-period and control-system dynamics. The purpose of this section is to summarize the analysis techniques in a form useful for design purposes, and to present a simplified version of the criterion which will be useful in the initial stages of a FCS/airframe design.

8.1 Criterion for Fighter Maneuvering Dynamics

The acceptability of an airplane's maneuvering dynamics to perform a given job can be stated in terms of the pilot compensation required to achieve some minimum "standard of performance" with the least possible tendency to oscillate or PIO. The standard of performance is dictated primarily by the mission requirements. For the combat phase of a fighter's mission, precise control of pitch attitude is a fundamental and critical task. Control of pitch attitude can be crudely modelled in the following way:

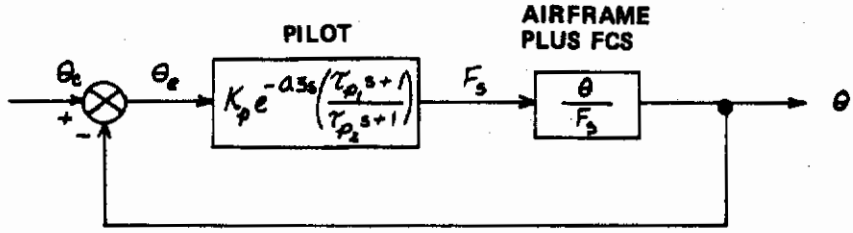

Using this model, the following terms are defined:

Bandwidth (BW): Bandwidth is defined as the frequency for which the closed-loop Bode phase, $\angle(\theta/\theta_c)$, is equal to -90 degrees. It is a measure of how quickly the pilot can move the airplane's nose toward the target.

Droop: Droop is defined as the maximum excursion of closed-loop Bode amplitude, $|\theta/\theta_c|$, below the 0 dB line for frequencies less than BW. In the absence of large oscillations, droop is a measure of how slowly the nose settles down on target.

Standard of Performance: A minimum bandwidth, $(BW)_{min}$, of 3.5 rad/sec, and a maximum droop of 3 dB:

$\angle(\theta/\theta_c)$ greater than (-90) degree
and $|\theta/\theta_c|$ greater than (-3) dB
} for ω less than 3.5

PIO Tendency: The tendency to oscillate or PIO is defined in terms of the Bode magnitude of any closed-loop resonant peak, $\left|\theta/\theta_c\right|_{max}$, that results from the pilot's efforts to achieve the performance standards.

Pilot Compensation: The pilot's physical and mental workload required to achieve the standard of performance is defined in terms of the phase of his compensation at $\omega = (BW)_{min}$:

$$\angle_{pc} = \angle \left(\frac{j\omega \tau_{p_1} + 1}{j\omega \tau_{p_2} + 1} \right)_{\omega = (BW)_{min}}$$

Thus, by analogy to the way in which the pilot controls pitch attitude, the designer's job in analyzing a given configuration is to select values of K_p, τ_{p_1}, and τ_{p_2} which will minimize $\left|\theta/\theta_c\right|_{max}$, while maintaining a minimum bandwidth of 3.5 rad/sec and a maximum droop of 3 dB. The values of $\angle_{pc}$ and $\left|\theta/\theta_c\right|_{max}$ determined in this way can then be compared against the boundaries of Figure 50 to determine the acceptability of the airplane's maneuvering characteristics.

The details of how $\angle_{pc}$ and $\left|\theta/\theta_c\right|_{max}$ can be determined for a given configuration are explained in Sections 6.5 through 6.8, and are summarized below.

(1) Obtain the Bode amplitude and phase characteristics of the airplane's pitch-attitude response to stick-force inputs (including the effects of the FCS), $\left|\frac{\theta(j\omega)}{F_s(j\omega)}\right|$ and $\angle \left(\frac{\theta(j\omega)}{F_s(j\omega)}\right)$. These characteristics can be obtained from computed $\frac{\theta}{F_s}$ transfer functions or from in-flight frequency responses (see Section 8.4). The frequency range of interest is from about 0.5 rad/sec to at least 10 rad/sec.

(2) Obtain the complete open-loop Bode amplitude and phase characteristics for the airplane and pilot delay at some nominal K_p (say 1.0):

$$\left(\frac{\theta}{\theta_e}\right)^* = 1.0e^{-0.3s} \left[\frac{\theta}{F_s}\right]$$

This can be accomplished by simply adding the 0.3 sec time delay to $\angle \theta/F_s$:

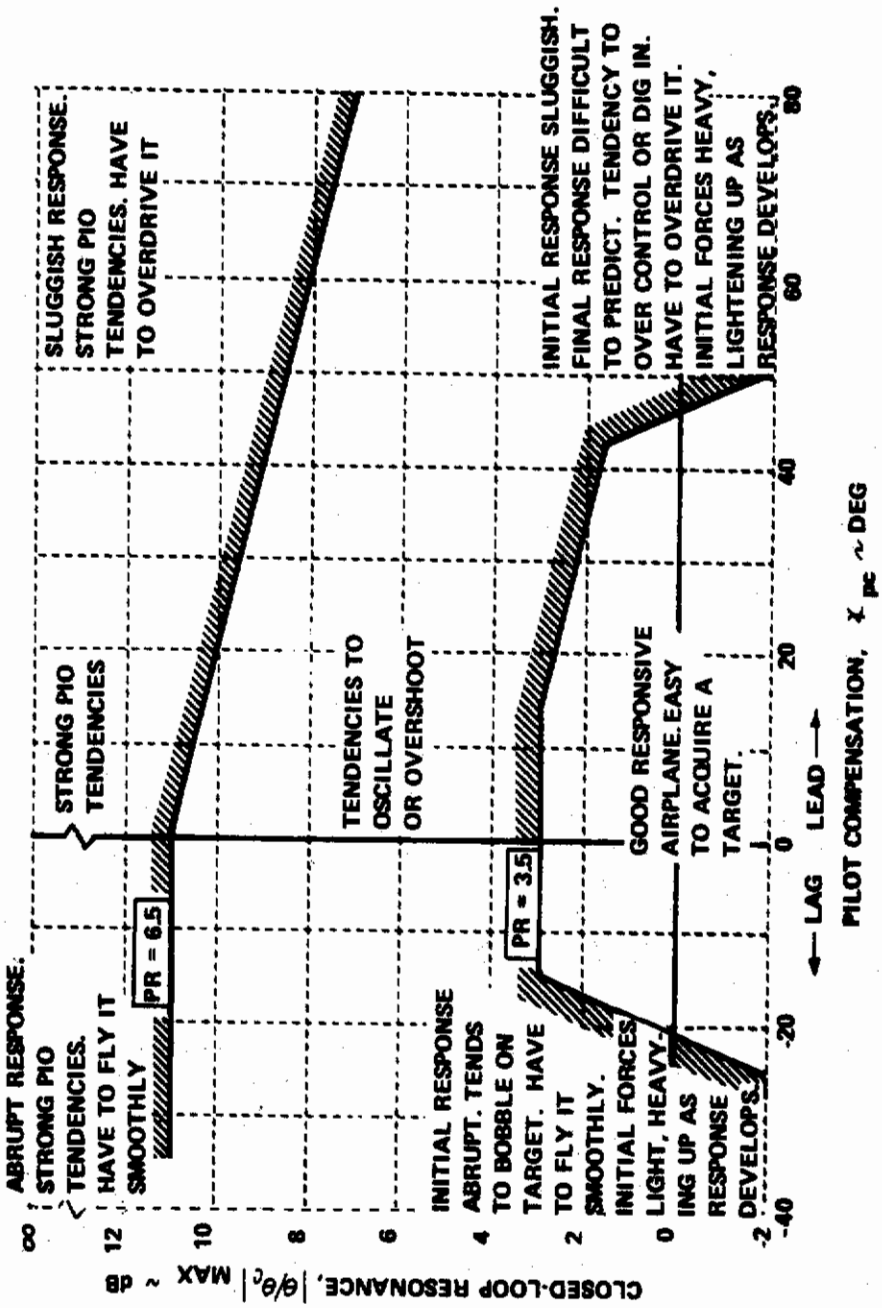

Figure 50. Proposed Criterion for Fighter Maneuvering Dynamics

$$\angle (\theta/\theta_e)^* = \angle \theta/F_s + 57.3\,(0.3)\omega \qquad \text{(deg)}$$

$$|\theta/\theta_e|^* = |\theta/F_s| \qquad \text{(dB)}$$

(3) Plot $|\theta/\theta_e|^*$ versus $\angle (\theta/\theta_e)^*$ and overlay the resulting curve on a Nichols chart, positioning the curve vertically so that the performance standards are just barely met (see Figure 51).

(4) If $|\theta/\theta_c|_{max}$ is greater than 0 dB, pilot compensation is required (lead compensation is needed for the example shown in Figure 51). The compensation can be determined by adding the amplitude and phase of Figure 52 to the uncompensated amplitude-phase curve, for several trial values of τ_{p_1} or τ_{p_2}/τ_{p_1}. The value of τ_{p_1} or τ_{p_2}/τ_{p_1} resulting in the smallest value of $|\theta/\theta_c|_{max}$ will be that which causes the bandwidth to exactly equal 3.5 rad/sec and the maximum droop to exactly equal -3 dB, as shown in Figure 51.

(5) $|\theta/\theta_c|_{max}$ can then be obtained from Figure 51 and $\angle_{pc}$ can be read directly from Figure 52 (for ω = 3.5 and the particular value of τ_{p_1} or τ_{p_2}/τ_{p_1} used).

8.2 Simplified Criterion.

The design criterion discussed above seems to satisfy all the requirements mentioned in Section I. It relates directly to the pilot's difficulties in performing the mission, it is applicable to airplanes having complex FCS dynamics, and is not dependent on how the control system is mechanized. However, it would be desirable to have a "quicky" method for making initial design estimates. Referring to Figure 51, it can be seen that the amount of compensation that the pilot will apply is related to the open-loop phase of the uncompensated pilot plus airplane, at $\omega = (BW)_{min}$. This phase angle, which is the phase of the airplane plus pilot delay, is defined as follows:

$$\angle_{ad} = \angle \left(\frac{\theta}{F_s} e^{-0.3j\omega}\right) \quad \text{at} \quad \omega = (BW)_{min} \qquad \text{(deg)}$$

It can also be seen from these figures that the slope of the compensated amplitude-phase curve in the vicinity of $\omega = (BW)_{min}$ is a crude measure of how large the closed-loop resonance will be; a large positive slope will

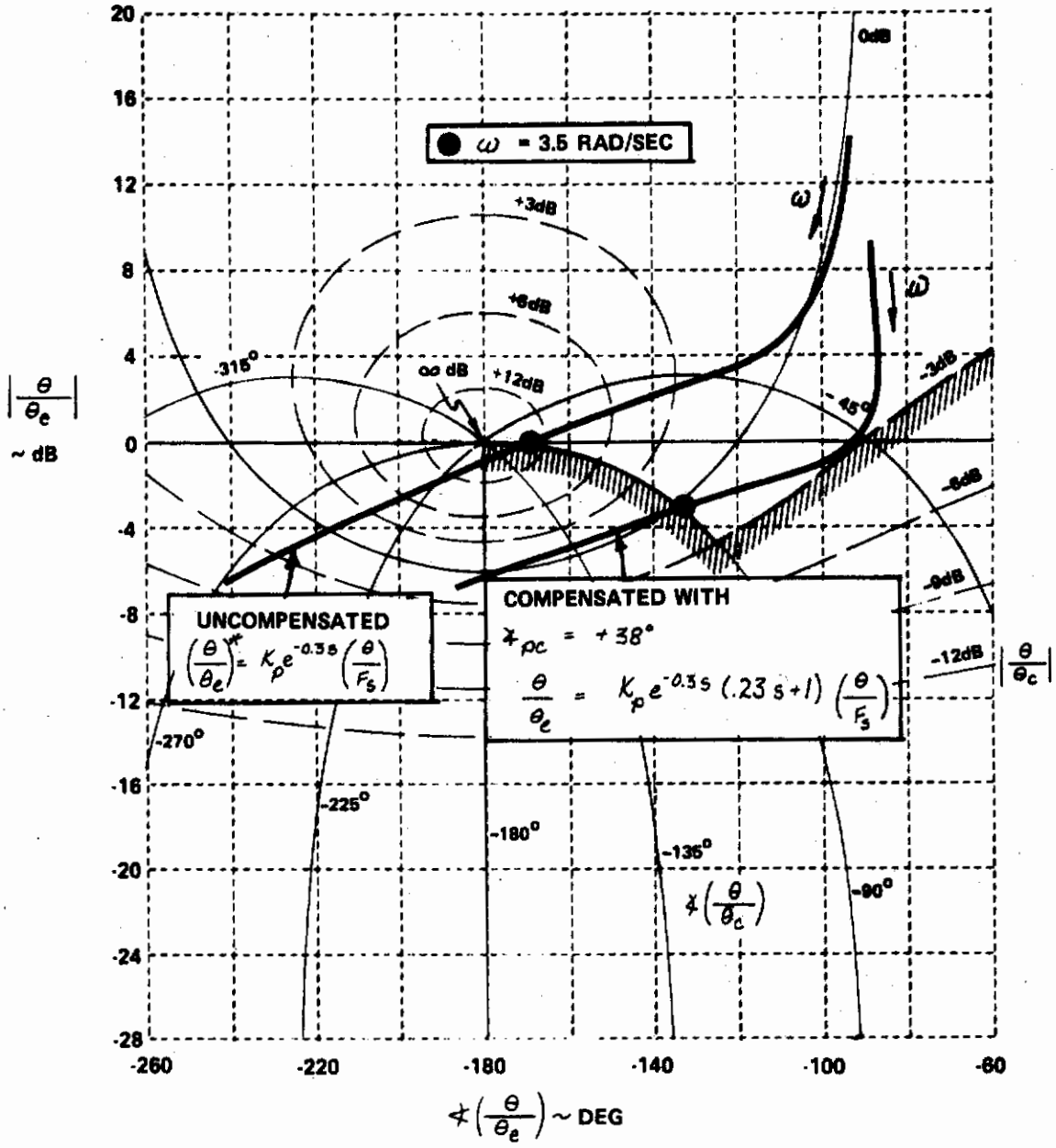

Figure 51. Nichols Chart Showing Typical Amplitude-Phase Overlays

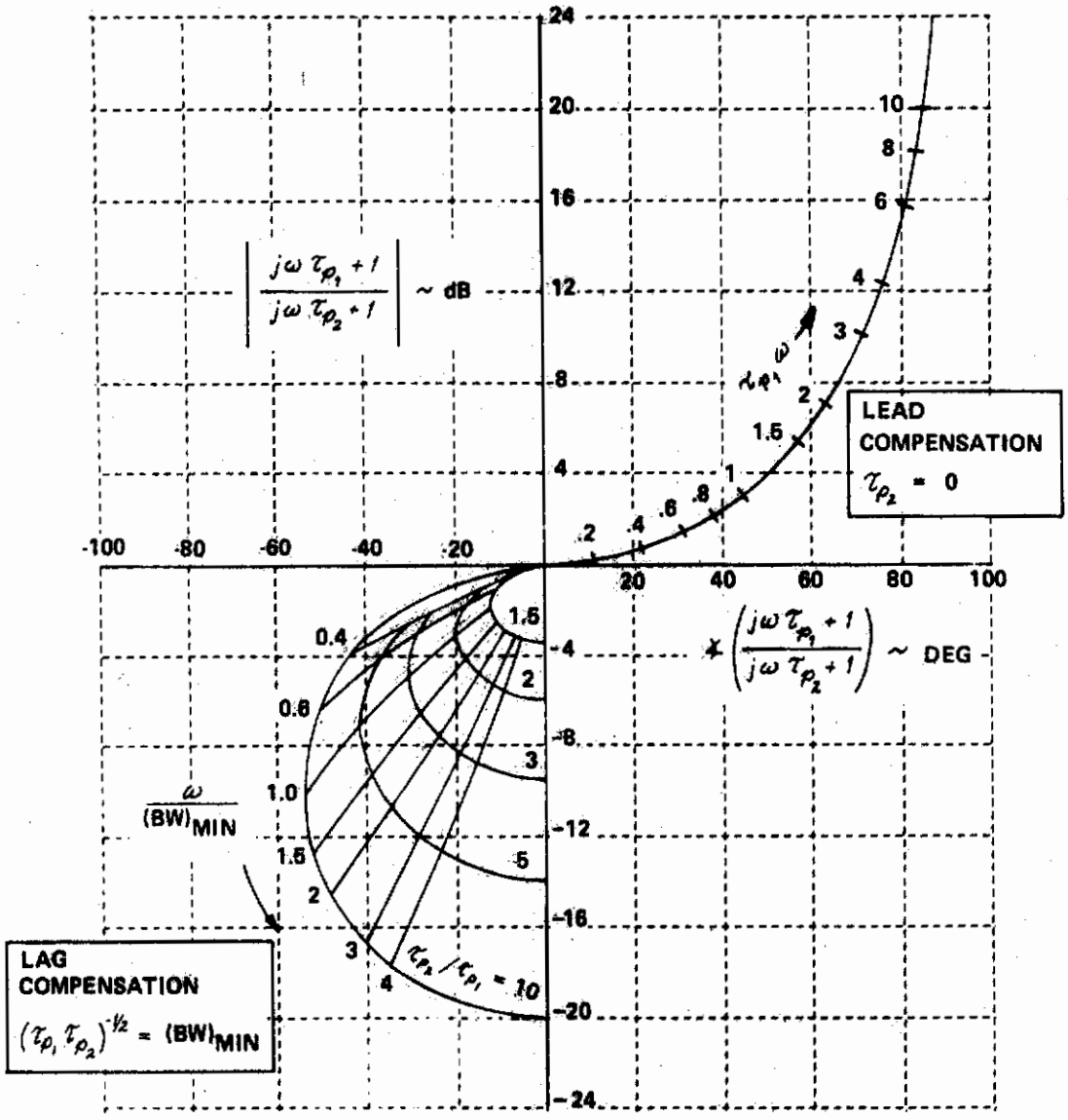

Figure 52. Amplitude-Phase Curves for "Optimum" Pilot Compensation

produce no resonance, and a small or negative slope is likely to produce a large resonance. Notice that the slope of the compensated curve is related to the slope of the uncompensated curve at $\omega = (BW)_{min}$ and to the amount of compensation needed. That is, lag compensation will tend to make the slope become more positive and lead compensation will tend to make the slope become slightly less positive. The slope of the uncompensated curve is defined as follows:

$$\left(\frac{dA}{d\angle}\right)_{ad} = \frac{d\left|\frac{\theta}{F_s} e^{-0.3j\omega}\right|}{d\left(\angle \frac{\theta}{F_s} e^{-0.3j\omega}\right)} \quad \text{at } \omega = (BW)_{min} \quad \text{(dB/deg)}$$

Thus, it would appear that the pilot compensation required and the closed-loop resonance are determined, in a crude sense, by the parameters $\angle_{ad}$ and $(dA/d\angle)_{ad}$.

These two open-loop parameters can be easily determined by making three measurements from the θ/F_s Bode plots at $\omega = (BW)_{min}$: $d\left|\theta/F_s\right|/d(\log\omega)$ (in dB/decade), $d(\angle\,\theta/F_s)/d(\log\omega)$ (in deg/decade), and $\angle\,\theta/F_s$ (in degrees). The relationships between these three measurements and $\angle_{ad}$ and $(dA/d\angle)_{ad}$ can be derived as follows:

$\angle_{ad}$:

$$\angle\left(e^{-0.3j\omega}\right)_{(BW)_{min}} = -17.2\,(BW)_{min}, \text{ degrees}$$

$$\angle_{ad} = \left[\angle\left(\frac{\theta}{F_s}\right)_{(BW)_{min}} - 17.2\,(BW)_{min}\right], \text{ degrees}$$

$(dA/d\angle)_{ad}$:

$$\left(\frac{d(\angle e^{-0.3j\omega})}{d(\log\omega)}\right)_{(BW)_{min}} = -39.6\,(BW)_{min}, \text{ deg/decade}$$

$$\left(\frac{d\left(\angle \frac{\theta}{F_s} e^{-0.3j\omega}\right)}{d(\log\omega)}\right)_{(BW)_{min}} = \left[\left(\frac{d\left(\angle\frac{\theta}{F_s}\right)}{d(\log\omega)}\right)_{(BW)_{min}} - 39.6\,(BW)_{min}\right] \text{ deg/decade}$$

$$\left(\frac{d\left|\frac{\theta}{F_s}\, e^{-0.3j\omega}\right|}{d(\log\omega)}\right)_{(BW)_{min}} = \left(\frac{d\left|\frac{\theta}{F_s}\right|}{d(\log\omega)}\right)_{(BW)_{min}}, \quad dB/decade$$

$$\left(\frac{dA}{d\angle}\right)_{ad} = \left[\frac{d\left|\frac{\theta}{F_s}\, e^{-0.3j\omega}\right| / d(\log\omega)}{d\left(\angle \frac{\theta}{F_s}\, e^{-0.3j\omega}\right) / d(\log\omega)}\right]_{(BW)_{min}}$$

$$= \left[\frac{\left[d\left|\frac{\theta}{F_s}\right| / d(\log\omega)\right]_{(BW)_{min}}}{\left[d\left(\angle \frac{\theta}{F_s}\right) / d(\log\omega)\right]_{(BW)_{min}} - 39.6\,(BW)_{min}}\right], \quad dB/deg$$

Using the above expressions, the parameters $\angle_{ad}$ and $(dA/d\angle)_{ad}$ were computed from Bode plots for each FCS/short-period configuration evaluated in the present program. The pilot ratings associated with each combination of $\angle_{ad}$ and $(dA/d\angle)_{ad}$ are shown in Figures 53 and 54. As with the more general criterion, it was necessary to use $(BW)_{min}$ of 3.5 rad/sec for the high-speed data and 3.0 rad/sec for the low-speed data. Boundaries were drawn on the plots, which separate the data very nicely into three bands of pilot ratings. These boundaries form a simple design criterion. In applying the criterion, it is recommended that $(BW)_{min}$ = 3.5 rad/sec be used:

$$\angle_{ad} = \angle\left(\frac{\theta}{F_s}\right)_{\omega=3.5} - 60$$

$$\left(\frac{dA}{d\angle}\right)_{ad} = \left[\frac{\left[d\,\frac{\theta}{F_s} / d(\log\omega)\right]_{\omega=3.5}}{\left[d\left(\angle \frac{\theta}{F_s}\right) / d(\log\omega)\right]_{\omega=3.5} - 139}\right]$$

To illustrate the computations involved, consider Configuration 6C from the present experiment. From the open-loop θ/F_s Bode characteristics given in Appendix I, the following measurements can be made

$$\left[\frac{d\left|\theta/F_s\right|}{d(\log\omega)}\right]_{\omega=3.5} = -28 \quad dB/decade$$

$$\left[\frac{d\left(\angle\, \theta/F_s\right)}{d(\log\omega)}\right]_{\omega=3.5} = -135 \quad deg/decade$$

$$\angle\left(\theta/F_s\right)_{\omega=3.5} = -130 \quad deg$$

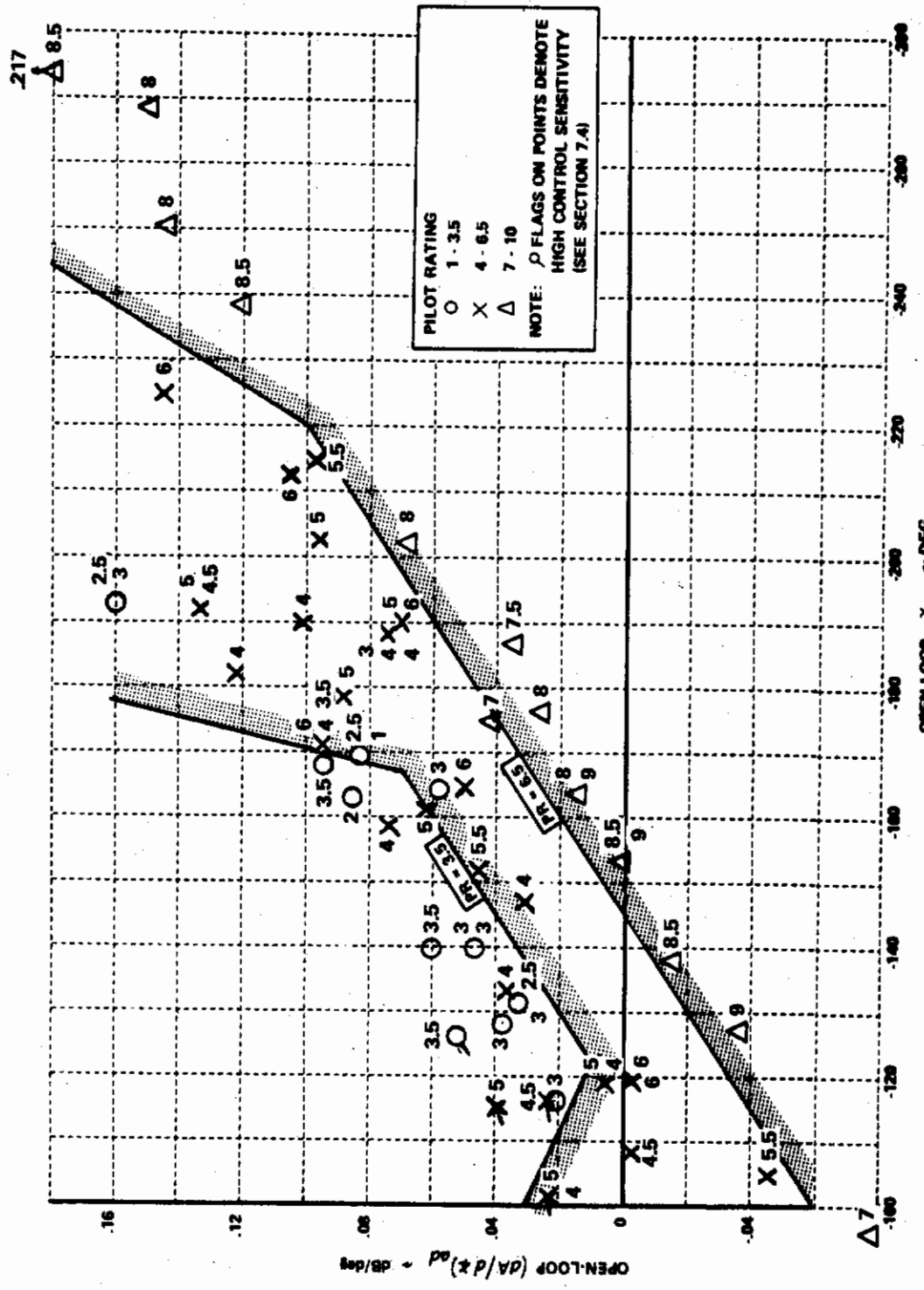

Figure 53. Correlation of Pilot M Rating Data with Simplified Analysis Parameters (Configuration 1A to 8E)

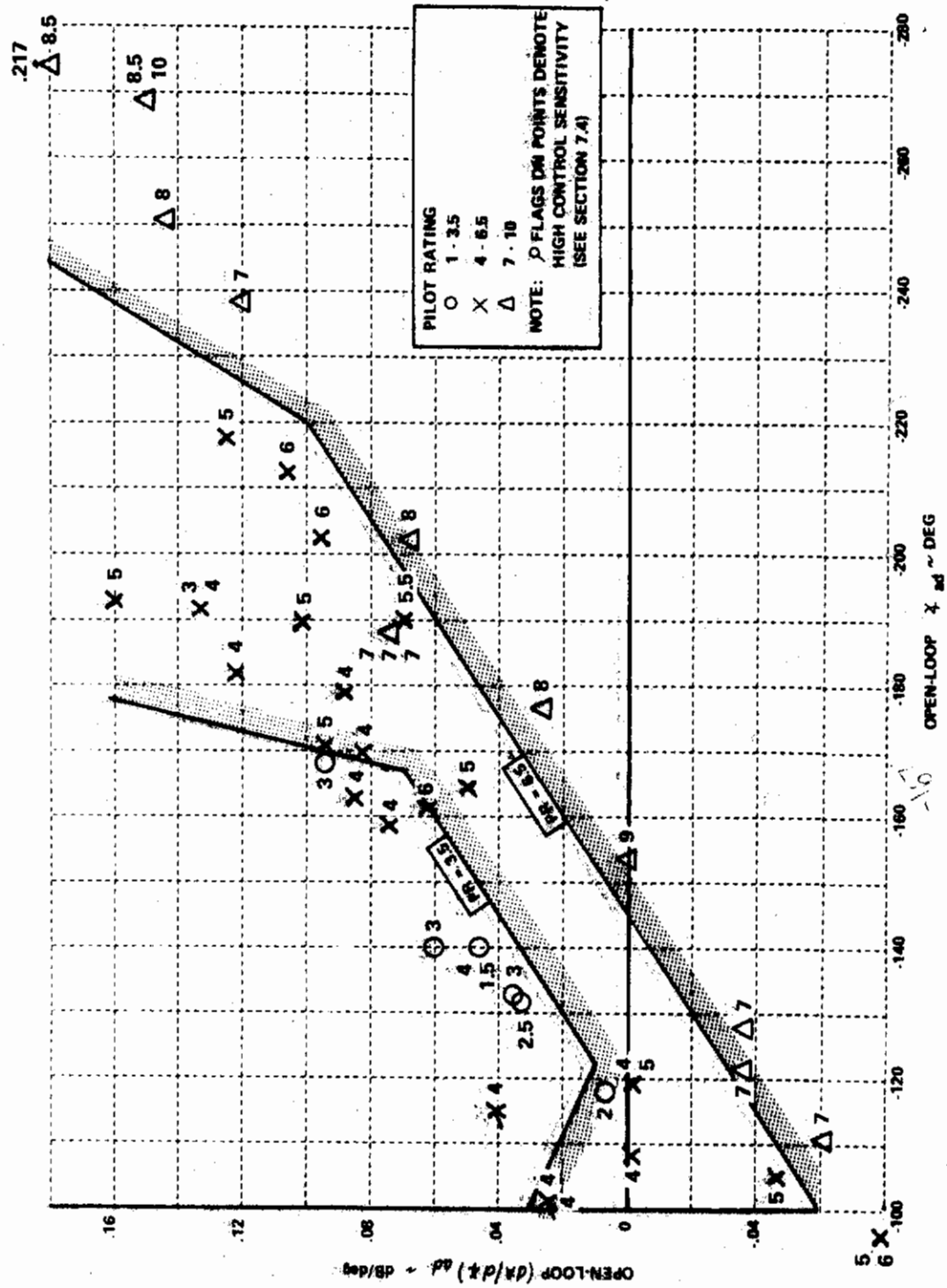

Figure 54. Correlation of Pilot W Rating Data with Simplified Analysis Parameters (Configurations 1A to 8E)

Thus,

$$\left(\frac{dA}{d\chi}\right)_{ad} = \frac{-28}{-135-139} = \frac{-28}{-274} = +.102 \quad dB/deg$$

$$\chi_{ad} = -130 - 60 = -190 \text{ deg}$$

It should be mentioned that the simplified criterion does not take into account as many details of the airplane's θ/F_s dynamics as the more complete criterion. For this reason, the simplified criterion is probably not as generally applicable. Nevertheless, Figures 53 and 54 do show what characteristics a good airplane should have: $\chi_{ad} \approx -120$ deg ($\chi_{\theta/F_s} \approx -60$ deg at ω = 3.5 rad/sec), plus a high positive value of $(dA/d\chi)_{ad}$.

8.3 Additional Considerations

Although the criteria discussed in Sections 8.1 and 8.2 adequately describe the more important aspects of fighter longitudinal flying qualities (for the "combat" flight phase), there are some other factors which must be considered separately.

For example, the elevator-to-stick-force gearing must be selected to provide good values of F_s/n without causing difficulties due to tracking forces or control sensitivity. The appropriate values of F_s/n for a fighter are adequately set by the high n/α requirements of MIL-F-8785B (Reference 12). For high n/α, the requirements show a range of 3.5 to 9.3 lb/g for satisfactory values of F_s/n (based on a limit load factor of 7.0g).

Control sensitivity, $\left|\ddot{\theta}/F_s\right|_{max}$, can cause difficulties if it becomes too large, as explained in Section 7.4. Although not well documented, values of sensitivity greater than 0.5 $\frac{rad/sec^2}{lb}$ are likely to cause problems.

It should be noted that for an airplane with $\omega_{sp} > 1/\tau_{\theta_2}$, good ζ_{sp}, a linear control system, and negligible control system dynamics, sensitivity is related to F_s/n in the following way (as shown in Appendix IV):

$$\left|\frac{\ddot{\theta}}{F_s}\right|_{max} = \frac{\omega_{sp}^2}{\left(\frac{n}{\alpha}\right)\left(\frac{F_s}{n}\right)}$$

As also explained in Section 7.4, K_{BW} can become a problem. However, because the effects of K_{BW} are so closely related to the effects of χ_{pc}, the present experiment gives little guidance in establishing limits on K_{BW}.

Another factor which is not handled by the criteria is the airplane's response to atmospheric turbulence. Since turbulence is a complex subject in itself, its effects were not treated in detail in this experiment. The subject is only mentioned to remind the designer that there are many ways to achieve the desired θ/F_s dynamics (prefilters, feedback loops, compensation networks, etc), and a particular design which has good θ/F_s characteristics will not necessarily result in good response to turbulence. For example, use of a first-order prefilter lag will often improve the θ/F_s characteristics of an airplane having high ω_{sp}, but will not affect the airplane's abrupt pitching response to vertical gusts.

8.4 Flight Test Measurements

It is evident that the usefulness of the criteria discussed in Sections 8.1 and 8.2 is dependent on the availability of θ/F_s Bode characteristics for the airplane being considered. Since the criteria are primarily intended for design purposes, these characteristics can easily be computed from the θ/F_s transfer function, which can be derived by combining the airframe characteristics (Appendix IV) with the FCS dynamics. For flight test purposes, generation of the Bode characteristics is a bit more complicated, but can be accomplished.

The most straightforward way to obtain in-flight frequency-response data is to have the pilot pump the stick at various frequencies, while recording stick force and pitch attitude (or pitch rate). One technique for accomplishing this is described in Reference 21.

For fly-by-wire control systems, i.e., systems with no direct mechanical link between the stick and the elevator, the frequency responses can be obtained by feeding an oscillating electrical signal into the control system at the stick-force transducer. This technique was applied several times during the present program with good results. The technique was not used as the primary method for identifying the dynamic characteristics evaluated in this program, because the particular mechanization of the dynamics in the T-33 made it easier to use a combination of ground and in-flight measurements (see Appendix V).

Whatever in-flight methods are used to generate frequency-response data, there is one essential element in the data reduction techniques which must be accounted for. The records from which the data is reduced include the effects of sensor dynamics as well as the airplane's dynamics. Thus, the dynamics of rate gyros, attitude gyros, filter networks, etc. must be identified and subtracted from the raw data. Even if the sensor dynamics have natural frequencies as high as 50 rad/sec, they can have a significant effect on θ/F_s in the frequency range of interest.

One last point should be mentioned. Since rate gyros are generally more available than attitude gyros, it is quite acceptable to measure pitch rate instead of pitch attitude. The θ/F_s frequency response characteristics can then be obtained from the $\dot{\theta}/F_s$ characteristics as follows:

$$\left|\frac{\theta(j\omega)}{F_s(j\omega)}\right| = \frac{1}{\omega}\left|\frac{\dot{\theta}(j\omega)}{F_s(j\omega)}\right|$$

$$\angle\left(\frac{\theta(j\omega)}{F_s(j\omega)}\right) = \angle\left(\frac{\dot{\theta}(j\omega)}{F_s(j\omega)}\right) - 90 \text{ degrees}$$

SECTION IX

CONCLUSIONS

(1) For the "combat" phase of a fighter's mission, those tasks which require precision control of pitch attitude will usually be the most critical, from the standpoint of longitudinal flying qualities.

(2) When allowed to select the elevator-to-stick-force gearing, neither pilot in the present experiment was willing to compromise the ability to pull high load factors with reasonable stick forces. Thus, it would appear that F_s/n is more of a performance parameter than a flying qualities parameter, in the sense that it forms a prerequisite to good flying qualities.

(3) The results of this experiment concerning short-period dynamics are consistent with the requirements of MIL-F-8785B (paragraph 3.2.2.1), with the exception of the low ζ_{sp}, high ω_{sp} region. In this region, the data indicates that the MIL-F-8785B requirements may be too lenient.

(4) The results of this experiment show that the dynamic modes of the flight control system can cause serious flying-qualities problems, but the data does not correlate with the control system requirements of MIL-F-8785B (paragraph 3.5.3). In addition, the C* criterion does not adequately account for control-system dynamics.

(5) The results also show that low ζ_{sp} can cause PIO tendencies, which are stronger at moderate values of ω_{sp} than when ω_{sp} is high. The strongest PIO tendencies, however, are obtained when control-system lags are added to configurations having low ζ_{sp} or low ω_{sp}.

(6) The pilot-in-the-loop analysis techniques presented in this report can be used to effectively describe the pilot's difficulties in precision tracking and to provide insight into the manner in which the pilot flies the airplane. These techniques are shown to be applicable to a wide range of control-system and short-period dynamics.

(7) A criterion, based on the pilot-in-the-loop analysis, can be used for the design of good fighter maneuvering characteristics. This criterion appears applicable to airplanes having high-augmented flight control systems, as well as unaugmented airplanes.

(8) A simplified version of the criterion, based on open-loop parameters, can be used to provide the flight control system designer with a "quicky" method for estimating the effects of his control-system design on the airplane's flying qualities.

(9) The performance standards used by the pilot in performing the required tasks can have a strong influence on the evaluation results. Clear definition of the tasks to be performed is necessary before meaningful flying qualities data can be obtained.

(10) More data on the effects of high ω_{sp} is needed, to better understand what the pilot describes as high frequency "bobbling" tendencies. In particular, the influence of control sensitivity and low ζ_{sp} on configurations having high ω_{sp} is poorly understood.

(11) A better understanding is needed of the effects of pilot gain, per se, on flying qualities.

(12) The techniques and criteria developed in this report should be applied to the rather considerable amount of existing data from other sources, concerning the influence of short-period dynamics on fighter flying qualities.

TABLE I

SUMMARY OF EXPERIMENTAL RESULTS (PILOT M)

NUMBERS IN BLOCKS REFER TO THE FOLLOWING: CONFIGURATION NO. / FLIGHT NO./PR/PIOR/$\frac{F_s}{n}$

CONTROL SYSTEM CHARACTERISTICS				SHORT PERIOD CHARACTERISTICS							
				n/α = 16.5 g/rad, $1/\tau_{\theta_2}$ = 1.25 sec^{-1}, V_T = 480 ft/sec					n/α = 50 g/rad, $1/\tau_{\theta_2}$ = 2.4 sec^{-1}, V_T = 675 ft/sec		
				3.21	3.42	ω_{SP}/ζ_{SP}	.41	.08	ω_{SP}/ζ_{SP}		
$1/\tau_1$	$1/\tau_2$	ω_3	ζ_3	2.2/0.69	4.8/0.70	8.7/0.63	5.0/0.26	5.1/0.18	3.4/0.67	7.3/0.78	16.5/0.68
0.5	2	63	0.75	1A 1032*/2/1/14.4 1065/6/2.5/7.2 1071/6/1.5/7.2		7.76			1.42	3.04	6.88
0.8	3.3								6A 1033/5/2/8.9		
2	5			1B 1046/3.5/1/6.0	2A 1046/4.5/2/5.8						
3.3	8								6B 1047/2.5/1.5/2.8 1075/1/1/5.4	7A 1046/6/2/3.7 1075/6/2/6.2	
5	12				2C 1044/3/1.5/4.6						
8	19									7B 1044/3/1.5/3.1	
∞	∞	75	0.67	1D 1028/5/2.5/9.0 1047/4.5/2/4.8	2D 1021/3/2/9.9 1045/2.5/1/3.7	3A 1023/5/3/10.8 1044/4/1.5/5.4	4A 1032/5.5/2.5/8.7	5A 1026/7/3/10.0	6C 1026/4/2.5/6.5	7C 1022/3/2/5.6 1053/3/2/3.9	8A 1028/5/2.5/6.3
.053	19	63	0.75							7D 1046/5.5/3/3.0	8B 1046/3.5/1.5/3.3
.083	12				2E 1045/4/1/3.6	3B 1048/4.5/2/4.3	4B ——	5B ——			
.125	8								6D 1038/5.5/2.5/4.9	7E 1050/6/3/5.1	8C 1036/3.5/2/5.7
.200	5			1E 1035/6/3.5/8.0	2F 1039/3/1/5.5	3C 1035/4/2/7.2	4C 1047/5.5/4/3.9	5C 1039/9/5/7.3			
.333	3.3								6E 1040*/5.5/2.5/3.2 1071/6.5/5/5.7	7F 1032/3/2/5.6 1067/4/2/4.5 1065/4/2/4.8	8D 1050/2/1/5.5
.5	2			1F 1033/6/4/14.4	2H 1022/5/2.5/8.2 1040/6/2.5/4.9	3D 1058/4/2/5.1	4D 1040/8/3.5/3.9 1057/9/5/5.9	5D 1033/8.5/4/11.0 1057/9/5/5.4		7G 1056/6/2/4.9	
.25	0.8								6F 1030*/6/2.5/7.8 1070/6/4/6.7	7H ——	8E 1063/2.5/1/4.6 1070/3/1/4.6
2	0.5			1G 1030/8.5/4.5/6.0	2J 1063/6/2/5.5	3E 1063/4/1.5/4.8	4E 1052/7.5/4/3.9	5E 1030/8/4/6.3			
2	5	16	0.75	1C 1036*/2/1/8.0 1054/5/2.5/7.2 1066/3.5/2/9.0	2B 1036*/2.5/1.5/5.4 1054/6/2.5/6.0 1066/6/3/6.6						
∞	5				2G 1053/7/3/5.5						
↓	2	↓	↓		2I 1036/8/4.5/4.6						

SIX ADDITIONAL CONFIGURATIONS: STICK POSITION COMMANDS USED (SEE SECTIONS 3.2 AND 3.3)

$1/\tau_1$	$1/\tau_2$	ω_3	ζ_3	ω_{SP}/ζ_{SP}				ω_{SP}/ζ_{SP}		
∞	∞	75	0.67	2.3/1.7	2.3/1.2	3.3/1.1		10/0.45	13/0.34	16.6/0.28
↓	↓	↓	↓	9 1070/6/2/9.7	10 1075/4/1.5/8.2	11 1065/3/1/7.8		12 1052/5/2.5/4.9 1071/6/2.5/8.4	13 1053/7/3/6.0 1068/5.5/2.5/8.1	14 1052/4.5/2/5.4 1066/6/3/8.4

*THESE RATINGS NOT USED IN DATA ANALYSIS (SEE DISCUSSION IN APPENDIX I).

TABLE I (cont.)

SUMMARY OF EXPERIMENTAL RESULTS (PILOT W)

NUMBERS IN BLOCKS REFER TO THE FOLLOWING: CONFIGURATION NO. / FLIGHT NO./PR/PIOR/$\frac{F_s}{n}$

CONTROL SYSTEM CHARACTERISTICS				SHORT PERIOD CHARACTERISTICS							
				n/α = 18.5 g/rad, $1/\tau_{\theta_2}$ = 1.25 sec^{-1}, V_T = 480 ft/sec					n/α = 50 g/rad, $1/\tau_{\theta_2}$ = 2.4 sec^{-1}, V_T = 675 ft/sec		
				ω_{SP}/ζ_{SP}					ω_{SP}/ζ_{SP}		
$1/\tau_1$	$1/\tau_2$	ω_3	ζ_3	2.2/0.69	4.0/0.70	9.7/0.63	5.0/0.28	5.1/0.18	3.4/0.67	7.3/0.73	16.5/0.69
0.5	2	63	0.75	1A 1043*/2/1/6.0 1073/6/2/7.2							
0.8	3.3								6A 1034/6/3/3.5		
2	5			1B 1074/3/1.5/6.5	2A 1051/4/2/5.1						
3.3	8								6B 1074/4/1.5/5.4	7A 1074/2/1/4.7	
5	12				2C —						
8	19	↓	↓							7B —	
∞	∞	75	0.67	1D 1043/3/1/4.2 1067/4/2/6.0	2D 1031/2.5/1/5.9	3A 1024/4/1/11.5 1072/4/1.5/5.7	4A 1041/5/2/5.3	5A 1029/6/1.5/6.3 1051/6/3/5.5	6C 1029*/2.5/1/3.9 1072/5/2/5.4	7C 1027/4/1/3.2 1062/1.5/1/4.7	8A 1041/4/1/4.0
↓	19	63	0.75							7D —	8B —
	12				2E —	3B —	4B 1062/7/4/5.6	5B 1062/7/4/7.1			
	8								6D —	7E 1056/5/2/3.5	8C 1051/3/1/3.9
	5			1E —	2F —	3C 1066/3/1/5.1	4C —	5C 1056/7/4/7.3			
	3.3								6E 1073/7/4/5.4	7F 1024/7/-/5.0 1043/7/3.5/3.2 1064/7/4/4.7	8D 1064/4/2/4.6
	2			1F 1034/8/4/6.0	2H 1027/5.5/2/5.7	3D 1059/4/1/5.4	4D —	5D 1034/8/4/7.3		7G 1059/6/2/4.9	
	0.8								6F 1031/8.5/4/3.0 1067/10/5/5.4	7H 1061/5/2/4.7	8E 1067/5/2/4.6
↓	0.5	↓	↓	1G 1061/8.5/4/4.6	2J 1060/6/2/4.9	3E 1061/4/1/4.5	4E —	5E 1041/8/4/4.4			
2	5	16	0.75	1C 1038/4/1.5/6.0	2B 1038/4/1.5/4.9 1072/5/2.5/5.9						
∞	5	↓	↓		2G —						
↓	2	↓	↓		2I 1038/8/4/4.9						

SIX ADDITIONAL CONFIGURATIONS: STICK POSITION COMMANDS USED (SEE SECTIONS 3.2 AND 3.3)

$1/\tau_1$	$1/\tau_2$	ω_3	ζ_3	ω_{SP}/ζ_{SP}
∞	∞	75	0.67	10/0.45
↓	↓	↓	↓	12 1073/6/3/6.3

* THESE RATINGS NOT USED IN DATA ANALYSIS (SEE DISCUSSION IN APPENDIX I)

TABLE II

SUMMARY OF PILOT-IN-THE-LOOP PARAMETERS

NUMBERS IN BLOCKS REFER TO THE FOLLOWING:

CONFIGURATION NO.

$$\left|\frac{\theta}{\theta_C}\right|_{MAX} / \omega_{pc} \Big/ \frac{1}{\tau_{P_1}} \Big/ \frac{1}{\tau_{P_2}}$$

CONTROL SYSTEM CHARACTERISTICS				SHORT PERIOD CHARACTERISTICS							
				n/α = 18.5 g/rad $1/\tau_{\theta_2}$ = 1.25 sec^{-1} $(BW)_{min}$ = 3.0 rad/sec					n/α = 50 g/rad $1/\tau_{\theta_2}$ = 2.4 sec^{-1} $(BW)_{min}$ = 3.5 rad/sec		
				ω_{SP}/ζ_{SP}					ω_{SP}/ζ_{SP}		
$1/\tau_1$	$1/\tau_2$	ω_3	ζ_3	2.2/0.69	4.9/0.70	8.7/0.63	5.0/0.28	5.1/0.18	3.4/0.67	7.3/0.73	16.5/0.69
0.8	2	6.3	0.75	1A +7.0/+20/5.6/0							
0.8	3.3								6A +9/+11/17.5/0		
2	5			1B +0.5/+35/4.3/0	2A +3.0/-26/5.0/1.9						
3.3	8								6B +0.5/+38/4.4/0	7A +8/-10/4.1/2.8	
5	12				2C +2.0/-16/8.8/2.3						
8	19	↓	↓							7B +2/0/0/0	
∞	∞	75	0.67	1D 0/+60/1.7/0	2D +2.0/ -5/3.3/2.7	3A -1.0/-25/4.8/1.8	4A +10/-28/5.0/1.8	5A >12/-35/6.0/1.5	6C +1.5/+57/2.3/0	7C 0/+13/15.9/0	8A 0/-10/4.1/2.8
		19	0.3							7D +1.5/+23/6.3/0	8B +1.5/0/0/0
		12			2E +3.5/+14/12.0/0	3B +1.0/-12/3.7/2.5	4B +12/-17/4.0/2.2	5B >12/-25/4.6/1.8			
		8							6D +8/+67/1.4/0	7E +3.5/+35/4.9/0	8C -1/+14/14.0/0
		5		1E +9.0/+73/.91/0	2F +2.5/+29/5.5/0	3C +2.5/0/0/0	4C >12/-6/3.2/2.9	5C >12/-10/3.6/2.6			
		3.3							6E +12/+78/0.7/0	7F +4.0/+57/2.3/0	8D 0/+35//4.4/0
		2		1F >12/+80/.50/0	2H +3.0/+55/2.1/0	3D -2.0/+31/5.0/0	4D +10/+31/5.0/0	5D > 12/+21/7.5/0		7G +4.0/+70/1.3/0	
		0.8							6F ∞/+60/0.6/0[**]	7H +5.5/+60/0.58/0	8E -0.5/+70/1.25/0
↓		0.5	↓	1G ∞/+90/.50/0[*]	2J +3.5/+76/0.6/0	3E -2.0/+55/2.1/0	4E +10/+57/2.0/0	5E > 12/+50/2.5/0			
2	5	16	0.75	1C +2.0/+42/3.3/0	2B +7.0/-20/4.3/2.1						
∞	5	↓	↓		2G +6.0/+35/4.3/0						
↓	2	↓	↓		2I +7.0/+58/1.8/0						

SIX ADDITIONAL CONFIGURATIONS: STICK POSITION COMMANDS USED (SEE SECTIONS 3.2 AND 3.3)

$1/\tau_1$	$1/\tau_2$	ω_3	ζ_3	ω_{SP}/ζ_{SP}					ω_{SP}/ζ_{SP}		
∞	∞	75	0.67	2.3/1.7	2.3/1.2	3.8/1.1			10/0.45	13/0.84	15.6/0.23
↓	↓	↓	↓	9 -1.0/+61/1.5/∞	10 -1.0/+63/1.5/∞	11 -1.5/+45/3.0/∞			12 4/-/∞/∞	13 2.0/-6/3.9/2.1	14 1.0/-10/4.1/3.0

[*] $(BW)_{min}$ = 2.7 RAD/SEC FOR CONFIGURATION 1G

[**] $(BW)_{min}$ = 3.3 RAD/SEC FOR CONFIGURATION 6F

TABLE III

SUMMARY OF AVERAGE[1] CONTROL SENSITIVITIES AND PILOT GAINS

NUMBERS IN BLOCKS[1] REFER TO THE FOLLOWING:

CONFIGURATION NO.
$\left\lvert \frac{\ddot{\theta}}{F_S} \right\rvert_{MAX} / K_{BW}$

[1]WHERE $\ddot{\theta}/F_S$ max AND K_{BW} ARE AVERAGE VALUES BASED ON THE FOLLOWING:

F/n = 6.0 LB/g USED FOR CONFIGURATIONS WITH n/α = 18.5 g/RAD

F/n = 4.5 LB/g USED FOR CONFIGURATIONS WITH n/α = 50 g/RAD

CONTROL SYSTEM CHARACTERISTICS				SHORT PERIOD CHARACTERISTICS							
				n/α = 18.5 g/rad, $1/\tau_{\theta_2}$ = 1.25 sec^{-1}, $(BW)_{min}$ = 3.0 rad/sec					n/α = 50 g/rad, $1/\tau_{\theta_2}$ = 2.4 sec^{-1}, $(BW)_{min}$ = 3.5 rad/sec		
				ω_{SP}/ζ_{SP}					ω_{SP}/ζ_{SP}		
$1/\tau_1$	$1/\tau_2$	ω_3	ζ_3	2.2/0.69	4.9/0.70	8.7/0.63	5.0/0.28	5.1/0.16	3.4/0.67	7.3/0.78	16.5/0.69
0.5	2	6.3	0.75	1A 0.17/0.96							
0.8	3.3								8A 0.21/1.9		
2	5			1B 0.10/1.6	2A 0.51/0.89						
3.3	8								6B 0.115/2.9	7A 0.52/1.8	
5	12				2C 0.44/1.1						
8	19	↓	↓							7B 0.48/2.0	
∞	∞	75	0.67	1D 0.044/2.6	2D 0.22/1.3	3A 0.88/1.1	4A 0.43/0.92	5A 0.67/0.80	6C 0.054/3.1	7C 0.24/2.0	8A 1.18/2.1
		19	63	0.75						7D 0.19/2.2	8B 0.70/2.2
		12			2E 0.17/1.4	3B 0.53/1.1	4B 0.39/0.99	5B 0.60/0.83			
		8							6D 0.045/4.1	7E 0.190/2.4	8C 0.37/2.1
		5		1E 0.036/4.0	2F 0.12/1.7	3C 0.31/1.8	4C 0.29/1.2	5C 0.46/1.1			
		3.3							6E 0.033/5.0	7F 0.070/3.8	8D 0.17/2.8
		2		1F 0.024/6.7	2H 0.058/2.4	3D 0.18/2.0	4D 0.15/1.7	5D 0.23/1.6		7G 0.043/4.6	
		0.8							6F 0.031/16.0**	7H 0.019/12.0	8E 0.042/8.5
↓		0.5	↓	1G 0.008/16.5*	2J 0.016/8.0	3E 0.095/6.4	4E 0.041/5.4	5E 0.065/4.6			
2	5	16	0.75	1C 0.094/1.7	2B 0.46/0.94						
∞	5				2G 0.12/1.7						
↓	2	↓	↓		2I 0.058/2.6						

SIX ADDITIONAL CONFIGURATIONS: STICK POSITION COMMANDS USED (SEE SECTIONS 3.2 AND 3.3)

$1/\tau_1$	$1/\tau_2$	ω_3	ζ_3	ω_{SP}/ζ_{SP}				ω_{SP}/ζ_{SP}		
∞	∞	75	0.67	2.9/1.7	2.3/1.2	3.3/1.1		10/0.45	13/0.34	16.6/0.23
↓	↓	↓	↓	9 0.035/4.9	10 0.041/3.6	11 0.079/2.2		12 0.47/2.0	13 0.86/1.9	14 1.85/1.9

*$(BW)_{min}$ = 2.7 RAD/SEC FOR CONFIGURATION 1G

**$(BW)_{min}$ = 3.3 RAD/SEC FOR CONFIGURATION 6F

TABLE IV

SUMMARY OF PARAMETERS FOR SIMPLIFIED CRITERION

NUMBERS IN BLOCKS REFER TO THE FOLLOWING: CONFIGURATION NO. $\left(\frac{dA}{d\phi}\right)_{ad} / \phi_{ad}$

CONTROL SYSTEM CHARACTERISTICS				SHORT PERIOD CHARACTERISTICS							
				n/α = 18.5 g/rad; $1/\tau_{\theta_2}$ = 1.25 sec^{-1}; $(BW)_{min}$ = 3.0 rad/sec					n/α = 50 g/rad; $1/\tau_{\theta_2}$ = 2.4 sec^{-1}; $(BW)_{min}$ = 3.5 rad/sec		
				ω_{SP}/ζ_{SP}					ω_{SP}/ζ_{SP}		
$1/\tau_1$	$1/\tau_2$	ω_3	ζ_3	2.2/0.69	4.9/0.70	9.7/0.63	5.0/0.28	5.1/0.18	3.4/0.67	7.3/0.73	16.5/0.69
0.5	2	6.3	0.75	1A 0.084/-170							
0.8	3.3								6A 0.062/-161		
2	5			1B 0.094/-168	2A -0.002/-108						
3.3	8								6B 0.062/-169	7A 0.005/-119	
5	12				2C 0.021/-116						
8	19	↓	↓							7B 0.038/-126	
∞	∞	75	0.67	1D 0.134/-182	2D 0.033/-132	3A 0.022/-101	4A -0.046/-105	5A -0.060/-96	6C 0.102/-180	7C 0.045/-140	8A 0.060/-115
	19	63	0.75							7D 0.045/-152	8B 0.052/-126
	12				2E 0.032/-147	3B 0.022/-116	4B -0.036/-121	5B -0.062/-111			
	8								6D 0.098/-215	7E 0.060/-165	8C 0.060/-140
	5			1E 0.143/-226	2F 0.058/-164	3C 0.036/-133	4C -0.016/-138	5C -0.037/-128			
	3.3								6E 0.120/-238	7F 0.075/-188	8D 0.065/-163
	2			1F 0.143/-251	2H 0.069/-190	3D 0.075/-159	4D 0.014/-164	6D 0/-154		7G 0.086/-203	
	0.8								6F 0.150/-289**	7H 0.125/-218	8E 0.100/-183
↓	0.5	↓	↓	1G 0.217/-274*	2J 0.106/-213	3E 0.122/-182	4E 0.037/-187	5E 0.027/-177			
2	5	16	0.78	1C 0.089/-179	2B -0.002/-119						
∞	5				2G 0.041/-175						
↓	2	↓	↓		2I 0.064/-202						

*$(BW)_{min}$ = 2.7 RAD/SEC FOR CONFIGURATION 1G

**$(BW)_{min}$ = 3.3 RAD/SEC FOR CONFIGURATION 6F

REFERENCES

1. Chalk, C. R.: Fixed-Base Simulator Investigation of the Effects of L_α and True Speed on Pilot Opinion of Longitudinal Flying Qualities. ASD-TDR-63-399, November 1963.

2. Chalk, C. R.: Flight Evaluation of Various Short-Period Dynamics at Four Drag Configurations for the Landing Approach Task. FDL-TDR-64-60, October 1964.

3. Chalk, C. R.: Flight Evaluation of Various Phugoid Dynamics and $1/T_{h_1}$ Values for the Landing Approach Task. AFFDL-TR-66-2, February 1966.

4. DiFranco, D. A.: Flight Investigation of Longitudinal Short-Period Frequency Requirements and PIO Tendencies. AFFDL-TR-66-163, April 1967.

5. Parrag, Michael L.: Pilot Evaluations In a Ground Simulator of the Effects of Elevator Control System Dynamics in Fighter Aircraft. AFFDL-TR-67-19, July 1967.

6. DiFranco, D. A.: In-Flight Investigation of the Effects of Higher-Order System Dynamics on Longitudinal Handling Qualities, AFFDL TR-68-90, July 1968.

7. Hall, G. W.: In-Flight Investigation of Longitudinal Short-Period Handling Characteristics of Wheel Control Airplanes, AFFDL-TR-68-91, July 1968.

8. Newell, F. D. and Wasserman, R.: In-Flight Investigation of Pitch Acceleration and Normal Acceleration Bobweights. AFFDL-TR-69-3, April 1969.

9. Cooper, G. E. and Harper, R. P., Jr.: The Use of Pilot Rating in the Evaluation of Aircraft Handling Qualities, NASA TN D-5153, April 1969.

10. Moses, K., et al: Adaptive Control Using Sampled Data -- A Flight-Proven Concept, AIAA/ION Guidance and Control Conference, Minneapolis, Minnesota, 16-18 August 1965.

11. Rubertus, D. P.: Correlation of a Fighter Aircraft's Augmented Response with the C* Longitudinal Handling Qualities Criterion, Master's Thesis, Ohio State University, 1967.

12. Anon: Military Specification, Flying Qualities of Piloted Airplanes. MIL-F-8785B(ASG), 7 August 1969.

13. Chalk, C. R., Neal, T.P., Harris, T. M., Pritchard, F. E., and Woodcock, R. J.: Background Information and User Guide for MIL-F-8785B(ASG), "Military Specification-Flying Qualities of Piloted Airplanes", AFFDL-TR-69-72, August 1969.

14. Hall, G. W. and Huber, R. W.: System Description and Performance Data for the USAF/CAL Variable Stability T-33 Airplane, AFFDL-TR-70-71, July 1970.

15. Tobie, H. N., Elliott, E. M., and Malcom, L. G.: A New Longitudinal Handling Qualities Criterion, National Aerospace Electronics Conference, Dayton, Ohio, 16-18 May 1966.

16. Shomber, H. A. and Gertsen, W. M.: Longitudinal Handling Qualities Criteria: An Evaluation. AIAA Paper 65-780, November 1965.

17. McRuer, D. T., Ashkenas, I. L. and Guerre, C. L.: A Systems Analysis View of Longitudinal Flying Qualities. WADD TR 60-43, USAF, January 1960.

18. Jex, Henry R. and Cromwell, Charles H., III: Theoretical and Experimental Investigation of Some New Longitudinal Handling Qualities Parameters. ASD-TR-61-26, June 1962.

19. Ashkenas, I. L., Jex, H. R., and McRuer, D. T.: Pilot-Induced Oscillations: Their Cause and Analysis. TR-239-2, Systems Technology, Inc., 20 June 1964.

20. McRuer, D., Graham, D. et al: Human Pilot Dynamics in Compensatory Systems, AFFDL-TR-65-15, July 1965.

21. Klung, H. A., Jr.: Frequency Response Method of Determining Aircraft Longitudinal Short-Period Stability and Control System Characteristics in Flight. FTC-TR-66-24, USAF, August 1966.